1-1-2013

Cervical Spine Tolerance And Response In Compressive Loading Modes Including Combined Compression And Lateral Bending

Daniel Toomey
Wayne State University,

CERVICAL SPINE TOLERANCE AND RESPONSE IN COMPRESSIVE LOADING MODES INCLUDING COMBINED COMPRESSION AND LATERAL BENDING

by

DANIEL E. TOOMEY

DISSERTATION

Submitted to the Graduate School

of Wayne State University,

Detroit, Michigan

in partial fulfillment of the requirements

for the degree of

DOCTOR OF PHILOSOPHY

2013

MAJOR: BIOMEDICAL ENGINEERING

Approved by:

_____

Advisor Date

_____

Co-Advisor Date

_____

_____

_____

ACKNOWLEDGMENTS

The author gratefully acknowledges his advisors Dr. King Yang and Dr. Chris Van Ee for their support throughout his graduate studies at Wayne State University. The author gratefully acknowledges the guidance provided by his dissertation committee: Dr. Albert King, Dr. Michele Grimm, and Dr. Priya Prasad.

PMHS testing conducted at the Bioengineering Center was funded by Nissan Motor Co. This experimentation would not have been possible without the efforts of Matt Mason, Jim Kopacz and Dr. Warren Hardy. Their unselfish support of this research in working late evenings was essential to the completion of these experiments. Additionally, the author is very grateful for the training and expertise in experimental protocols and biomedical instrumentation provided by Dr. Hardy.

The author would like to acknowledge Drs. Pintar and Yoganandan at the Medical College of Wisconsin who welcomed him into their laboratory so data from their previous experimentation could be included in the PMHS cervical spine compressive tolerance analysis. This collaboration greatly enhanced the current research.

Finally, the author would like to acknowledge the support of Design Research Engineering whose encouragement and generosity made this research possible. The author would like to offer deep appreciation for his family and friends who have supported him during the course of this work, especially his wife Erin. This would never have been possible without your love and support.

TABLE OF CONTENTS

LIST OF TABLES

LIST OF FIGURES

CHAPTER 1

INTRODUCTION

1.1 Statement of the Problem

Injuries in motor vehicle accidents continue to be a serious and costly societal problem. Protecting occupants from cervical spine compressive injuries during rollover dynamics has been a significant challenge to automotive safety engineers. Since 2005, motor vehicle accidents have accounted for 42.1% of all reported spinal cord injuries in the United States (NSCISC Apr 09). The development of effective countermeasures to decrease the incidence of these spinal cord injuries must be guided by meaningful and reliable injury criteria.

Rollover researchers have regularly used the Hybrid III anthropomorphic test device (ATD) as a tool in understanding the magnitude of neck forces and moments during rollover tests for assessment of injury causation and evaluation of the efficacy of various vehicle structural and restraint designs (Orlowski et al. 1985, Bahling et al. 1990, Hare et al. 2002, Moffatt et al. 2003, McCoy and Chou 2007, Raddin et al. 2009, and Viano et al. 2009). Investigators have observed noticeable lateral bending of the ATD neck prior to impact or in conjunction with head impact with the vehicle roof in rollover crash tests (Figure 1.1). Since there is scant data available about the effects of lateral bending on overall compressive tolerance of the human cervical spine, it is unknown if the presence of lateral bending is important to consider when interpreting the data from rollover testing. As the Hybrid III ATD continues to be used in automotive rollover applications, interpretation of measured neck loads in this testing mode would be aided by a better understanding of human cervical spine response and tolerance in compression dominated combined loading scenarios and their correlation to Hybrid III ATD neck responses.

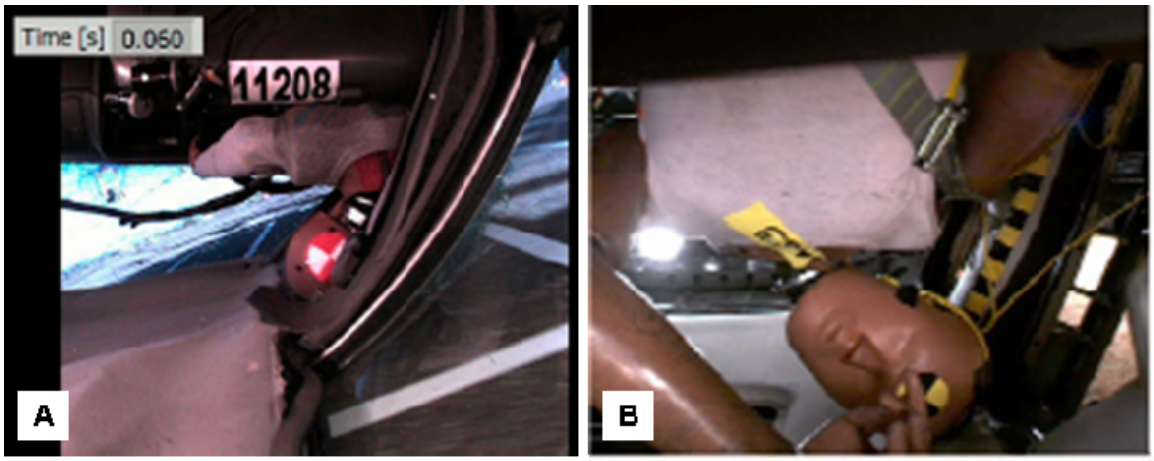

Figure 1.1: ATD neck compressive loading with lateral bending present from (A) Raddin et al. (2009) and (B) McCoy and Chow (2007)

1.2 Background

The response of the human cervical spine to compressive loading has repeatedly been demonstrated to vary with the direction of the applied loading vector, head and neck constraint and initial head and neck posture (Nusholtz et al. 1983, Yoganandan et al. 1986, McElhaney et al. 1988, and Myers et al. 1991a). While sagittal plane human cervical spine compressive loading has been well explored, human cervical spine compressive loading combined with lateral bending remains largely unexplored other than in computational studies (Eggers et al. 2005 and Hu et al. 2008). The influence of lateral bending on injury dynamics and tolerance has yet to be quantified in the human cervical spine.

In the vehicle rollover environment, several potential loading scenarios are feasible consisting of a laterally angled impact surface, a laterally angled posture or a combination thereof. Yamaguchi et al. (2005) have demonstrated the response of human surrogates during vehicle dynamics leading up to the initiation of vehicle trip prior to rollover. Results indicated that people on the near side of vehicle, or side that first approaches the ground in a rollover, tend to move their heads' away from the window opening against the lateral inertial loads of their heads' creating a laterally bent neck posture (~20 degrees) in the process (Figure 1.2). Since the

influence of these effects is unknown, the significance of lateral bending phenomena previously identified by automotive researchers has not been fully addressed.

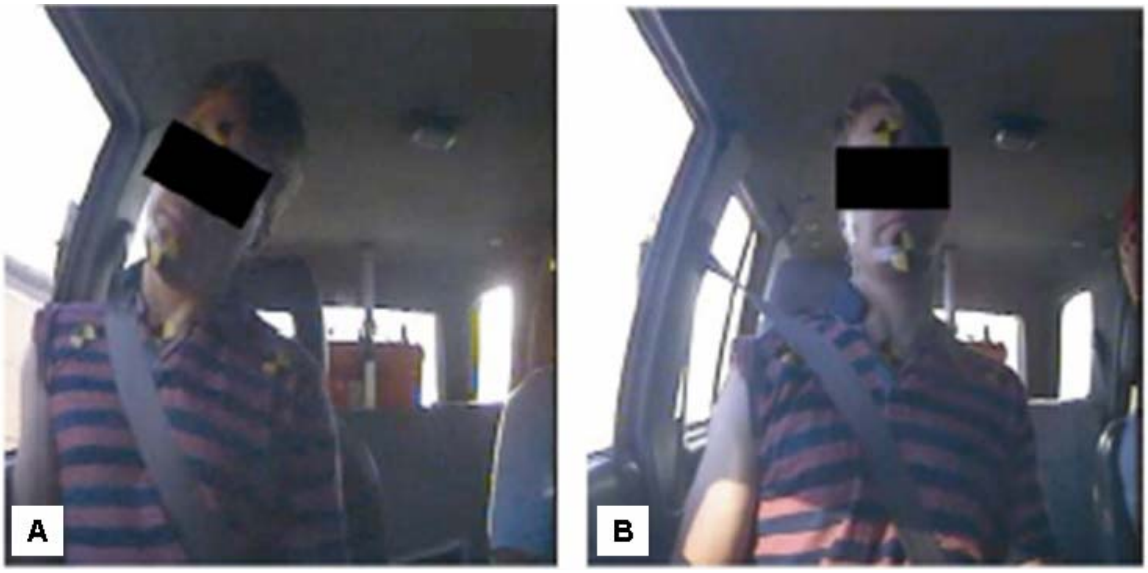

Figure 1.2: Human surrogate response during vehicle kinematics leading up to near-side (A) and far-side (B) rollovers from Yamaguchi et al. (2005)

Biomechanical investigations using post mortem human subjects (PMHS) have been an essential element in the current understanding of the complex dynamics of compressive cervical spine injury including cervical column buckling, injury timing with respect to head motion, and the effects of contact surface padding on neck injury risk (Nusholtz et al. 1983, Alem et al. 1984, Yoganandan et al. 1986, Pintar, Nightingale et al. 1996a, 1996b, Camacho et al. 2001). Compressive injury tolerance has historically been reported by identifying the peak axial force at injury measured at the base of the neck (Pintar et al. 1995 and Nightingale et al. 1997a). However, as an injury predictor, compressive force at failure exhibits variation and this has been attributed to the alignment of the cervical vertebra and the end conditions of test methodology used. Robust and sensitive injury metrics for human compressive cervical spine tolerance that can be applied to a wide range of initial test conditions and head-neck postures would be useful in evaluating and developing mechanically meaningful and robust anthropomorphic test devices

(ATDs) and their associated injury assessment reference values (IARVs). Previous PMHS studies that include the entire human head-neck complex and measure the dynamic forces and moments at the base of the neck include Pintar et al. (1995 and 1998a) and Nightingale et al. (1997a). By combining the available data sets from these previous studies with the data from the experiments conducted as part of this research, a more refined and statistically relevant tolerance was identified based on the underlying cervical spine mechanics.

Repeatable and reliable ATDs are important for assessing the risk of injury during various impact loading events in automotive, motor sports or athletic sports environments. The current neck compressive injury assessment reference value (IARV) for the midsized male was originally based on reconstructions of injurious football impacts using the Hybrid III ATD (Mertz et al. 1978). The normalized neck injury criteria, or Nij, takes into account neck axial load and sagittal plane bending moment and was initially introduced to address the risk of neck injury due to airbag deployment (Eppinger et al. 1999). The current compressive Nij intercepts have been set equal to that of the derived tension intercepts. The tension intercepts were formulated from matched airbag deployment testing on porcine subjects and the Hybrid 3-year-old ATD (Mertz et al.1982a, Mertz et al. 1982b, Prasad and Daniel, 1984). Porcine tests resulting in tension–extension cervical injury were correlated to the response of the Hybrid 3-year-old ATD and scaled up to the Hybrid III 50th male ATD. As the Hybrid III continues to be used in automotive rollover applications, the interpretation of measured neck loads and moments in the Hybrid III ATD neck during primarily compressive loading scenarios would be aided by a more complete understanding of the correlation between these mechanical responses and the risk of compressive injury in the human cervical spine.

Similar to the approaches taken by Mertz et al. (1978) for football impacts and by Mertz et al. (1982a and 1982b) and Prasad and Daniel (1984) for primarily tension-extension combined loading scenarios, further understanding about the relationship between the Hybrid III ATD neck response and the risk of injury to the human cervical spine during primarily

compressive loading scenarios can be evaluated by performing matched tests of PMHSs and the ATD. A matched data set was created by reconstructing the PMHS tests of Nightingale et al. (1997a) and those performed as part of the current study with the Hybrid III head and neck assembly. Using the matched data set, the injury predictability of ATD neck dynamics was evaluated and refined injury probability relationships identified for evaluating compressive loading scenarios.

1.3 Specific Aims

The specific aims of the study are to:

1. Investigate the effects of lateral bending on compressive cervical spine response and tolerance through the use of PMHS head-neck complex experimentation.

2. Identify more robust injury metrics for human compressive cervical spine tolerance that can be applied to a wider range of initial test conditions and initial cervical spine postures by combining the data collected in Aim 1 with data from prior studies.

3. Evaluate the Hybrid III ATD neck Injury Assessment Reference Values (IARVs) and new potential neck injury metrics under dynamic compressive loading conditions comparable to those of PMHS tests with known injury outcomes.

CHAPTER 2

CERVICAL SPINE ANATOMY, EPIDEMIOLOGY, INJURY CLASSIFICATION AND INJURY MECHANISM

2.1 – Bony and Ligamentous Anatomy

The cervical spine functions to connect the head to the torso and provide structure for controlled articulation of the head. It serves as a conduit for the spinal cord and the vertebral arteries, the major blood supply to the brain stem and posterior portions of the brain, and provides functional strength that protects the other soft tissue structures of the neck including the carotid arteries. The majority of this anatomical review is taken from McElhaney et al. (2002). Unless otherwise indicated, no explicit citing will be provided if the basis is taken from this reference.

The ligamentous cervical spine consists of seven vertebral bodies connected by intervertebral discs and connective ligaments that form a total of eight motion segments (see Figure 2.1). The vertebrae are often separated into two categories, the upper and lower cervical spine. The upper cervical spine extends from the atlanto-occipital joint at the base of the skull to the C2-C3 junction. The morphology of C1 (atlas) and C2 (axis) are differentiated from the remaining cervical vertebrae. The atlas (C1) is comprised of an anterior and a posterior arch which connect to form a ring. At the junction of these arches are the lateral masses which form superior facets that articulate with the occipital condyles of the skull. The odontoid process (or dens) of C2 and the spinal cord pass through this ring separated by the transverse ligament. Laterally, on each side of the ring, the transverse processes connect and form the transverse foramen for the vertebral arteries to pass through. The axis (C2) is made up of a vertebral body and laminae which connect to similarly form a foramen for the spinal cord. At the posterior connection of the laminae, a spinous process is present. Superior to the axis body, the odontoid process projects into the atlas. Superior and inferior facets are present laterally on the axis body

for articulation with the atlas and C3 respectively. Both upper cervical spine vertebrae have transverse processes, albeit significantly smaller than those of the lower cervical spine. Based on this structural makeup, no intervertebral discs are present between the occiput and the atlas or the atlas and the axis. This structure allows for a large range of motion of the head.

The lower cervical spine extends from the C2-C3 junction to the cervical spine connection with the thoracic spine at T1. Adjacent vertebral bodies are connected and articulate with each other through the intervertebral discs. The posterior elements of the vertebrae, including the laminae and pedicles, create the vertebral foramen through which the spinal cord passes. Lateral to each pedicle are the bony transverse process and posterior to the laminae is the spinous process. At each pedicle-lamina junction are the inferior and superior facets which serve as the articulating joints for the inferior and superior vertebrae respectively. The intervertebral discs are not discussed in detail because they do not contribute significantly to the structural stability of the cervical column. Additionally, in the absence of bony fracture, disc rupture has been shown to be a degenerative process that typically occurs over many loading cycles rather than a single impact event. Researchers have continually found that under compressive load, the vertebral body was always damaged prior to visible damage of the adjacent intervertebral disc (King, 2002).

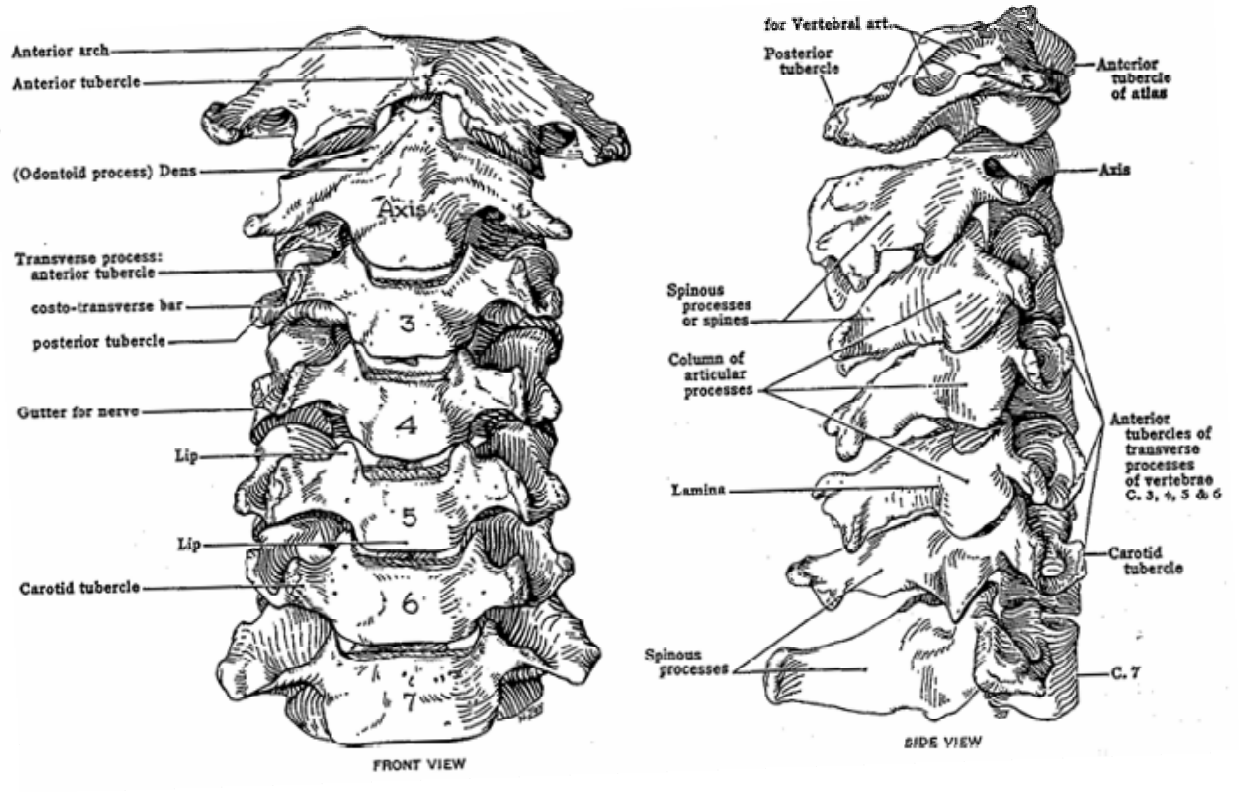

Figure 2.1: Anterior and lateral views of the bony cervical column (from McElhaney et al. 2002)

In addition to the bony joints, several ligaments are present and serve as connective tissue for the various vertebrae and base of the skull. The cruciate ligament consists of the transverse ligament of C1 and a vertical portion that connects the anterior inferior aspect of the foramen magnum of the skull to the C2 body. The apical ligament connects the C2 dens directly to the skull and the alar ligaments connect the lateral aspects of the dens to the base of the skull. The anterior and posterior longitudinal ligaments and the flaval ligaments attach directly to the base of the skull and descend to the lower cervical spine (see Figure 2.2).

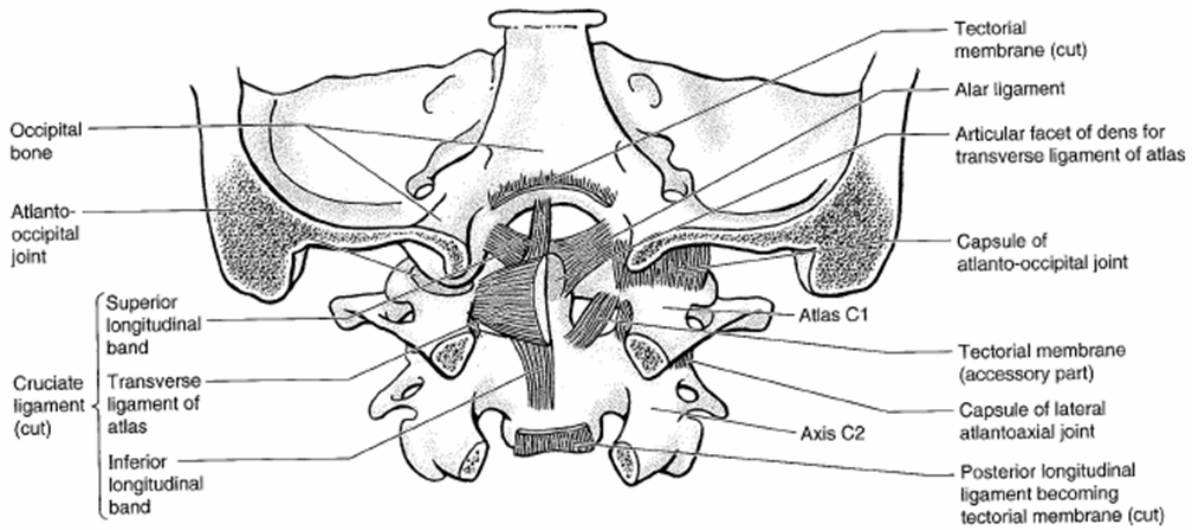

Figure 2.2: A posterior view of the upper cervical column ligaments (from Moore and Daley, 1999)

The anterior longitudinal ligament (ALL) connects the anterior surfaces of the vertebral bodies and the posterior longitudinal ligament (PLL) connects the posterior surfaces of the vertebral bodies. Additionally, the interspinous, supraspinous, and flaval ligaments connect adjacent vertebral spinous processes and laminae (see Figure 2.3).

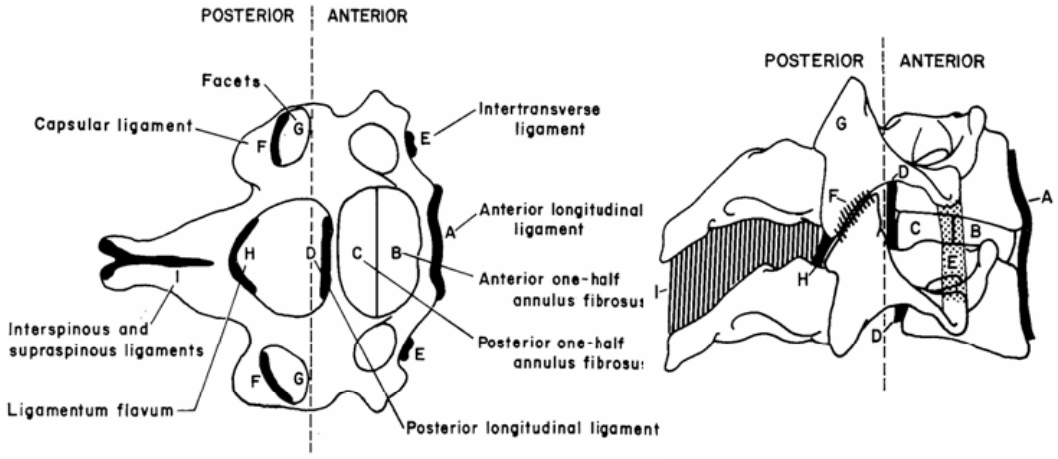

Figure 2.3: The ligaments of the cervical vertebrae (from White and Panjabi, 1990)

2.2 Cervical Spine Kinematics and Engineering Descriptions

In order to discuss the complex motion and loading scenarios of the human cervical spine, it is important that there be clarity in the definition of the various head and neck motions, orientations and engineering loading polarities. Additionally, clarity is vital for accurate description of injury classifications and mechanisms. Medically, flexion is defined as bending of a part or decreasing the angle between body parts while extension means the inverse (Moore and Agur, 2002). With respect to the head and cervical spine, flexion is defined as forward rotation of the head about the lateral axis of the head as the chin moves closer to the chest, while extension is rotation in the opposite direction. The medical definition of compression is synonymous with that of engineering; however, engineering tension is often referred to as distraction medically. Figure 2.4 taken from Portnoy et al. (1972) depicts the various orientations of the entire head-neck complex. Figure 2.5, also from Portnoy et al., outlines the various modes of applying loads to a cervical spine segment. Bending moments and shear forces can be applied in either the anterior-posterior direction or the lateral direction.

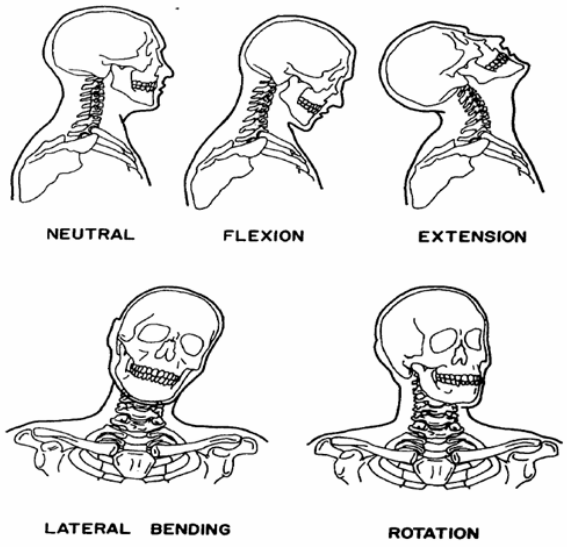

Figure 2.4: Descriptions of head / neck orientations (from Portnoy et al. 1972)

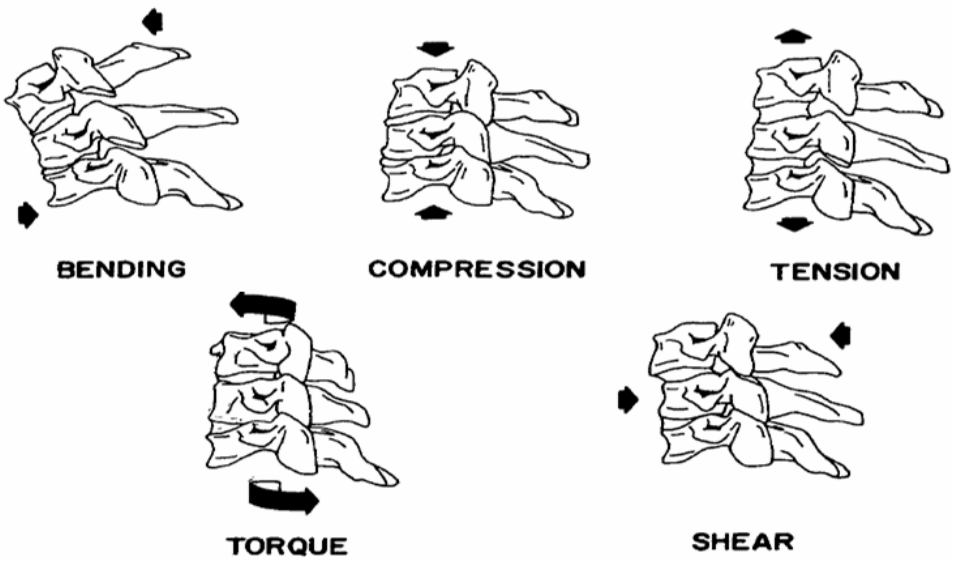

Figure 2.5: Descriptions of cervical loading modes (from Portnoy et al. 1972)

The Society of Automotive Engineers (SAE) defines the three orthogonal axis and their polarities with respect to the human body or anthropomorphic test device (SAE Surface Vehicle Recommended Practice J211-1). The X-axis is positive in the anterior direction, the Y-axis is positive in the rightward direction, and the Z-axis is positive in the inferior direction (Figure 2.6). The resulting positive local cervical forces and moments for each of the three axes, defined in SAE sign conventions, are anterior shear force and a rightward lateral bending oriented moment, rightward shear force and extension oriented moment, and tensile axial force and, when viewed from above, clockwise oriented axial rotation moment. Confirming proper polarity with a PMHS test specimen or ATD can be confusing. Recommended practices outline the following dummy manipulation polarity checks to confirm positive polarity; head rearward, head leftward, head upward, left ear to left shoulder, chin to sternum and chin to left shoulder. These manipulations are opposite of the respective neck reactive forces which are consistent with the orthogonal SAE axes.

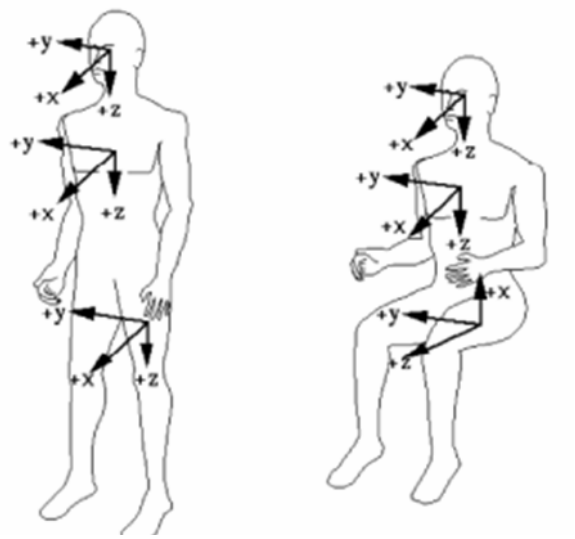

Figure 2.6: Standard SAE coordinate system and polarity (from SAE J211-1)

2.3 Injury Epidemiology

Approximately 12,000 spinal cord injuries occur each year in the United States, not including those who sustain fatal injuries at the scene. Fife and Kraus (1985) found approximately 42% of spinal cord injury were motor vehicle occupants and 68% of these lesions were in the cervical region. Since 2005, motor vehicle accidents have accounted for 42.1% of reported spinal cord injuries (NSCISC Apr 09). When considering cervical spinal cord injury only, McElhaney et al. (2002) reports that automobile accidents compromise the most frequent injury associated activity at 36.7% of reported cases. Most injury epidemiology studies are based on the Abbreviated Injury Scale (AIS). Miller (2001) has estimated medical costs alone for spinal cord injuries in vehicle accident survivors range from 330,000 dollars for AIS 3 injuries to over 1 million dollars for an AIS 5 injury on a per case basis.

Cervical spine injuries in the automobile collision environment can be separated into two categories, those caused by direct head contact and those without. Non-head contact neck injures are rare, but can be sustained by lap-shoulder belted occupants as reported by Huelke et al. (1978, 1992). Portnoy et al. (1972) reported on 55 cervical spine injuries in the automotive

crash environment caused by head contact, and categorized them by three frequent injury mechanisms including tension-extension, compression-flexion, and compression-extension. The authors note that these basic groups are further delineated by lateral bending and rotation. As the focus of the current research is cervical spine response and tolerance in compression and the effect of lateral bending, the focus will be on cervical spine injuries that occur with head contact.

Alker et al. (1975) reported on 146 fatal traffic accident victims and found that 21% had demonstrable neck injury most of which were localized to a single level at the cranio-cervical junction or the upper two cervical vertebrae. Similarly, Bucholz et al. (1979) looked at 100 fatal traffic accident victims and found incidence of cervical spine injury was 24% and all but 4 of the 24 fractures and/or dislocations were localized between the occiput and the axis. Yoganandan et al. (1989a) conducted a clinical study as well as an analysis of cervical spine injury in the automotive environment through analysis of data in the National Automotive Sampling System (NASS) database. They found that cervical injuries were more prevalent than thoracolumber injuries and that 20% of the AIS 3+ neck injuries involved the spinal cord, while 65% involved the vertebrae. McElhaney et al. (2002) reported that estimates of neurological injury in compression related cervical fractures ranges between 40% and 75% with an increased risk of neurological injury with increased fracture severity. Similar to the findings of Alker et al. and Bucholz et al., Yoganandan et al. (1989a) found that upper cervical spine injuries (occiput to C2) were predominant in fatal spinal injuries. In contrast, lower cervical spine injuries were more predominant in survivors, with the most common clinical fracture being flexion-compression related to and including vertebral body fractures and posterior element disruption. Other findings included a strong relationship between cranio-facial injury and serious cervical spine injury and that belted occupants were less frequently seriously injured. When the collision mode was taken into account, frontal collisions accounted for approximately 40% of the annual AIS 3+ cervical injuries, while rollovers accounted for only 25%. However, when the frequency of frontal

collisions and rollovers are taken into account, the rollover crash mode clearly had the highest incidence rate of AIS 3+ cervical injuries.

Hu et al. (2007a, 2007b) used the NASS Crashworthiness Data System (CDS) database to look at head, face and neck injuries specifically in rollover collisions. The frequency of AIS 3+ neck injury in rollover, based on weighted estimates, was found to be 0.4%. They found that occupant age, weight, and the number of quarter turns during the rollover event correlated with neck injury (predominately fracture related) and that seat belted occupants had a statistically significant reduced risk of injury. Additionally, the authors postulated that lateral deformation of vehicle structure may be more crucial than vertical deformation for prediction of head, face and neck injury in rollovers but noted that these correlations did not show causality.

2.4 Injury Classification and Mechanism

Cervical spine injury classification, particularly fractures and dislocations, has not historically had a uniform reporting method. Several classifications have been proposed (Roaf 1972, Babcock 1976, Allen 1982, Harris 1986, Myers and Winkelstein 1995, and Winkelstein and Myers (1997). Most early studies relied on a retrospective review of injured patient data. Roaf (1972) outlined this confusion, describing as an example that all cervical injuries in which the patient has facial or frontal injuries are depicted as “hyperextension” injuries regardless of the anatomical lesion created. He further commented on cervical injuries categorized as flexion injuries, stating that unless the cervical spine was pathologically stiff, hyperflexion could not occur without a broken mandible or manubrium sterni.

Hyperextension and flexion as referenced above by Roaf refer to global head-neck motions. One of primary confusing factors related to cervical injury classification is that head motion associated with both contact and non-contact cervical spine injury is often used to describe the cervical fractures and dislocations identified. Nightingale et al. (1996a) have clearly demonstrated that in compressive cervical loading modes caused by impact to head, cervical

injury occurs prior to any substantial movement of the head. As early as 1972, Roaf advocated for describing cervical injuries by the displacing forces at the local level. Similarly, Portnoy et al. discussed that classification of injuries should result from dynamic analysis of forces applied to the spine. This idea was formalized by White and Panjabi (1978) as the Major Injury Vector or MIV. The MIV is defined as the internal injury producing load at a particular level in the spine. Winkelstein and Myers (1997) described a classification system based on the applied forces with experimental validation. This mechanistic classification system is based on the force and the eccentricity at which it is applied for a given damaged cervical motion segment. This system can be found in Figure 2.7.

The current study is focused on primarily compressive cervical injuries with some contribution from combined lateral and anterior-posterior loading modes. Although rare, several cervical injuries have been previously associated with lateral bending dynamics in the literature. Roaf (1963) presented five cases of what he considered to be lateral flexion cervical spine injuries. There was often brachial plexus injury in addition to asymmetric separation between lower vertebrae (C5 to C7) but only one case included a compressive fracture. Babcock et al. (1976) opined that lateral forces can produce cervical injury but rarely occur as isolated injuries and are typically in combination with flexion or extension injuries. Allen et al. (1982) presented fives cases in which they classified as lateral flexion injuries. They are classified by an asymmetric compression fracture of the centrum plus vertebral arch fracture on the ipsilateral side. The authors went on to say that it is conceivable that compressive and distractive lateral flexion injuries may exist but that their case material is too limited to evaluate the probability. Harris et al. (1986) described lateral flexion as more commonly seen as modifying a primary vector force and presented an asymmetric fracture of the body of C2. The authors further describe an uncinate process fracture as the only discrete cervical fracture attributable to lateral flexion. When the scope is narrowed to include only compression driven cervical injuries,

asymmetric injury is the only injury class currently attributed to lateral bending in combined loading modes.

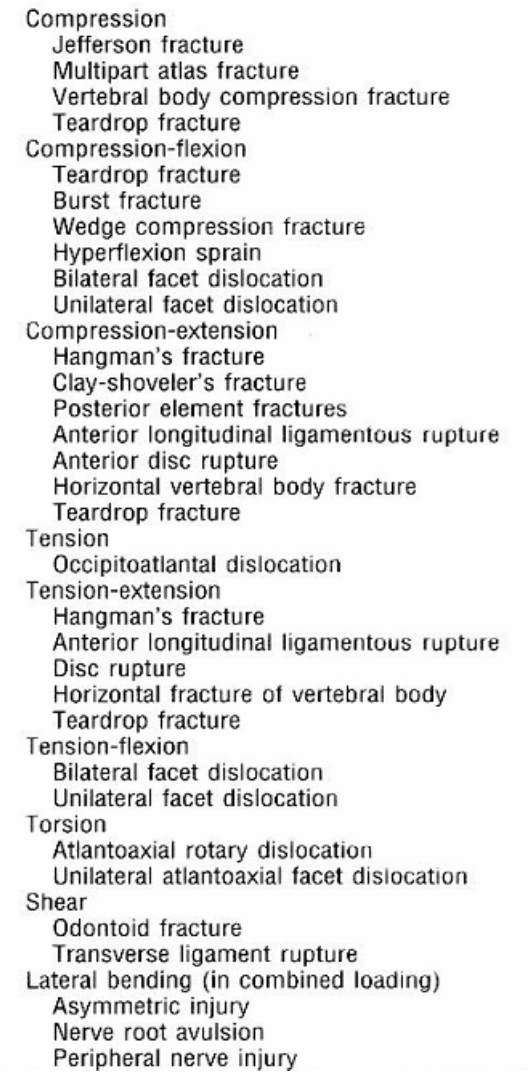

Figure 2.7: Cervical spine injury classification based on applied forces with experimental validation (from Winkelstein and Myers, 1997)

The mechanism of cervical injury at the local level can be caused by various head, neck and torso loading modes. During compressive loading events, the resultant force vector location (eccentricity) defines the local loading environment at each vertebral level based on the overall

geometry of the cervical spine. Additionally, buckling causes local geometry changes and adds local inertial loading which contributes the resultant loading at each level and often times produces several different classes of cervical spine injury at various vertebral levels for any single impact loading event. For the purposes of the current study, the actual applied loads will be described from an overall specimen stand point. Forces and moments will be measured globally at the impact point and at the base of the neck, not at each individual spinal segment; however, injuries will be classified by the forces at the local level required to create the observed damage.

CHAPTER 3

LITERATURE REVIEW – CERVICAL SPINE RESPONSE AND TOLERANCE IN COMPRESSIVE LOADING MODES AND CERVICAL INJURY CRITERIA

Published static and dynamic testing strategies using post mortem human subject cervical spine specimens can be grouped into three types based on the type of test specimen used: whole body cadaver, isolated head and neck and cervical spine motion segments. Human tissue, including bone and ligament, is viscoelastic or loading rate dependant (Mow and Hayes, 1997). McElhaney et al. (1983, 1988) has reported on these mechanical properties specifically for the ligamentous cervical spine. As rollover crashes are dynamic events, the focus of this literature review is on cervical spine dynamic response under realistic loading scenarios. Additionally, the various effects of the applied loading vector, head and neck constraint and initial head and neck orientation on compressive response and tolerance and the likelihood of sustaining a bony cervical injury are also of interest.

3.1 Whole Body PMHS Compressive Cervical Spine Experimentation

In order to load the cervical spine in non-trivial compression loading scenarios, compression of the spine is achieved when load is applied either through the head or the torso and resisted by the other. Hence, all meaningful compression loading events are head contact events and can be divided into superior to inferior impacts by an impactor on the apex of the head or inverted drop tests in which the cervical spine is loaded by the torso in an inferior to superior direction. The use of whole body human cadaveric specimens allows for direct evaluation of various loading scenarios but is limited in that only applied loads at the specimen head can be easily measured. Several historical whole body cadaver studies have provided some insight into the magnitude of applied loads that cause damage in the PMHS cervical spine

and the general effects of various initial head, neck and torso orientations. These studies are briefly reviewed in the section below.

3.1.1 Dynamic Whole Body PMHS Experimentation in Superior - Inferior Impacts

Eleven unembalmed PMHS were subjected to dynamic superior – inferior impact by Culver et al. in 1978. The cervical spine was aligned vertically with a 9.9 kg padded impactor's axis in order to maximize the load carrying capability of the cervical spine and increase the likelihood of basilar skull fracture. The authors reported that fractures began to occur at peak impact forces over 5.7 kN, impactor velocities over 7.5 m/s and initial impact energy values of 380 J. The authors also observed compressive arching of the spine that followed the normal lordotic curvature and appeared to depend on the initial alignment of the spine.

Hodgson and Thomas, 1980, applied static and dynamic loading to the heads of embalmed cadavers wearing helmets. Their results stated that the extent of head constraint imposed by the impactor's surface, the impact location, and the impact force alignment with the spine were the most influential factors on the site of fracture and the level of strain measured.

In 1981, Nusholtz et al. tested twelve unembalmed cadavers with a 56 kg impactor at impact speeds ranging form 4.6 to 5.6 m/s Each subject was instrumented to measure head, T8 and sternum accelerations. The orientation of the head, cervical spine and torso was adjusted relative to the impactor axis in order to investigate the initial orientation effect on damage patterns. The peak forces produced during impacts ranged from 1.8 to 11.1 kN. The authors concluded that the initial orientation of the spine was a critical factor influencing spine response and damage produced. They also found that descriptive head motion relative to the torso was not a good indicator of neck damage and finally, that the complex nature of spinal kinematics and damage may preclude the determination of a single tolerance criterion such as force.

Maiman et al. (1983) subjected three specimens, including the head, neck and intact torso, to compressive loading using a constant rate Materials Testing System (MTS) machine at

rates ranging from 1.12 to 1.42 m/s and measured the force applied by the MTS piston. The specimen torsos were oriented upright and supported under the arms with rigid yokes. Two specimens had their heads oriented horizontal with the Frankfort plane and one specimen head was extended 25 degrees. It is not clear what the head's translational orientation was with respect to the base of the neck or torso. Loading to the vertex of the head resulted in upper cervical spine posterior ligament disruption at loads of 1,868 and 2,936 N, respectively, and large piston displacements of 72 mm and 92 mm at failure. The pre-extended specimen sustained an avulsion fracture at C4 and anterior longitudinal ligament disruption at C5 and C6 at a load of 1,512 N and piston displacement of 36 mm. The authors emphasized the variety of injuries produced by specific force vector and the difficulty in retrospectively assigning forces given a specific lesion.

Alem et al. subjected 19 unembalmed cadavers to superior – inferior impact in 1984. A 10 kg impactor was utilized at impact speeds ranging from nominally 8 m/sec in five non-injurious tests up to 11 m/sec. Measurements taken were similar to those by Nusholtz et al. (1981) but Alem et al. measured the acceleration responses at T1, T6 and T12 instead of at T8 and the sternum. The authors found that impact force was not a reliable predictor of cervical injury, however, both the time integral of the impact force or impulse (impactor momentum) and the maximum head velocity correlated well with cervical spinal damage.

3.1.2 Dynamic Whole Body PMHS Inverted Drop Experimentation

Inverted drops of whole body PMHSs allows for easier control of head and neck initial positioning. Additionally, with regard to the automobile rollover environment and other types of diving injury scenarios, inverted drop testing of PMHS replicates the loading mode of the torso continuing to move towards the head after head motion is arrested. In 1983, Nusholtz et al. conducted inverted drop tests of eight whole body PMHSs. The purpose of the study was to investigate the effect of head and spinal configuration on damage patterns. Injurious and non-

injurious tests were conducted on either 6 mm or 25 mm of ensolite padding and divided into two series; the first which constrained the head in the mid-sagittal plane and the second which did not (included head, neck and torso lateral pre-positioning). Figure 3.1 depicts the experimental setup. Cervical damage was documented in tests with drop heights ranging from 0.9 to 1.8 m. The authors reported that when the initial positioning was not in the mid-sagittal plane, flexion type damages to the PMHS were observed in the cervical spine. A review of the damage summary provided by the authors indicates only one of the four tests not constrained in the mid-sagittal plane resulted in cervical fractures biased to one lateral side. The authors also noted that the acceleration response and mechanical impedance at T1 was strongly dependant on the initial position of the head, neck and thorax.

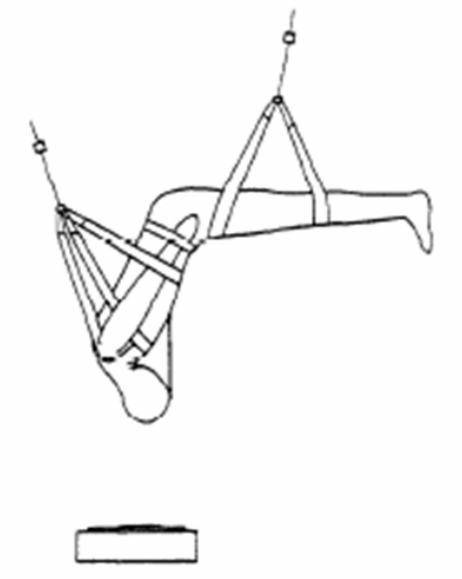

Figure 3.1: Schematic from Nusholtz et al. (1983) depicting setup of a sample test subject prior to release

Yoganandan et al. reported on a similar study of inverted PMHS drop tests in 1986. The tests were divided between constrained and unconstrained groups. In eight specimens, the skull was fixed to a halo ring and flexible steel cables were used to flex the head forward approximately 15 degrees. The cables were adjusted to maintain cervical compression in the 70

to 110 N range and released upon contact. This setup was intended to simulate muscle tone. In the other seven specimens, the head was unconstrained. In six specimens (three from each group), the mid-sagittal portion of either C5 or C6 was surgically removed and a single axis force gauge was inserted. Despite adding a 12 mm thick ensolite pad to the steel impact surface in 6 of the 8 constrained tests, the peak forces on the head ranged from 10 to 14 kN (three skull fractures) versus 3 to 7 kN (one skull fracture) for the unconstrained tests with drop heights ranging between 0.9 and 1.5 m. During the unconstrained tests, the contact point was at or posterior to the vertex of the head, the head slid forward (flexion) and ultimately the chin made contact with the chest. Secondary contact with the load plate was made by the lower cervical / upper thoracic region. Cervical injuries were documented in 3 of the 7 tests. In the constrained test, contact was at the vertex of the head in all but one test and cervical injury was identified more frequently, 6 out of 8 tests. It was also observed that cervical vertebral body damage was observed most commonly when the PMHS remained in contact with the load surface without substantial rotation or rebound.

3.2 Head-Neck Complex Compressive Cervical Spine Experimentation

Isolated cervical PMHS testing has taken many forms and been conducted in various manners. PMHS head – neck complex (specimen includes head, cervical spine, and upper thoracic vertebrae) experimentation has been used extensively to understand cervical spine compressive kinematics and kinetics and serves as the primary method in which cervical tolerance has been investigated since loads can be measured directly at the base of the neck. Similar to whole body cadaver tests, head – neck complex experimentation has been conducted by impacting the apex of the head in a superior to inferior direction or by conducting inverted drops in which an effective torso mass was added to load the cervical spine.

3.2.1 Dynamic Head-Neck Complex Experimentation in Superior to Inferior Impacts

Sances et al. (1981) conducted an extensive study on monkey and human cadaveric cervical spine tensile response and tolerance. For comparative purposes, two isolated fresh human cadaveric cervical columns were mounted at T1 / T2 and the skull and tested in compression. A MTS machine was used to apply a constant rate compressive displacement of 1.2 to 1.3 m/s at the skull. A 4.50 kN load was applied to the first specimen and resulted in a C5 burst fracture and anterior subluxation of C5 on to C6. The second specimen was applied a load of 4.41 kN which resulted in C5 vertebral fractures without subluxation. No other detail of specimen initial orientation was given. In addition to the three specimens with intact torsos tested by Maiman et al. (1983), ten isolated specimens were also evaluated and reported on by the authors. Two of the isolated specimens appear to be the same specimens reported by Sances et al. in 1981. Similar to the whole body cadaver testing, detail regarding initial orientation of the isolated specimens was lacking other than the initial skull orientation with respect to the Frankfort plane. The overall average failure load reported for “axial” tests in which the head angle was neutral, including whole body and isolated specimens, was 3,567 +/- 2,069 N. However, when only specimens including the atlanto-occipital joint are considered and “slow rate” studies are excluded, the mean failure load for this head orientation is approximately 3,205 +/- 1,203 N and mean piston displacement at failure was 62 +/- 25 mm.

Similar to the methodology employed by Sances et al. and Maiman et al., Pintar et al. (1990) and Yoganandan et al. (1991) used an electro-hydraulic actuator to impact the vertex of the skull of ligamentous head – neck complexes, axially loading the cervical spine and creating clinically relevant damage. In addition to a better description of the methodology, including initial specimen orientation, these studies included measurement of the resulting distal load measured at the base of the neck. Peak axial loads and displacements for a total of nine unique specimens at loading rates ranging from 2.95 to 8.5 m/s were reported. The head-neck complexes were pre-flexed prior to loading in order to align the vertebral column. Head position

was maintained with simulated muscle tension through a system of pulleys, dead weights and spring tension. The pre-test anterior weights and posterior spring tension were approximately 40 to 70 N and the posterior spring tension never exceeded 250 N during the loading event. Figure 3.2 depicts the experimental setup. A comparison of the skull impact force time history and the lower neck distal force suggested a decoupling between the head and spinal column. Additionally, the inertia of the specimens' heads continued to load the spinal column after the actuator piston began to rebound. Fractures were documented to occur in the first 2.5 to 6 milliseconds (ms) after initial contact.

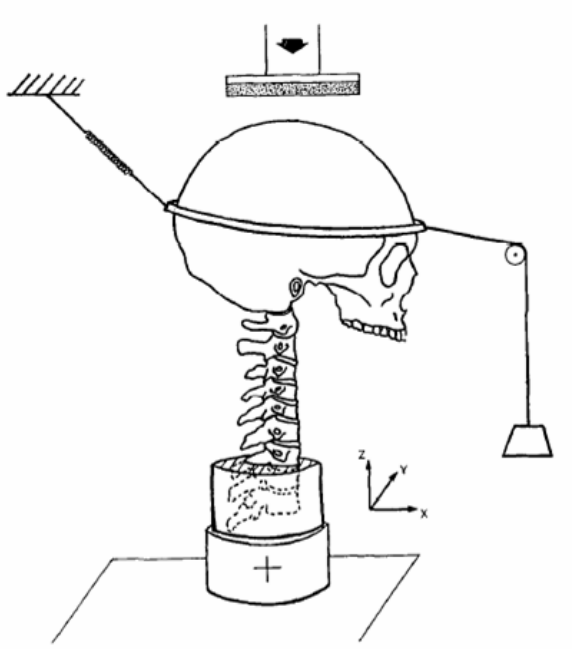

Figure 3.2: Schematic from Pintar et al. (1990) depicting sample specimen test setup and orientation

In a subsequent study, Pintar et al. (1995) reported cervical failure loads and displacements for 20 specimens tested using the same methodology. Pre-alignment of the specimen was documented in detail. The occipital condyles' initial location ranged from 25 mm anterior to 5 mm posterior of the center of T1. Additionally, a force displacement response corridor was presented based on the distal neck load and the actuator displacement. Failure

loads ranged from 744 to 6,431 N with a mean of 3,326 N. Specimen donors ages ranged from 29 to 95 years of age with a mean of 62 years. The average displacement at failure was reported as 18 +/- 3 mm. Figure 3.3 is the force displacement corridor derived by Pintar et al. The dashed line represents the mean response curve based on the mean force and deformation at failure and the mean stiffness.

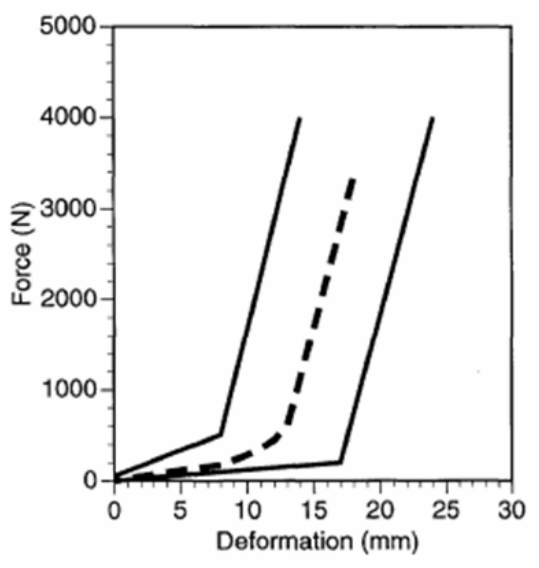

Figure 3.3: Derived human neck dynamic force-deflection corridor from Pintar et al. (1995)

In follow up study, Pintar et al. (1998a) used the same test methodology described above but investigated cervical injury patterns and tolerance with increased forward pre-flexion of the cervical spine resulting in increased anterior head eccentricity. A total of ten additional PMHS were tested and analyzed with three of the previous experiments (Pintar et al. 1995) that included anterior head pre-positioning. The authors used logistic regression techniques and reported the 25% probability of major neck injury occurred at 1,850 N of axial force and 62 Nm of forward bending moment.

3.2.2 Head-Neck Complex Inverted Drop Experimentation

A series of publications by Nightingale et al. (1996a, 1996b, 1997a and 1997b) utilized a different methodology to investigate cervical spine compressive kinematics and mechanical response. Similar to the research by Pintar, ligamentous head-neck complexes were utilized and head contact and lower neck loads were measured, but the specimens were inverted and dropped head first onto various orientation and material contact surfaces. The distinct advantage of this methodology is the ability to investigate the effect of variable head constraints on the probability of cervical damage and the relative ease in which the resting lordosis of the cervical spine can be maintained. Another fundamental advantage is that the cervical spine response is driven by contact surface and specimen characteristics and not influenced by the prescribed displacement of a constant velocity electro-hydraulic actuator.

The Nightingale methodology utilized a linear drop track apparatus that constrained the base of the neck to vertical translation while the head remained unconstrained. The effective torso mass was determined using Generator of Body Data (GEBOD) software to be 16 kg., the fraction of a 50^{th} percentile male torso mass acting on the neck during dynamic injury. The nominal drop height chosen was 0.5 m resulting in impact speeds of approximately 3.1 m/s. The drop height was chosen based on swimming pool diving accident reconstructions performed by McElhaney et al. in 1979 and along with the effective torso mass, proved to be sufficient to achieve cervical fracture in the inverted head-neck complex drop tests. Figure 3.4 outlines the Nightingale experimental setup.

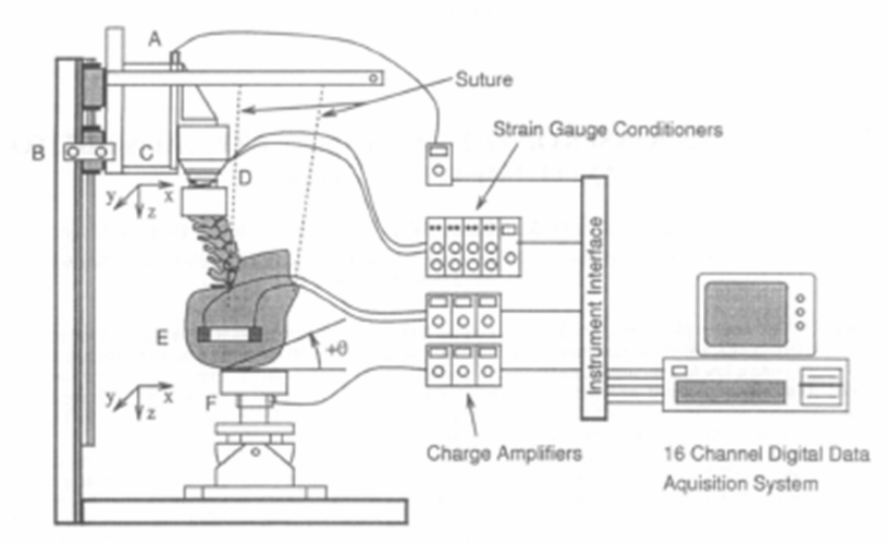

Figure 3.4: Diagram from Nightingale et al. (1996b) depicting the test setup and specimen orientation. The impact surface (F) material and angle in the sagittal plane was varied

Numerous findings were reported based on the 21 specimens tested by Nightingale et al. (1996b and 1997a). Cervical damage was documented to occur early in the impact event, generally within the first 10 or 20 ms for rigid and padded impact surfaces respectively. This was prior to an appreciable translation or rotation of the head quantitatively confirming what many previous studies had inferred, that head motion was not indicative of compressive spinal injury. Similar to the finding of Pintar et al. (1990), the dynamic response of the head and spine indicated that the two are decoupled. During head impacts with rigid surfaces, the contact force on the head was documented to be bimodal in nature, an initial pulse that corresponded with arresting the motion of the head and a subsequent pulse corresponding with arresting the motion of the torso mass. The onset of load measured at the neck lagged that at the head and head rebound contributed significantly to measured neck loads. Several sagittal plane impact surface orientations were investigated. Head inertia provided enough constraint in rigid vertex impacts to result in cervical fracture. The frequency and severity of documented cervical fracture was greater for vertex and anterior impacts and decreased for posterior impacts. Posterior impacts resulted in the least amount of measured neck impulse or torso momentum managed

by the neck, indicating that the head was able to escape the following torso to some extent. The addition of padding to impact surfaces increased head constraint thereby increasing the frequency of documented fracture. The mean resultant neck failure load for male specimens was 2,243 +/- 572 N with a mean age of 61.8 +/- 11.9 years. Head and neck force responses were provided for each specimen (Nightingale et al. 1997a).

3.3 PMHS Cervical Segment Level Experimentation

Functional spinal units or segment level testing has also been conducted giving insight into cervical tolerance at the local vertebral level and differences between various regions of the cervical spine. However, it neglects complex spinal buckling kinematics and physiologic loading vectors. Since the current study is motivated by ATD neck loading in rollover scenarios and lateral bending effects on entire cervical column, only a brief review relevant finding will be conducted.

Panjabi et al. (1991) impacted 13 upper cervical spine segments (occiput – C3) with a variable magnitude falling mass from 1.0 meter height (4.4 m/s impact speed). The tests were split into two groups, one in which the orientation of the segment was maintained in a neutral position, the second in which a 30 degree wedge was placed between the impactor and the specimen to force an extended orientation. Of the 13 tests, 10 sustained injury. Average axial failure loads and overall axial impulse were reported to be 3050 +/- 437 N and 34.9 +/- 8.3 Ns for the eight specimens in a neutral position and 2100 +/- 282 N and 17.6 +/- 1.8 Ns for the two specimens in an extended position. It should be noted that the authors indicated the failure loads were computed as the maximum compressive load.

Qingan et al. (1999) impacted C2-C4 segments with a 3.3 kg mass at high impact velocities. The 14 specimens were split into two groups. Impact energy was specified for the two groups, the first group at 30 J and the second at 50 J. No injuries were documented in the lower impact energy group and every specimen was damaged in the higher energy group. Damage

ranged from vertical and wedge fractures to burst fractures. The average peak compressive force for the non-damaged group was 4.11 +/- 0.11 kN and the damaged group was 4.89 +/- 0.38 kN.

Carter et al. (2002) tested 24 lower cervical spine segments using an MTS machine with a loading rate of approximately 1 m/s. The specimens were split into three groups and loaded in compression-flexion, compression-extension or pure compression loading environments. They reported average axial failure loads and sagittal plane moments of 765.5 +/- 240 N and 21.4 +/- 6.9 Nm for the compression-flexion group, 3472 +/- 684.4 N and -47.8 +/- 13.6 Nm for the compression-extension group and 3260.9 +/- 707.7 N and -15.0 +/- 5.7 Nm for the pure compression group.

Nightingale et al. (2002) tested 52 cervical spine segments from 16 female spines in a test fixture that was designed to load segments in pure sagittal plane bending. The average donor age was 50.8 +/- 8.8 years. The segments were divided into four groups, O-C2, C3-C4, C5-C6 and C7-T1 and loaded until failure. Loading rates were dependant on specimen flexibility but were near 90 Nm/s. Upper cervical spine failure moments were 23.66 +/- 3.42 Nm and 43.30 +/- 9.26 Nm in flexion and extension respectively. Lower cervical spine failure moments were 17.41 +/- 6.22 Nm and 21.22 +/- 7.61 Nm in flexion and extension respectively. This was followed up by a similar study by Nightingale et al. (2007) on 41 cervical segments from 16 male cervical spines. The average donor age was 66 +/- 7.2 years. In this study, the segments were divided into three groups, O-C2, C4-C5 and C6-C7. The authors reported failure moments for the upper cervical spine of 39.0 +/- 6.3 Nm and 49.5 +/- 17.5 Nm in flexion and extension respectively. The overall average failure moments for the lower cervical spinal segments were 20.2 +/- 5.3 Nm and 17.1 +/- 4.5 Nm in flexion and extension respectively.

Ching et al. (2004) evaluated the lateral bending tolerance of 27 lower cervical spinal segments from 9 cadaver cervical spines (6 male and 3 female). The average donor age was 65.0 +/- 4.2 years. The segments were split into three regions, C3-C4, C5-6, and C7-T1 and

tested at an average angular displacement rate of 10.8 +/- 2.9 Nm/rad. An overall average failure moment of 26.3 +/- 5.5 Nm was reported. A statistical difference was reported for the tolerance of the C3-C4 segments (23.6 +/- 5.3 Nm) versus the C7-T1 segments (30.9 +/- 5.3 Nm).

3.4 Role of End Conditions, Applied Load Eccentricity and Musculature, Age and Gender on Cervical Spine Tolerance and Response in Compressive Loading Modes

3.4.1 Effects of End Conditions / Constraint on Cervical Spine Compressive Response

Yoganandan et al. (1986) devised one of the first studies that directly evaluated the influence of head constraint and initial head / neck orientation on cervical spine response. As discussed previously, half of the drop tested specimens' skulls were fixed to a halo ring and flexible steel cables were used to flex the head forward approximately 15 degrees simulating the muscle tone necessary to maintain this pre-flexed orientation. The cables were adjusted to maintain cervical compression in the 70-110 N range and released upon contact. This pre-flexed, constrained orientation resulted in much larger impact forces on the head and an increased frequency of documented cervical damage.

McElhaney et al. (1988) reported on the change in cervical spine mechanical response, specifically bending stiffness, due to either pinned-pinned or fixed-pinned end conditions. The influence of end condition was evident across the test battery including relaxation, cyclic, and constant velocity tests. A small number of failure tests were also conducted and the axial load at failure was an order of magnitude larger for the fixed-pinned condition versus the pinned-pinned condition. Myers et al. (1991a) has demonstrated that changes in end conditions of the cervical spine during dynamic loading produces significant changes in axial stiffness and the type of injury produced in specimens that included the base of skull to T1. Axial displacement imposed on a fully constrained cervical spine resulted in wedge and compression fractures at an average

load of 4,810 +/- 1,286 N. Axial displacements applied to rotationally constrained specimens resulted in bilateral facet dislocations at an average load of 1,720 +/- 1,234 N and no injury was documented in the unconstrained specimens. The authors suggested that risk of cervical injury may be strongly dependant on the degree of head constraint imposed by the contact surface. This was confirmed by the studies of Nightingale et al. in which padded impact surfaces resulted in a higher frequency of cervical injury than rigid surfaces.

Through the use of computer modeling, Camacho et al. (1999) demonstrated that it was increased friction between the head and contact surface, not necessarily the padding, which increased the head constraint resulting in increased resultant neck forces and moments in the Nightingale tests. Similarly, Eggers et al. (2005) found that increases friction also increased the risk of compressive injury to the neck during apex head impacts with laterally inclined contact surfaces. Eggers et al. (2005) also predicted higher loads in the vertebral facet joints than the intervertebral discs and an increased risk of injury for the upper cervical spine versus the lower cervical spine from these simulations. Subsequently, Hu et al. (2008) reported that for impact surface coefficients of friction greater than zero, lateral impact surface orientations less than 30 degrees increased the average maximum principal strain in the vertebrae.

3.4.2 Effects of Loading Vector Eccentricity on Cervical Spine Response

The direction, magnitude and point of application of external load to either the apex of head or base of the neck are critical in determining whether compressive cervical spine injury is likely to occur. The more obliquely a load is applied with respect to the axis of the cervical column, the more likely that the head or torso will translate perpendicular to the cervical column and the applied load will not be resisted through the neck. The closer the applied load is to being parallel with spine, the greater the chance of compressive injury. This principle is demonstrated by results of tests presented by Nightingale et al. (1997a). The flat impact surface (0 degrees) and the 15 degree anteriorly biased impact surface (+15 degrees) are nearest to

perpendicular to a cervical column that has its resting lordosis maintained. Impacts with these surface orientations resulted in the highest frequency of unstable cervical injuries.

When considering near parallel loads, the distance from the center of the vertebral column that the load is applied, or magnitude of eccentricity, has been demonstrated to influence the type of cervical damage and the magnitude of axial force necessary to create it. Eccentricity has long been considered important in whole cervical spine kinematics and injury outcomes but it has rarely been quantified. When discussing the cervical spine, magnitudes of eccentricity are typically referenced to the center of either the vertebral body or the inferior vertebral disc at the point of load measurement and can be assumed as such unless indicated otherwise. McElhaney et al. 1983 found that small changes in eccentricity (+/- 10 mm) in the load axis could change the buckling mode and fractures produced. The results of Myers et al. (1991a) demonstrated increased failure loads in fully constrained cervical columns (~30 mm eccentricity) versus those that were only rotationally constrained and able to translate anteriorly (~60 mm eccentricity). Finally, Carter et al. (2002) reported on anterior – posterior eccentricity effects on cervical spine segment level tolerance using an MTS machine with a loading rate of approximately 1 m/s. They found that applying the compressive load with 10 mm of anterior eccentricity reduced the average axial compressive tolerance of the specimens tested to approximately 765 N versus approximately 3,260 N for segments loaded through the center of the vertebral disc.

Initial cervical column eccentricity has been quantified in the full head-neck complex tests and correlated with injury severity and mechanism by Maiman et al. (2002). The test methodology employed was that of Pintar et al. (1990, 1995) discussed previously in which the head was pre-flexed approximately 15 degrees to align the cervical column and load was applied by an MTS machine. Various eccentricities were achieved by translating the head anterior or posterior versus the center of T1 vertebral body and influenced the resulting injury produced and mechanism of injury. Winkelstein and Myers (1997) summarized the influence of

anterior eccentricity of the resultant force acting at the site of injury on the type of clinically recognized injuries that have been replicated in the laboratory (Figure 3.5).

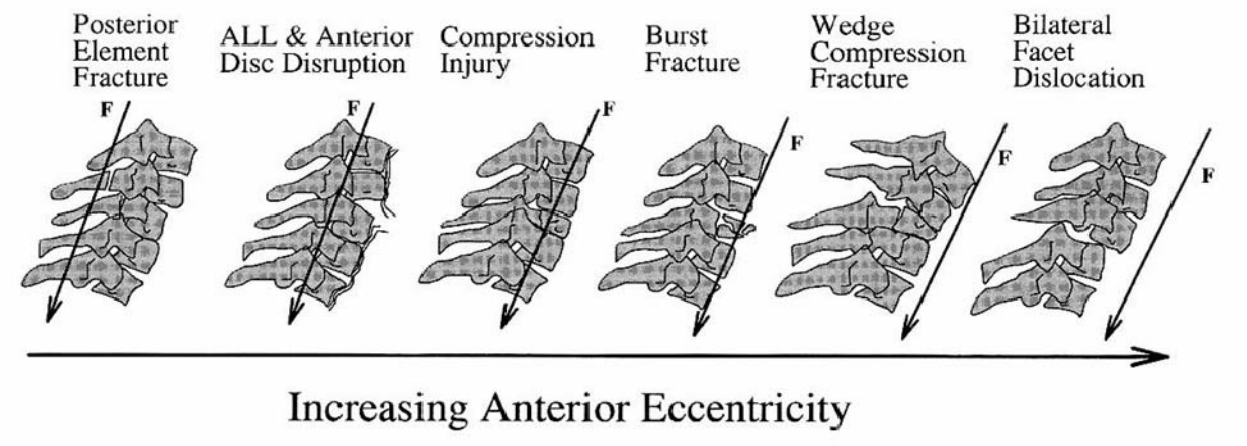

Figure 3.5: Influence of applied force eccentricity on the mechanism of cervical injury (from Winkelstein and Myers, 1997)

Fracture loads for the cervical spine in full head-neck complex tests have varied dependant on the cervical column orientation and resulting column eccentricity used during testing. Pintar et al. 1995 pre-flexed the PMHS head about 15 degrees prior to testing in order to align the cervical column. In this orientation, mean axial failure loads were 3,326 N for all specimens, including men and women. In a subsequent study, Pintar et al. (1998b) reported that the 50% probability of failure for a 50 years old man at a 4.5 m/s loading rate was 3.9 kN. Conversely, Nightingale et al. (1997a) maintained the natural lordosis resulting in greater eccentricity of the column prior to impact and found an average axial failure load of 2,243 +/- 572 N for male specimens.

3.4.3 Effects of Musculature, Age and Gender in Cervical Spine Compressive Response

A limitation of using the PMHS model as a surrogate for live humans is that muscle tone in cadaver specimens is absent. Active muscle response has been documented to occur at 50 to 65 ms following head loading (Foust et al 1973, Schneider et al. 1975). Since the occurrence

of injuries in the past studies have been identified to occur 2.5 to 20 ms following head contact (Pintar et al. 1990, Yoganandan et al. 1991, Nightingale et al. 1997a), the influence of cervical muscle reaction would be absent at the time of injury. Passive muscle response has not been well characterized. Muscle activations largest role in compressive cervical spine injuries appears to be its influence on pre-impact head and neck orientation and according to McElhaney (2002), may have a limited effect on flexural rigidity and buckling pattern. Passive cervical spine muscle response has been shown to only slightly increase compressive cervical spine injury risk in finite element modeling (Hu et al. 2008).

In 1971, McElhaney and Roberts found a correlation between test specimen age and vertebral cancellous bone ultimate strength in compression. The ultimate strength for specimens in their third decade was 70% greater than those in their sixth decade at the time of death. The effect of age on the difference in cortical bone ultimate strength for similar age groups has been reported to be closer to 10% (Keaveny and Hayes 1993). Riggs et al. (1981) studied the patterns of bone loss in osteoporotic and non-o osteoporotic men and women in the lumbar spine which is primarily trabecular (cancellous) bone. The authors reported unique linear relationships between bone mineral density and age for non- osteoporotic men and women. Women with osteoporosis and one ore more vertebral compression fractures had significantly lower bone mineral density on average than non- osteoporotic women of a similar age. Nuckley and Ching (2005) have reported a linear relationship between vertebral bone mineral density and yield strength.

Pintar et al. (1998b) similarly reported that the cervical spine failure force for loading rates between 2 and 4 m/s decreases with age. They analyzed 25 head-neck complex specimens tested to failure using the methodology previously described in Section 3.2.1. Regression analysis shows that comparing the failure force for specimens aged in their third decade was approximately 20% and 40% greater than specimens aged in their sixth decade at loading rates of 2 m/s and 4 m/s respectively. This is similar to the estimated scaling factor of

1.2 to 1.3 reported by Nightingale et al. (1997a) when attempting to derive a tolerance for the younger population from his data set composed of older specimens. The same Pintar et al. and Nightingale et al. studies reported decreased fracture tolerance for female specimens versus male specimens. Pintar et al. reported that male specimens were consistently 600 N stronger when comparing between similar aged specimens and similar experimental loading rates. Nightingale et al. reported a tolerance of 1,061 +/- 273 N for female specimens (mean age 58.3 +/- 14.1) and a tolerance of 2,243 +/- 573 N for male specimens (mean age 61.8 +/- 11.9 years).

3.4.4 Summary of PMHS Whole Cervical Spine Tolerance

Several different metrics can be defined to characterize human cervical spine tolerance to compressive injury. McElhaney et al. (1979) reconstructed swimming pool diving accidents resulting in cervical injury and determined head impact speeds of 3.11 m/s, approximately 0.5 m equivalent drop height, with a free following torso resulted in flexion-compression injuries. Subsequently, Nusholtz et al. (1983) and Yoganandan et al. (1986) documented cervical injury in the PMHS during inverted drop tests at heights ranging from 0.9 to 1.8 m. Viano and Parenteau (2008) analyzed the 33 PMHS inverted drop tests of Nusholtz et al. (1983) and Yoganandan et al. (1986) and 42 linear impactor or pendulum tests of Culver et al. (1978), Nusholtz et al. (1981) and Alem et al. (1984). Peak head velocity was used as a means to merge the data sets. A peak head velocity of 4.2 m/s corresponded to a 50% risk of serious injury.

3.4.4.1 Neck Compressive Force and Moment Tolerance

Existing cervical spine compressive force tolerance is largely influenced by experimental technique. When limiting the scope of studies to specimens that include the subject head and entire cervical spine and directly measure neck forces, average compressive failure forces range between approximately 2 and 4 kN (Pintar et al. 1995 and 1998a, Nightingale et al.

1997a). Nightingale et al. (1997a) averaged their reported failure loads with those of Pintar et al. and using a scale factor of 1.2 to 1.3 suggested a cervical tolerance for the young male of 3.64 to 3.94 kN. Pintar et al. (1995) also reported an axial displacement tolerance for injury in the aligned cervical column of 18 +/- 3 mm. Neck shear forces and moments have not been correlated with injury in these compressive loading scenarios.

Flexion and extension moment tolerance for the human cervical spine was originally based on volunteer and cadaver data of Mertz and Patrick (1971). During their experimentation, no flexion injuries were documented in cadaver studies so a flexion limit of 190 Nm was set based on the maximum measured moment that was sustained by a test subject. An extension moment limit of 57 Nm was derived for the 50^{th} percentile male from ligamentous damage in a small cadaver. Later, Cheng et al. (1982) reported on cervical flexion injuries in PMHS frontal sled tests in which the subjects' chest was decelerated by a pre-deployed airbag. Four of six specimens sustained cervical damage. The average peak flexion moment was 289 +/- 77 Nm and occurred simultaneously with significant tensile and shear forces.

Lateral bending has primarily been investigated in lateral sled test scenarios that do not include head contact. Wismans and Spenny (1983) subjected volunteers to 5 to 10 g lateral deceleration in sled tests and reported no injuries during exposure to lateral bending moments ranging from 20 to 60 Nm. Several researchers used PMHSs to investigate neck injury in lateral impacts (Kallieris and Schmidt 1990, McIntosh et al. 2007, and Yoganandan et al. 2009). This loading method typically results in complex three dimensional loading that is dominated by the tensile response at C0-C1. McIntosh et al. reported that peak lateral bending moment and / or lateral shear force did not have the greatest correlation with injury outcomes. In impacts with a change of velocity ranging from 8.7 to 17.9 m/s and utilizing various restraint configurations, Yoganandan reported average peak lateral neck moments ranging between 17.4 and 61.5 Nm, similar to the peak values reported by Wismans and Spenny, and documented various cervical injuries ranging in severity from AIS 1 through 3.

The torsion tolerance of the cervical spine was investigated by Myers et al. (1989, 1991b). Using six whole ligamentous cervical spines (Occiput – T1) and a loading rate of 500 deg/s, an average failure load of 17.2 +/- 5.1 Nm was reported. In each case, failure was documented to occur at the atlantoaxial joint. The specimens were subsequently recast at the axis and loaded until failure was documented in the lower cervical spine. The average load to failure for the lower cervical spine was reported as 21.0 +/- 5.4 Nm. By extrapolating torsion stiffness data reported by Wismans and Spenny (1983), McElhaney et al. (2002) estimates a human torsional tolerance of 28 Nm including muscular effects.

3.4.4.2 Neck Injury Metrics

Several neck injury metrics that combine measured neck responses have been proposed as human cervical spine injury criteria. The focus of this review will be on easily measurable quantities such as force, moment and acceleration. The use of relative displacements has been proposed by some researchers as a cervical tolerance metric, however, in practice this typically requires film analysis and is subject to greater error. Several injury metrics are simple linear combinations of force and moment which is consistent with basic mechanics and practical in calculation and an interpretation of results. The most utilized example is the normalized neck injury criterion, Nij. It is a linear combination of the Hybrid III ATD upper neck axial force and sagittal plane bending moment, details of which follow in section 3.5.1.

The beam criterion (BC) was proposed by Bass et al. (2006) for the lower human cervical spine in frontal collisions that do not include head contact. BC is the linear combination of the axial force and anterior-posterior moment measured at the center of the C7-T1 intervertebral disc and takes the form:

(Equation 3.1) $$BC = \frac{Fz}{Fzc} + \frac{My}{Myc}$$

The derived constants Fzc and Myc are 5,660 N, 5,430 N and 141 Nm in tension, compression and flexion respectively. A BC of 1.0 corresponded to a 50% risk of AIS 2 or greater human cervical spine injury. The neck anterior-posterior shear force was also considered in the BC but did not improve the predictive nature of the logistic regression curves.

A second neck injury metric applied the human cervical spine that uses a combination of measured neck responses is the neck injury index (NII) (ISO 1323-5:2005(E)). The NII was developed for the motorcycle ATD (MATD) upper neck and is based on the generalized stress ratio for the estimation of strength of materials and takes the form:

(Equation 3.2)

$$NII = \max\left(\left(\left(\frac{Fc}{Fcc}+\frac{F_T}{F_Tc}+\left(\left(\frac{Mx}{Mxc}\right)^2+\left(\frac{M_{Ext}}{M_{EC}}+\frac{M_{Flex}}{M_{FC}}\right)^2\right)^{1/2}\right)^2+\left(\frac{M_Z}{M_{ZC}}\right)^2\right)^{1/2}, 3.1\left(\frac{Fc}{Fcc}+\frac{F_T}{F_{TC}}\right)\right)$$

F_C and F_T are the measured compressive and tensile forces and M_{Flex}, M_{Ext}, M_X, and M_Z are the measured flexion, extension, lateral bending and torsion moments respectively. The respective force and moment constants are -6,530 N, 3,340 N, 204.2 Nm, -58 Nm, 62.66 Nm and 47.1 Nm. These constants and the probability of various AIS level neck injuries were derived by minimizing the difference between distributions of observed injuries in epidemiologic field databases and predicted injuries from computer simulations. The constant 3.1 found in the second term of Equation (3.2) was derived based on the 3% probability of an AIS 3 or greater injury when subjected to a 4.17 kN tensile force (Wilber 1998). Although the above metric was derived based on MATD simulations, subsequently, researchers have reformulated the probability function constants for AIS 3 or greater cervical spine injuries to be applicable to PMHS tests (Bass et al. 2010). Additionally, the axial loading constant in the second term of Equation (3.2) was reduced from 3.1 to 1.77 assuming a 50% risk of AIS 3 or greater injury to

the PMHS when subjected to a tensile load of 3,510 N (Bass et al. 2006) resulting in the NII_{PMHS} injury metric.

Several other neck injury criteria have been formulated for loading conditions observed in low speed rear impacts to address whiplash injuries. These criteria include the Neck Injury Criterion (NIC), the Neck Protection Criterion (Nkm), the Lower Neck Load index (LNL) and the Whiplash Injury Criterion (WIC). The NIC, introduced by Bostrom et al. (1996), takes into account the head acceleration and velocity relative to T1 and takes the form:

(Equation 3.3) $$NIC = a_{rel} * 0.2 + v_{rel}{}^2$$

Eriksson and Kullgren (2006) have correlated a NIC of 15 m^2/s^2 with an 18% probability of AIS 1 neck injury. The Nkm was introduced by Schmitt et al. (2002) and is the linear combination of anterior-posterior shear force and sagittal plane bending moment. It takes the form:

(Equation 3.4) $$Nkm = \frac{Fx(t)}{F\,\mathrm{int}} + \frac{My(t)}{M\,\mathrm{int}}$$

where Fint equals 845 N and Mint equals 47.5 Nm and 88.1 Nm for flexion and extension respectively. The intercepts were chosen to correlate with the human tolerance levels for AIS 1 injuries. Heitplatz et al. (2003) proposed the Lower Neck Load index as a predictor of lower neck soft tissue injury. LNL combines lower neck tensile force, shear forces, and anterior-posterior and lateral bending moments. It takes the form:

(Equation 3.5) $$LNL = \frac{\sqrt{Mx^2 + My^2}}{C_{moment}} + \frac{\sqrt{Fx^2 + Fy^2}}{C_{shear}} + \frac{Fz}{C_{tension}}$$

where the moment, shear and tension constants are 15 Nm, 250 N, and 900 N respectively. When LNL was calculated using the Rear Impact Dummy 2, the researchers reported qualitative

correlation to insurance claim frequency data. Finally, WIC was introduced by Munoz et al. (2005) and is simply the difference in sagittal plane moments measures at upper and lower neck load cells. This criterion has not been developed sufficiently to suggest an injury threshold level but is unique in that it incorporates measured loads and both the upper and lower neck load cells.

3.5 Hybrid III Anthropomorphic Test Device and Associated Injury Criteria

Reliable anthropomorphic test devices (ATDs) with meaningful injury assessment references values (IARVs) are important for assessing the risk of injury during various impact loading events and aiding in the design of effective injury mitigating devices. The Hybrid III ATD has been developed for and used extensively in automotive crashworthiness applications. The current Hybrid III neck evolved over several generations of ATDs developed by General Motors and has been validated to human flexion and extension moment corridors in dynamic sled tests (Foster et al. 1977). It is constructed out of rigid aluminum vertebral elements and molded butyl elastomer.

3.5.1 Hybrid III ATD IARVs and Nij

A summary of the Hybrid III upper neck IARVs were introduced by Mertz at General Motors in 1984. Upper neck peak flexion and extension moments, along with duration dependant peak tension, compression and fore-aft shear limits were proposed for the 50^{th} percentile male ATD (Mertz, 1984). The current compressive neck injury assessment reference value of 4 kN was originally derived from reconstructions of injurious football head impacts using the Hybrid III test device (Mertz et al., 1978). An upper and lower compressive limit was developed that is dependant on the duration of the impulse and ranged from 4 kN to 6.67 kN for very short duration events. Flexion moment IARVs for the Hybrid III were originally based on

volunteer and cadaver data of Mertz and Patrick (1971) discussed above and defined as 190 Nm.

In the 1990's, the National Highway Traffic Safety Administration (NHTSA) was upgrading Federal Motor Vehicle Safety Standard (FMVSS) 208 injury criteria for assessment of advanced restraint systems. It was during this time frame that both in-position and out-of-position IARVs were introduced. Out-of-position (OOP) IARVs are more stringent than in-position IARVs in tension and extension in order to decrease the risk of severe airbag induced injuries and due to the fact that in-position limits include an estimate for muscle activation in these loading modes. An extension, lateral bending and torsion moment IARV has been defined for both in-position and OOP occupants. The OOP extension moment IARV for the 50^{th} male is based on injury risk curves derived from matched paired tests of airbag deployments into OOP fetal pigs and the 3-year old ATD of Mertz et al. (1982a, 1982b) and Prasad and Daniel (1984) and scaled to 96 Nm for an in-position occupant assuming 80% muscle tone. IARVs for lateral bending and torsion have been proposed with the rationale that based on neck muscle size and location, that the strength in lateral bending would lie between the flexion and extension strength (143 Nm) and the torsion strength would be similar to that of extension (96 Nm) (Lund, 2003).

Prasad and Daniel (1984) proposed the first combined axial load and sagittal plane bending moment injury criteria. Injuries to porcine subjects from deploying airbags were correlated with measured three years old child ATD upper neck tension and extension response in a similar loading environment. It was suggested that the linear combination of tension and extension should be used as an injury metric. The concept of linearly combining axial load and sagittal plane bending moment was expanded to include compression and flexion and presented as Nij by Klinich et al. (1996). Nij is calculated using Equation (3.6) where the intercept values Fc and Mc vary for compression and tension, and flexion and extension respectively.

(Equation 3.6) $$Nij = \frac{Fz(t)}{F_C} + \frac{My(t)}{M_C}$$

In the NHTSA's second report on the development of improved injury criteria for the assessment of advanced automotive restraint systems, which included the addition of the Nij injury metric, the NHTSA proposed upper neck compressive force, flexion moment and extension moment intercept values of 4,500 N, 310 Nm and 125 Nm respectively for the Hybrid III 50th percentile male ATD (Eppinger et al., 1999). The compressive force limit was based on PMHS testing performed by Pintar et al. (1995) which the authors felt best represented pure axial compression of the cervical spine. The extension moment critical intercept of 125 Nm was based on scaling of the three years old ATD extension limit proposed by Prasad and Daniel (1984). Separately, a scale factor between human and ATD neck extension moments of 2.4 was determined using MADYMO, and when applied to the 57 Nm human cervical tolerance in extension proposed by Mertz and Patrick (1971), yields roughly the same extension intercept value. Finally, the flexion moment intercept was determined by maintaining a ratio of 2.5 between flexion and extension moment intercepts. The ratio of 2.5 between flexion and extension moment intercepts is the same as that proposed by the American Automobile Manufactures Association (AAMA) (190 Nm flexion / 78 Nm extension). The OOP upper neck Nij flexion and extension intercepts proposed as IARVs by Mertz et al. (2003) are 305 Nm and 122 Nm respectively. The difference between these values and those originally proposed by NHTSA are accounted for in rounding differences during the scaling process.

Lower neck IARVs have been reported by Mertz et al. (2003). The axial force limits and axial force Nij intercepts are identical to the upper neck. Prasad et al. (1997) recommended a lower neck extension IARV of 154 Nm based on rear impact sled tests. Using the ratio of this recommendation and the out of position upper neck extension IARVs (154 / 77 Nm) the in-

position flexion and extension IARVs are double that of the upper neck or 380 Nm and 192 Nm respectively. The lower neck Nij flexion and extension intercepts are also double that of the upper neck or 610 Nm and 266 Nm respectively. Table 3.1 summarizes the Hybrid III 50th male ATD upper and lower neck IARVs and Nij intercepts. Recently, Raasch et al. (2010) performed reconstructions of past PMHS testing of Clemons and Burrow (1972) using the Hybrid III 50th percentile male ATD. The original PMHS tests conducted were rigid seat frontal and rear impact sled tests. Updating the lower neck flexion and extension moment IARVs for the Hybrid III was proposed. An extension limit of 149 Nm for in-position occupants and an in-position flexion moment of 200 Nm maximum were advocated.

Table 3.1: Hybrid III 50th percentile male upper and lower neck IARVs proposed by Mertz et al. (2003)

	Fx & Fy	Fz		Mx	My		Mz	Nij Intercepts			
	Shear (N)	Tension (N)	Comp (N)	(Nm)	Flex (Nm)	Ext (Nm)	(Nm)	F_T (N)	F_C (N)	M_F (Nm)	M_E (Nm)
Upper Neck IP	3100	4170	4000	143	190	96	96	6780	6200	305	133
Upper Neck OOP	3100	3290	4000	134	190	78	78	6200	6200	305	122
Lower Neck IP	3100	4170	4000	286	380	192	96	6780	6200	610	266
Lower Neck OOP	3100	3290	4000	268	380	156	78	6200	6200	610	244

There are no currently utilized neck injury criteria for the 50th percentile male Hybrid III ATD that incorporate a combination of axial force and lateral bending or torsion moments. One study has been identified that has incorporated upper neck lateral bending in to the formulation of Nij for the 5th percentile female ATD (Duma et al. 2003). The authors evaluated small female neck interaction with a deploying side airbag and similar to the form of NII, adjusted Nij to include the square root of the sum of the squares of the measured anterior-posterior and lateral neck moments. The current 5th female Nij flexion moment intercept of 155 Nm for 5th female was utilized when evaluating the resultant moment.

3.5.2 Neck Injury Criteria Adopted as Legal Regulations

The upper neck Nij intercepts ultimately adopted by NHTSA and incorporated into FMVSS 208 for the Hybrid III 50th percentile male were published in a supplement to the aforementioned NHTSA report (Eppinger et al., 2000). The compression intercept was set at 6,160 N, equal to the tension intercept derived from scaling the three years old ATD tension intercept based on the work on Prasad and Daniel. The extension intercept was similarly scaled from the child ATD criteria for OOP testing but was increased to 135 Nm for in-position testing based on the assumption that adult occupant neck muscles would be flexed at 80% of their static strength. The flexion intercept was maintained at 310 Nm. The increased value of the compression intercept was deemed appropriate for the proper linear combination of sagittal moment and axial compressive load but a peak compressive load limit of 4,000 N was also incorporated consistent with the earlier work done by Mertz (1978). Figure 3.6 depicts the original NHTSA Nij kite and the ultimate Nij boundaries incorporated into Federal Motor Vehicle Safety Standard 208 (CFR 49 part 572.208). An in-position Nij of 1.0 in tension and extension has been equated to a 5% injury risk of AIS 3 or greater (Mertz et al., 2003). The Nij intercepts and peak tension and compression force limits for all ATDs currently included in FMVSS 208 are listed in Table 3.2.

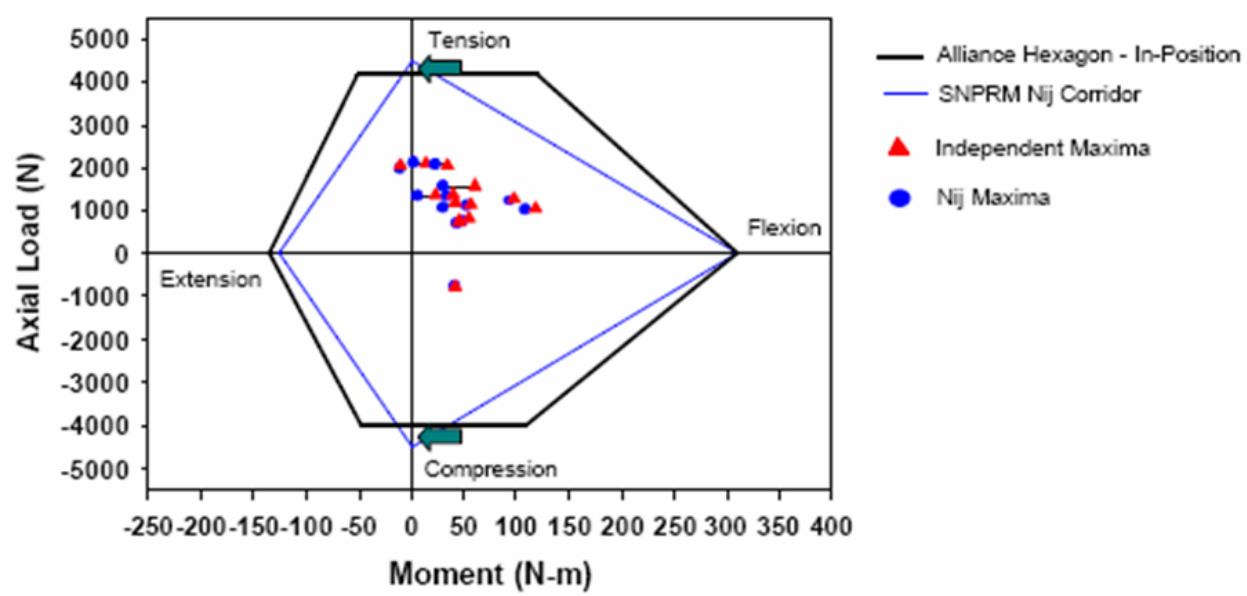

Figure 3.6: NHTSA proposed Nij kite corridor and AAMA proposed in-position hexagon corridor adopted as the FMVSS 208 final rule (from Eppinger et al. 2000)

Table 3.2: FMVSS 208 Nij intercepts and peak tension and compression force limits for various In-Position (IP) or Out-of-Position (OOP) ATD testing scenarios (CFR 49 part 571.208)

	Nij Intercepts				Peak Axial Load	
ATD - Position	F_T (N)	F_C (N)	M_F (Nm)	M_E (Nm)	F_T (N)	F_C (N)
50th Male - IP	6806	6160	310	135	4170	4000
5th Female - IP	4287	3880	155	67	2620	2520
5th Female - OOP	3880	3880	155	61	2070	2520
6yo - OOP	2800	2800	93	37	1490	1820
3yo - OOP	2120	2120	68	27	1130	1380
12mo - Crabi OOP	1460	1460	43	17	780	960

The United Nations Economic Commission for Europe (UNECE) Regulation No.94 addresses uniform provisions concerning the approval of vehicles with regard to the protection of occupants in the event of a frontal collision. Within this regulation, neck injury criteria are specified for the 50th percentile Hybrid III ATD for axial tension, anterior-posterior shear and the sagittal plane extension bending moment. The force tolerances are time dependent and can be found in Figure 3.7. The maximum allowable extension bending moment is 57 Nm. The European New Car Assessment Program (Euro NCAP) also evaluates vehicles for frontal impact protection and whiplash protection in low speed rear impacts. The same ECE Regulation

94 neck criteria are used for the frontal impact protection evaluation and NIC and Nkm are part of the whiplash injury criteria considered. The Euro NCAP tests are not regulatory in nature but rate vehicle performance for consumers.

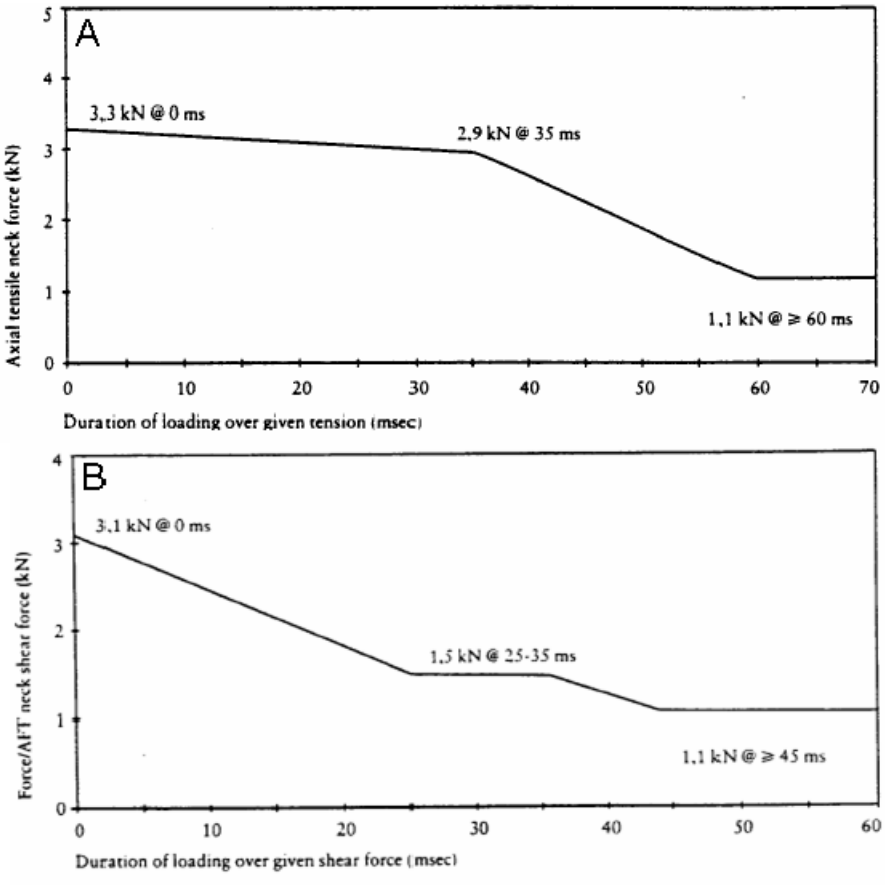

Figure 3.7: UNECE Regulation No. 94 neck tensile and anterior-posterior shear force criteria for frontal impact protection (taken from UNECE Transport Regulation No. 94)

3.5.3 Available Hybrid III Neck Data

Several researchers have reported on the isolated Hybrid III 50th percentile male neck response in various loading modes and rates (Yoganandan et al., 1989b, Myers et al. 1991a and Pintar et al., 1990). In quasi - static loading environments, the Hybrid III head-neck complex has been reported to be 1.5 to 3.5 times stiffer in axial compression than the human head and cervical spine complex. The Hybrid III neck needs to be robust enough to maintain its structural

integrity and repeatability so must withstand more load than the human cervical spine. Frechede et al. (2009) conducted 26 inverted drop tests of the entire Hybrid III 50th percentile male ATD in which upper and lower neck forces and moments were measured and analyzed. The Hybrid III neck showed the ability to deform in an S-shape during some of the inverted drop tests where the upper neck was in a compression - extension loading mode and the lower neck in a compression-flexion loading mode. For a given impact velocity (drop height), measured biomechanical parameters were significantly influenced by the impact orientation.

CHAPTER 4

INVESTIGATION OF THE EFFECT OF LATERAL BENDING ON THE CERVICAL SPINE COMPRESSION RESPONSE AND TOLERANCE IN PMHS HEAD-NECK COMPLEX TESTS

4.1 Introduction

Cervical spine compressive loading combined with lateral bending remains largely unexplored and the influence of lateral bending on injury dynamics, tolerance and injury classification has yet to be quantified. In crash tests of rollover type accidents, researchers have observed lateral bending of the dummy neck prior to head impact or in conjunction with head impact with the roof. Since the effects of lateral bending on compressive tolerance of the cervical spine are not well documented, the significance of this phenomenon cannot be addressed.

This study seeks to investigate the effects of lateral bending on cervical spine compressive injury dynamics and gross kinematics. Automotive testing in the rollover collision environment with Hybrid III ATDs has resulted in near apex head impact loading events generating significant cervical compressive load combined with both noticeable neck lateral bending and measured lateral bending moments. Potential effects of either a laterally oriented impact plate or initial lateral bending postures on cervical spine response have not been investigated experimentally using the PMHS model. Investigation of these effects has been conducted through execution and analysis of inverted drop tests of head-neck complexes resulting in injurious, near vertex head impacts. Results including injury patterns, buckling modes, mechanical response and the axial force at failure are compared with prior investigations of purely sagittal plane compressive experimentation. Further, whether or not asymmetric loading patterns are equivalent to symmetric loading patterns with asymmetric

postures is addressed. Portions of this chapter have been published in the 2009 American Society of Mechanical Engineers (ASME) International Mechanical Engineering Congress and Exposition (IMECE).

4.2 Methodology

Historical testing strategies can be grouped into three types based on the type of test specimen used: whole body cadaver, isolated head and neck and cervical spine motion segments. The primary drawback of historical studies of head impacts using whole body cadavers is the difficulty in accurately quantifying neck loads and developing injury reference values. Whole body cadaver studies allow for direct application of real-world loading scenarios but do not allow for direct measurement of neck loads because of the invasiveness of load measuring instrumentation. In contrast, isolated cervical segment testing facilitates direct measurement of load on the local spine segments. A drawback of segment testing, however, is that reproducing the dynamic loading vector present in a real world loading scenario is experimentally intractable since the real world loading vector temporally varies in position, magnitude and orientation. Given the limitations of these test methods, the isolated head and neck specimen strategy represents a compromise between collecting accurate neck loading data while maintaining relatively accurate kinematics and dynamic loading of the entire head and neck complex. This investigation begins by applying the techniques used in isolated head and neck investigations and adapting them to include the effects of lateral bending. Specifically, the methodology reported by Nightingale et al. (1996b, 1997a) to study sagittal plane compressive neck injury and the effects of padding on neck injury risk is the foundation for the methods used in this study. This testing was conducted at the Wayne State University Bioengineering Center.

4.2.1 Test Apparatus

A head and neck injury drop track apparatus was designed and fabricated to allow unconstrained head-first impacts on an adjustable oblique surface (Figure 4.1). Specimens were mounted to a cart attached to a vertical track with linear bearing sliders. The cart was weighted to 16.3 kg to simulate the effective mass of the torso. This value was reported by Nightingale et al. (1996a) and was estimated using GEBOD software to be the fraction of a 50th percentile male torso mass acting on the neck during dynamic injury.

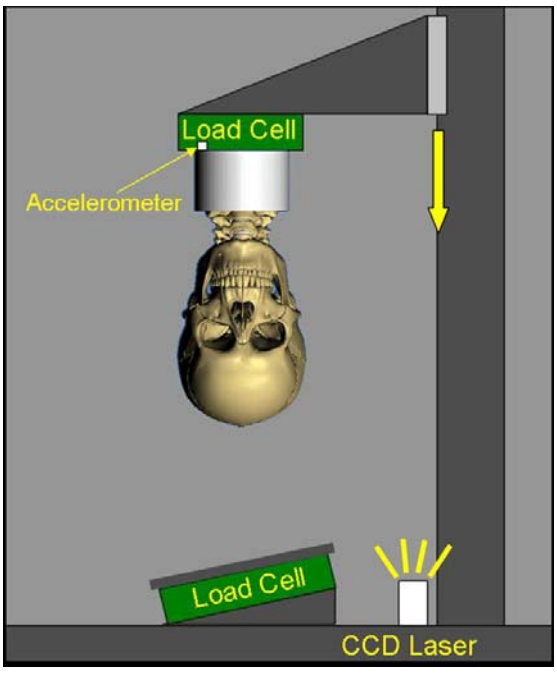

Figure 4.1: Schematic of drop test apparatus showing an initial 15-degree lateral impact angle

4.2.2 Specimen Preparation

Five unembalmed human cadaver heads and ligamentous cervical spine specimens including T2 were harvested, sealed in plastic bags and stored at -20 C. Pretest radiographs were taken of the specimens and were examined along with medical records to ensure that there were no unrecognized spinal pathologies. The inferior two vertebrae (T1 and T2) were cleaned of muscular tissue and cast into aluminum cups with reinforced polyester resin. Care was taken to ensure that the C7-T1 articulation was free of the casting and had unrestricted

range of motion. The C7-T1 intervertebral disc was oriented at approximately 25° to horizontal to preserve the resting lordosis of the cervical spine (Matsushita et al. 1994). Finally, photographic target pins (4.0 mm diameter) were inserted in the anterior vertebral bodies, the spinous processes and lateral masses of C2-C7. The mandible of specimen 1 was removed to allow better visualization of the C2-Occipital region during the test. Because of the possible influence this might have on the overall head inertia properties, the mandible was left in place on subsequent tests.

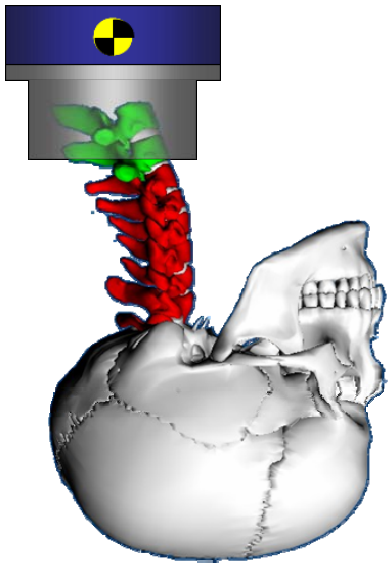

Figure 4.2: Schematic demonstrating method of specimen preparation cast in cup while maintaining natural lordosis and free articulation of C7-T1. The cervical spine is represented by the red vertebrae

Specimen anthropometry, age, and cause of death are given in Table 4.1. The average height of the specimens was 1.803 +/- 0.08 m and the average weight was 80.9 +/- 6.5 kg. The 50th percentile male stands 1.75 m tall and weighs 78.4 kg (Tilley 1993).

Table 4.1: Specimen anthropometry, age, and cause of death

Test ID	Gender	Age	Height (m)	Weight (kg)	Cause of Death
1	male	76	1.78	79.5	Congestive heart failure
2	male	80	1.93	90.9	Cardiac arrhythmia
3	male	77	1.73	72.7	Bacterial sepsis
4	male	81	1.83	81.8	Cardio respiratory failure
5	male	55	1.75	79.5	Carbon monoxide intox

4.2.3 Experimental Setup

Test specimens were inverted and mounted to the carriage of the drop track. Two different specimen/impact plate configurations were used during these tests, as shown in Figure 4.3. In Configuration 1, the initial position of the head and neck was in a neutral posture but the impact plate was inclined laterally at 15 degrees from horizontal. This is roughly comparable to a rollover event with a neck maintaining its initial posture and either the body rotating with respect to the vehicle prior to head impact or an impact with an upright torso and head into an angled roof structure. In Configuration 2 the head was pre-positioned with 15 degrees of lateral bending and the impact plate remained horizontal. The angle was defined by the head angle with respect to the neck load cell reference frame. This is roughly comparable to a rollover event with a flexible neck allowing the head and neck to be in a lateral bending posture at the time of head impact. Both configurations result in asymmetric compressive loading of the cervical spine. Figure 4.4 depicts test specimen 3 mounted to the drop track test apparatus prior to raising the cart and executing the test.

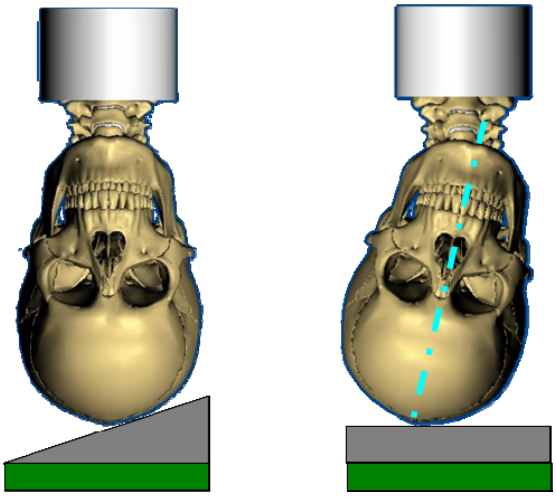

Figure 4.3: Two different initial positions were used in these tests

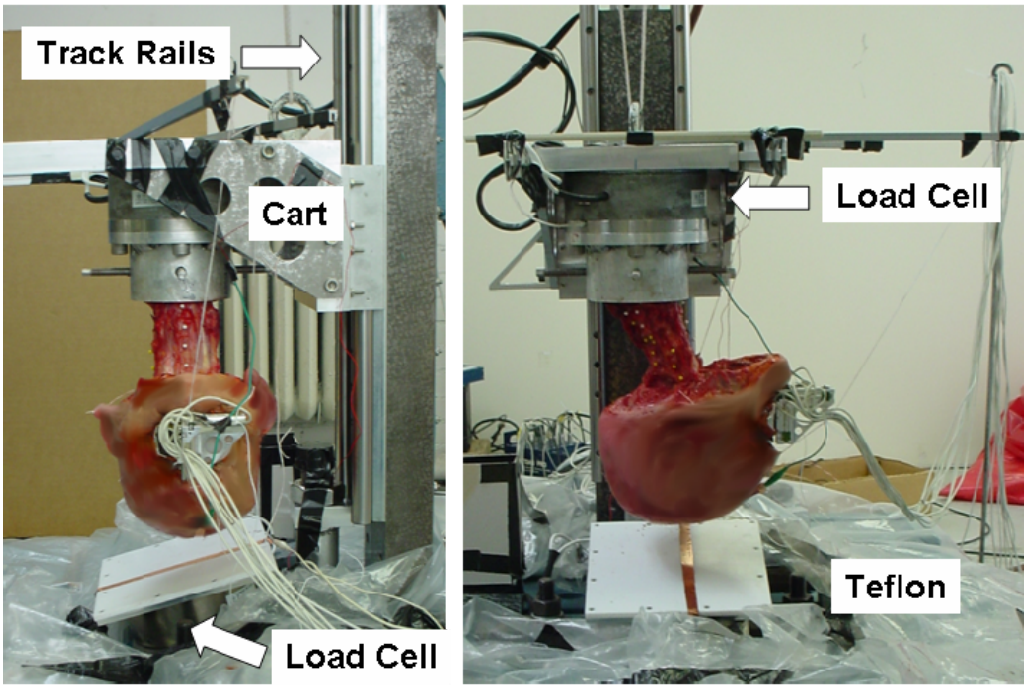

Figure 4.4: Test PMHS 3 mounted to the drop track test apparatus

After mounting, the specimen was raised into drop position and preconditioned by manually exercising the head and neck through 60° of combined flexion and extension and 20 degrees of lateral bending for 50 cycles (McElhaney et al. 1983). The initial position of the head

and neck posture in Configuration 2 was achieved using breakaway sutures attached through the skin. Drop heights of 0.45 m for tests 1, 2 and 4 and 0.53 m for tests 3 and 5 were used based on head impact velocities in diving accident reconstructions performed by McElhaney et al. (1979) and to be consistent with the study of Nightingale et al. (1997a). These heights have been shown to produce sufficient energy to cause cervical spine injury without producing skull fractures.

4.2.4 Instrumentation and High Speed Digital Video

Head impact forces were measured using a six-axis load cell located directly below a Teflon® impact surface. Lower neck forces and moments at the T1 level were measured using a six-axis load cell located between the neck and the carriage. T1/cart vertical acceleration response was measured with a linear accelerometer attached to the cart. Impact speed was calculated from cart displacement measured using a laser CCD displacement sensor. All transducer data were acquired in accordance to the SAE J211 standard. Two 1,000-fps digital cameras were synchronized with the data acquisition and used to record each test; one from the frontal perspective and one from the left lateral perspective. The impact surface provided variation of the impact angle to produce laterally oblique impacts.

Data processing was conducted in accordance was SAE J211. All head and neck forces were digitally filtered at SAE channel filter class 1000 (CFC 1000) and neck moments at CFC 600. The SAE coordinate system outlined in J211 was used. The neck vertical load and sagittal and frontal plane moments measured at the load cell were transformed to the center of the C7-T1 intervertebral disc. The actual vertical load at the center of C7/T1 was calculated by adding the measured load at the load cell to the product of the acceleration measured at C7/T1 and the mass of the casting cup, casting material, adapter plates, attachment hardware and the mass of the load cell between the sensitive axis of the load cell and the center of the C7-T1 intervertebral disc. The measured neck forces were filtered at CFC 600 for the sagittal and

frontal plane moment transformation process. The location of the C7-T1 intervertebral disc was determined using pre-test radiographs. Equations (4.1) and (4.2) were used to transform the measured moments and are depicted in Figure 4.5.

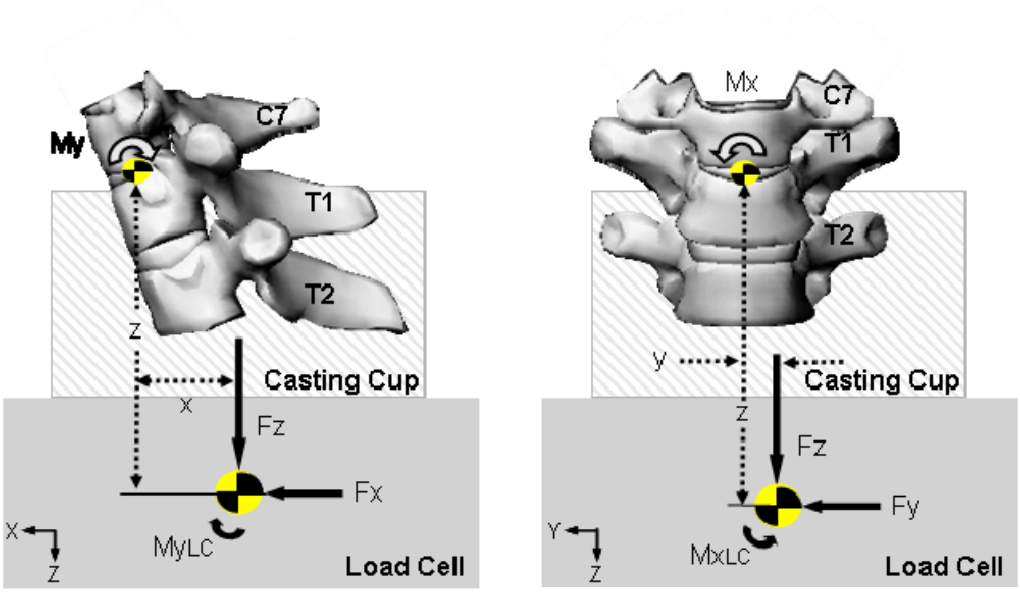

Figure 4.5: Transformation of flexion/extension moment (My) and lateral bending (Mx) moments to the center of C7-T1 intervertebral disc

(Equation 4.1) $$My = My_{LC} + (Fx \times z) + (Fz \times x)$$

(Equation 4.2) $$Mx = Mx_{LC} - (Fy \times z) - (Fz \times y)$$

In head-neck complex experimentation, the C7-T1 intervertebral disc represents a convenient and repeatable anatomical landmark nearest the tested specimen that does not move relative to the load cell sensitive axis. Combined with the relative ease in which the center of the disc can be defined in a radiograph, this ensures accurate moment transformation. There is flexibility in this approach in that alternate identifiable anatomical landmarks that may correlate better with the sensitive axes of ATD load cells can be used to report the moment response.

The head impact plate load cell was always aligned with the impact surface. The measured axial and lateral head contact forces in Configuration 1 tests were therefore

transformed so that the vertical axis aligned with the cervical spine vertical axis and was consistent with measured loads in Configuration 2 tests. The head and lower neck vertical impulse was calculated for each specimen by integrating the vertical force time history.

4.2.5 Injury Documentation

The presence of damage to the cervical vertebral column was documented through post test radiographs and dissection of the specimens. Antero-posterior and lateral radiographs were taken of each specimen preparation. Both the heads and cervical spines were then dissected and all damage was documented. For the three tests in which vertebral fractures were identified, the load at fracture was determined based on the measured neck load responses and the associated high speed video. Traditionally, compressive failure has been defined as a decrease in axial load while displacement is still increasing. In the case of the cervical spine, a change in geometry due to neck buckling or a change in end conditions (head translation on the impact surface) can also lead to a decrease in axial load on the spine. The fracture loads identified are the first decrease in axial load that could not be attributed to another cause. Similar approaches to identifying cervical vertebral failure loads have been used by other researchers (Nightingale et al. 1996b and Carter et al. 2002).

The Abbreviated Injury Scale (AIS) is widely used in automotive safety. The severity of cervical injuries in the AIS scaling system is highly dependent on neurological dysfunction and the magnitude of spinal cord involvement. Testing with PMHS limits the ability to determine neurological dysfunction, therefore cervical damage documented was limited to clinically recognized orthopedic injuries. The clinical stability of the orthopedic damage sustained by the PMHS specimens was documented. Damaged spinal segments were assessed manually and adjacent segments that were able to be manipulated beyond a typical physiologic range of motion were defined as unstable (White and Panjabi, 1990).

4.3 Results

Five tests were conducted in which PMHS were dropped from either 0.45 or 0.53 m, with resulting impact speeds ranging from 2.9 to 3.25 m/s. Three of the five specimens sustained compressive cervical vertebral fractures at lower neck loads ranging between 1,518 N and 3,472 N. Fracture patterns did suggest that the asymmetric postures and loading resulted in asymmetric fracture patterns. Overall compressive neck injury dynamics and tolerances appear similar to previous studies of purely sagittal plane dynamics based on these initial results.

4.3.1 General Kinetics and Kinematics

Typical plots of the head and neck vertical loads are shown in Figure 4.6. Figure 4.6 (A) represents a test in which no fracture occurred while Figure 4.6 (B) represents a test in which a fracture was identified. In both cases, the neck load initially lagged the head load due to decoupling of the head and neck. The head contacted the impact plate and began to rebound before the neck began to experience significant loading. The neck load increased rapidly initially, then the neck buckled or fractured and the load began to decline. The average peak axial neck force due to head rebound was 2,122 +/- 1,331 N or 59 +/- 25% of the overall neck axial force at that time. The neck impulse ended once the torso was arrested or the head moved out of the path of the torso. A primarily bi-model head response was observed in Tests 1-4, similar to previous findings (Nucholtz et al. 1981 and 1983 and Nightingale et al. 1996b and 1997a). In Test 5, a tri-modal head response was observed. Peak head and neck loads, head and neck impulse and the lag in neck force response are summarized in Table 4.2.

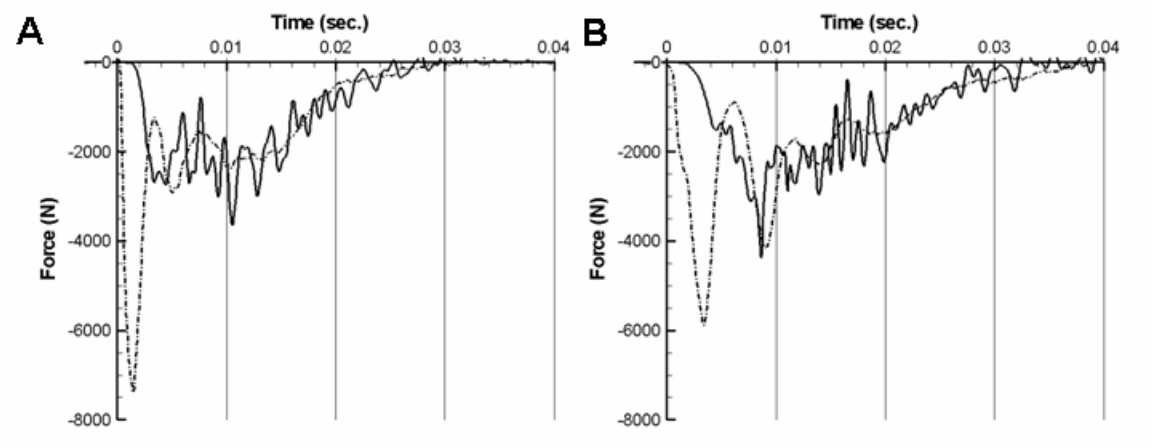

Figure 4.6: Test 2 head (dashed line) and neck (solid line) vertical loads for a non-fracture case (A) and Test 3 for a fracture case (B)

Cervical spine buckling modes do not appear to be a function of lateral bending and appear similar to sagittal plane tests reported by Nightingale et al. (1996b, 1997a). Based on high speed video, no observable high-order lateral bending mode was present in any of the tests. Buckling was observed after the rapid onset of compressive load. Relative anterior-posterior motion at individual cervical spine motion segments was visualized at approximately 4 ms after impact. This was consistent with a sizeable decrease in the measured axial load. In all five tests, the lower cervical spine (C6-C7) was flexed locally while the remaining vertebrae appeared to be in extension. The velocity of the anterior snap through of the cervical spine buckle was qualitatively greatest in Tests 4 and 5 which were tested in Configuration 2.

Table 4.2: Summary of peak head and neck kinetics

		First Mode of Head Response				Lower Neck Response					
	Impact	Resultant		Vertical		Peak Force			Torso Verical		Neck
Test ID	Speed (m/s)	Force (N)	Duration (msec.)	Impulse (N-s)	Momentum^ (N-s)	Res (N)	Axial (N)	Time (msec.)	Impulse (N-s)	Momentum^ (N-s)	Lag (msec.)
1	2.97	9492	3.4	-14.0	13.1	5146*	-5122	8.2	-38.8	48.4	1.6
2	3.07	7658	3.4	-13.2	13.5	3656*	-3643	10.6	-37.2	50.0	1.4
3	3.25	6064	6.1	-16.7	14.3	4407	-4371	8.7	-42.6	53.0	1.9
4	2.91	10828	4.1	-20.8	12.8	4695*	-4694	9.1	-64.0	47.4	1.0
5	3.26	17483	3.3	-20.5	14.3	4714	-4669	3.8	-50.5	53.1	1.0

^Based on head mass of (4.4 kg)

*Lateral shear force not used in resultant calculation

The vertical impulses and the momentum at impact were calculated for both the head and torso in each of the tests. The head impulse presented in Table 4.2 is the integration of the first mode of the head force response. The impulse calculated at the base of the neck is equivalent to the effective torso impulse or change in torso momentum. The torso impulse at the end of the first mode of the head response was approximately 25 +/- 4% of the head impulse, indicating torso inertial forces are contributing slightly to the head load during mode 1, but that the primary work that was being done during the first mode of the head response was the stopping and subsequent rebounding of the head. Since impulse is equivalent to change in momentum, comparing the calculated impulses to the momentum of the head and torso at impact gives some insight into the ability or inability of the head to escape out from underneath the falling torso and the extent to which the torso is arrested. Table 4.2 lists the calculated impulses as well as the momentum at impact for the head and torso. The head and torso impulses were greatest for Configuration 2 indicating that the head was less likely to escape the ensuing torso in this configuration. This is likely primarily due to the cervical spine being oriented nearly perpendicular to the impact surface.

4.3.2 Cervical Spine Response

Unlike primarily sagittal plane cervical spine response to near vertex head impacts, the two test configurations evaluated elicited a complex three-dimensional response dominated by the compressive axial load. The maximum response of all lower neck forces and moments was observed during the initial 30 to 40 ms after head contact. Following this initial impulse, the general head kinematics included forward and left translation and forward flexion, left lateral bending, and a small degree of head clockwise axial rotation when viewed in the superior to inferior direction. Test 4 was an exception in that primary post impact head motion was rearward rotation or extension with very little head translation. The torso impulse in this test was the largest observed and the vertical rebound of the torso was evident in the high speed video. In

Test 5, the head of the specimen briefly began to go into extension but reversed into forward flexion.

The following detailed descriptions of spinal responses are grouped by test configuration and only include the initial primarily compressive phase of the response which occurred prior significant head motion. Figures 4.7 – 4.11 are individual plots of the axial (Fz), anterior-posterior shear (Fx), sagittal plane moment (My), lateral shear and bending (Fy, Mx) and axial twist (Mz) responses at the base of the neck respectively. The lateral shear force channel was corrupt for tests 1, 2, and 4 so the lateral bending moment could not be transformed to C7/T1, therefore, Figure 4.10 does not include these tests.

.

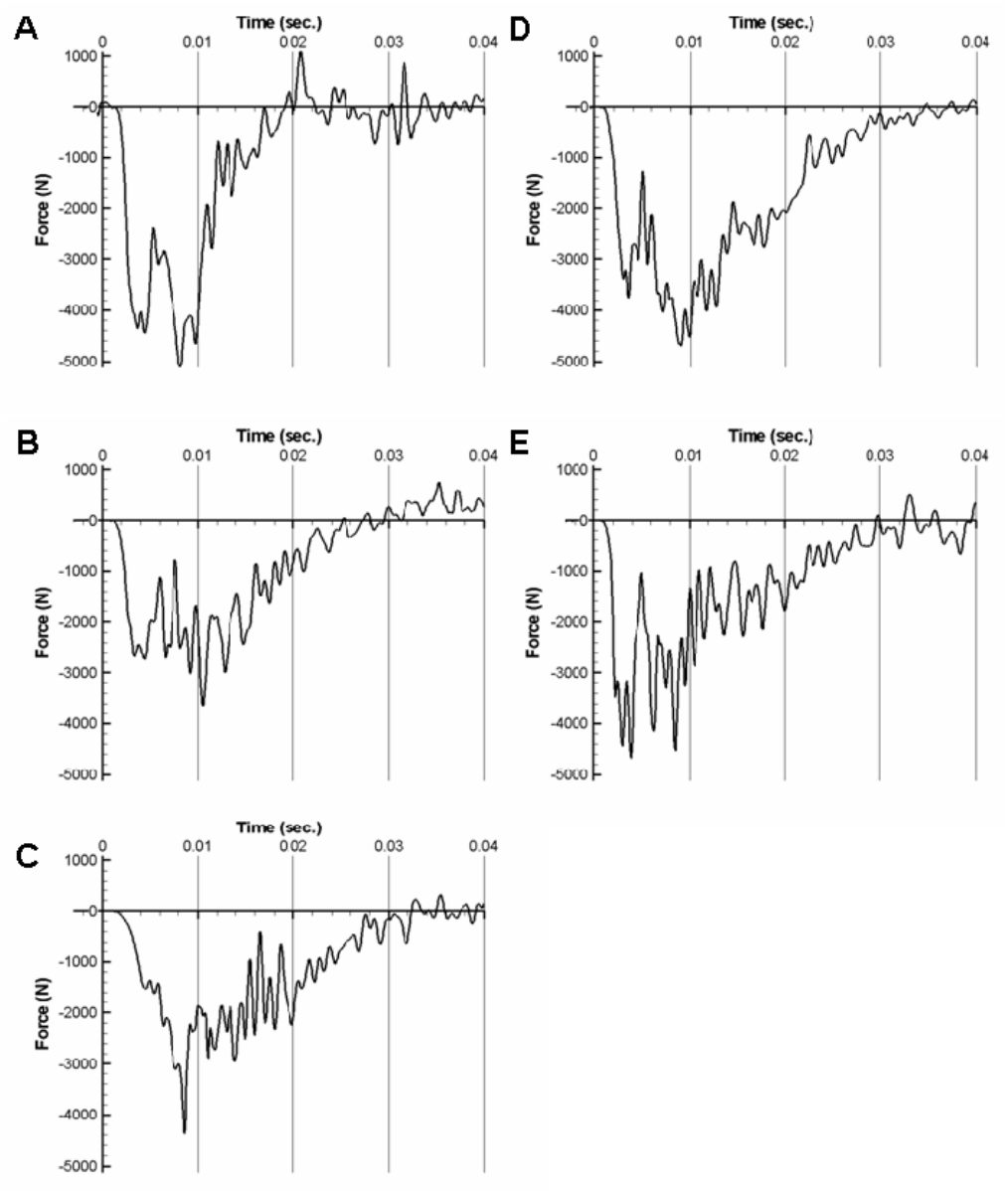

Figure 4.7: Axial force response of the cervical spine in tests 1 (A) – 5 (E). A negative axial force indicates compression

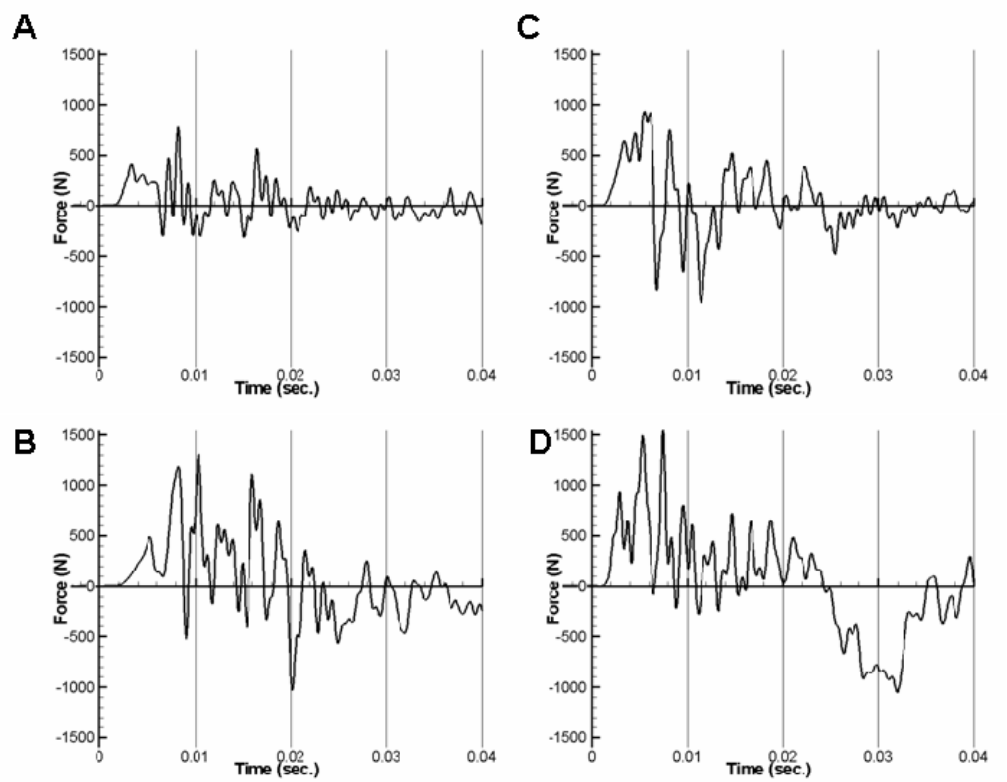

Figure 4.8: Anterior-posterior shear force (Fx) response of the cervical spine in tests 2 (A) – 5 (D)

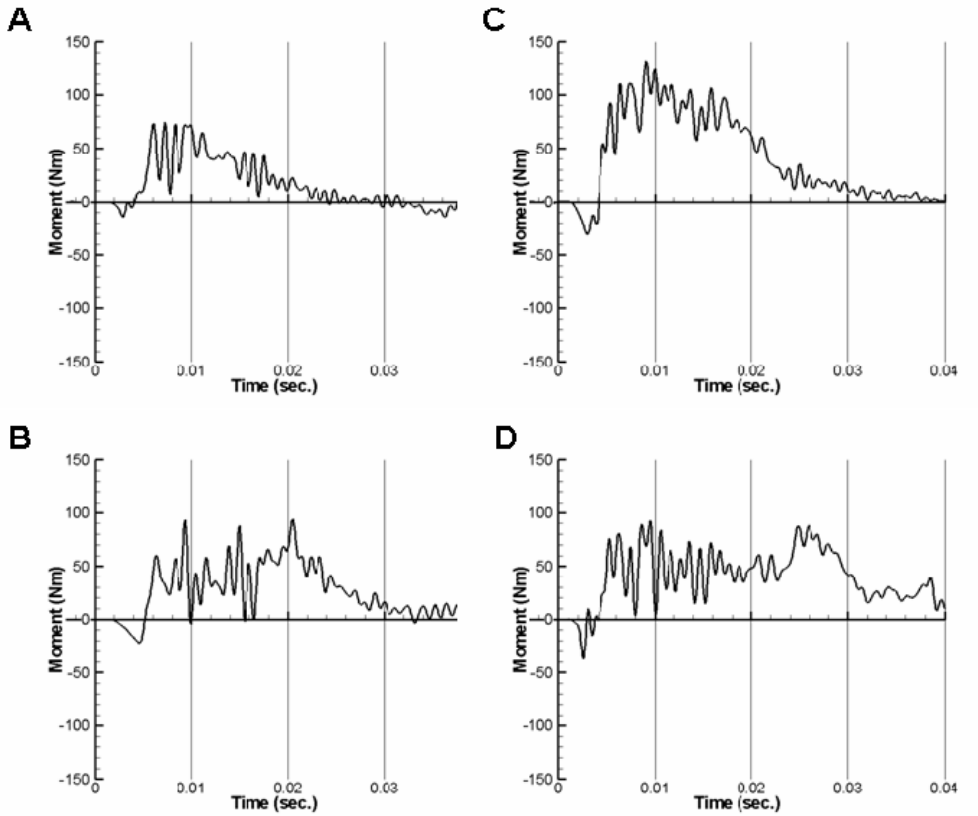

Figure 4.9: Sagittal plane moment (My) response of the cervical spine in tests 2 (A) – 5 (D)

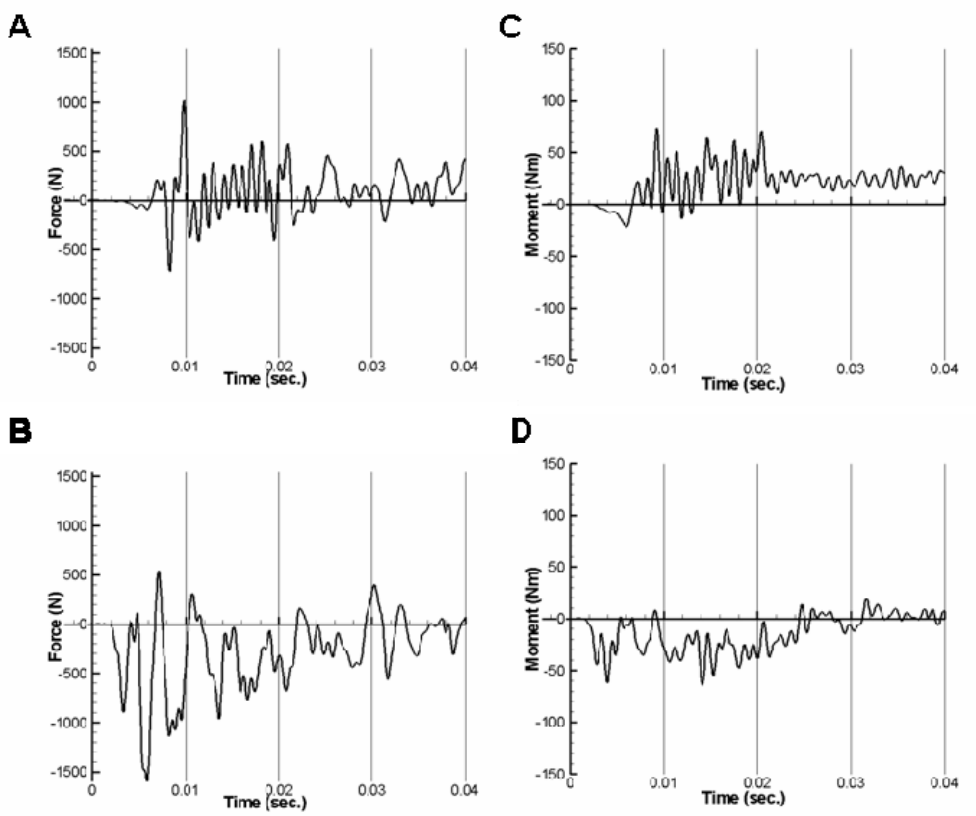

Figure 4.10: Lateral shear force (Fy) and moment (Mx) response for test 3 (A and C) and 5 (B and D)

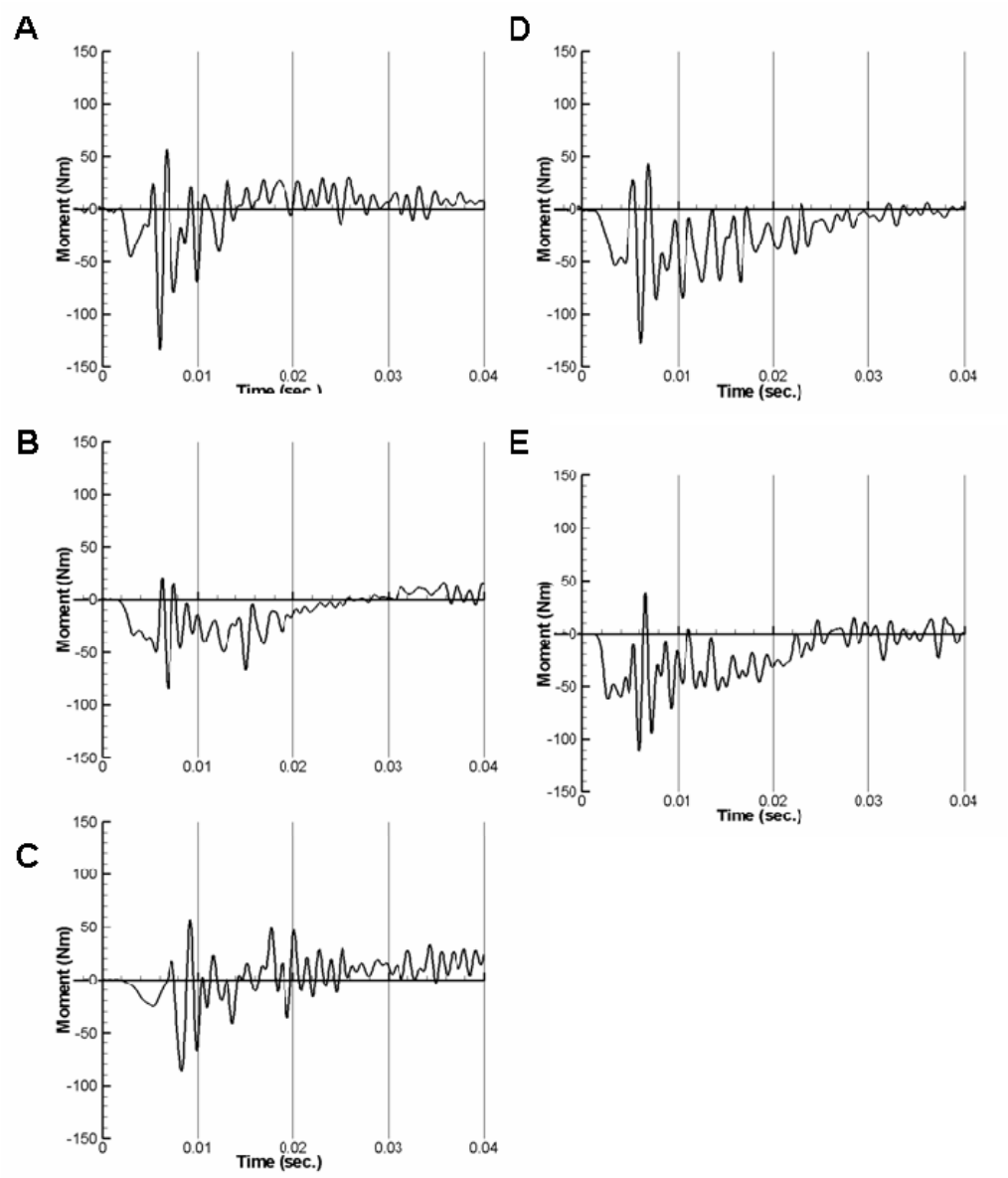

Figure 4.11: Axial twist moment (Mz) response for tests 1 (A) – 5 (E)

Test Configuration 1 consisted of a neutral neck impacting a fifteen degree laterally inclined plate. Each of the six neck load channels, including axial force to some extent, experience high frequency oscillation and in some cases polarity reversals at the specified SAE filter classes. Due to the overall geometry of the head-neck complex when the natural lordosis of the spine is maintained, the sagittal plane reaction forces were similar for both test configurations. The vertical head force is applied anterior to the base of the neck resulting in a

primarily positive moment around the lateral (Y) axis. Initially, a posterior shear force with a magnitude significantly less than that of the axial compression is applied at the head which subsequently dissipates with the decrease in axial load. The posterior shear force applied to the head acts to generate a negative moment around the lateral (Y) axis but is significantly less than the contribution of the axial force. Figure 4.12 depicts the primary forces applied to the head (blue arrows) and the cervical spine reaction forces and moments (black arrows) in each of the three orthogonal perspectives.

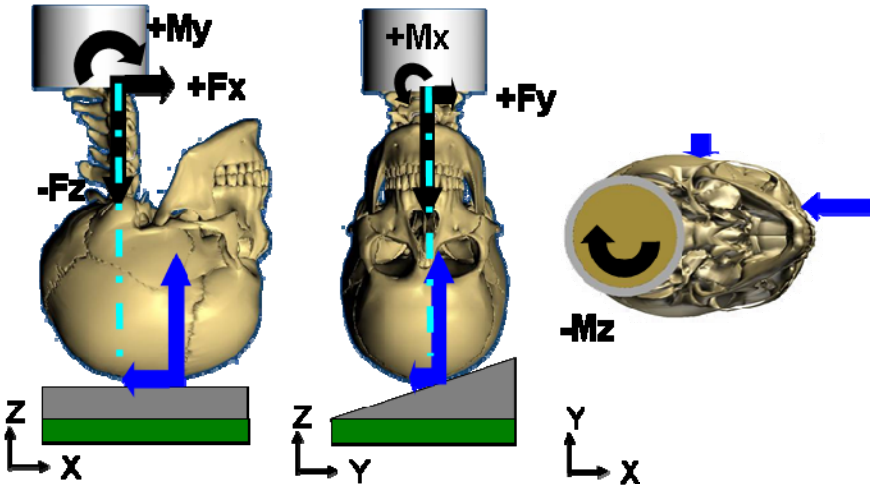

Figure 4.12: Primary force and moments in cervical spine in test Configuration 1

The lateral shear force reaction was small in magnitude compared to the axial force and the anterior-posterior shear force for test Configuration 1. The lateral bending moment (Mx) is primarily driven by the lateral shear force, not the axial compressive force because the lateral shear force moment arm is large whereas the axial force is being applied near to the lateral center line of spine. The direction of lateral shear and bending depicted in Figure 4.12 holds true for the majority of the compressive phase of the spinal response. Finally, Figure 4.12 depicts the anterior-posterior and lateral shear forces effect on the axial twist or torsional moment (Mz). In this configuration, the greater magnitude of the shear force applied in the posterior direction

versus the leftward direction results in a negative twist moment reaction at the base of the cervical spine.

Test Configuration 2 consisted of a pre-laterally flexed head and neck impacting a flat impact surface. The sagittal plane response is very similar to that of Configuration 1 but the magnitude of the pre-buckle axial response in this configuration is generally greater. The decrease in load due to buckling is very large and rapid and easily identified in the plot in Figure 4.7 beginning near 4 ms. The lateral shear response has a larger magnitude and lateral shear and bending moment responses are primarily in the opposite direction of that in Configuration 1. An initial left lateral bending posture resulted in an initial right lateral bending response due the location and direction of the applied force on the head. The lateral shear force and the moment arm at which it is applied, again exceed the contribution of the axial load due to it acting near the centerline of the cervical column. The magnitudes of both lateral shear and bending responses are larger than observed in Configuration 1 and approach the magnitudes of shear and bending in the sagittal plane (Fx, My). Figure 4.13 outlines the primary forces applied to the head and the respective neck reaction forces and moments.

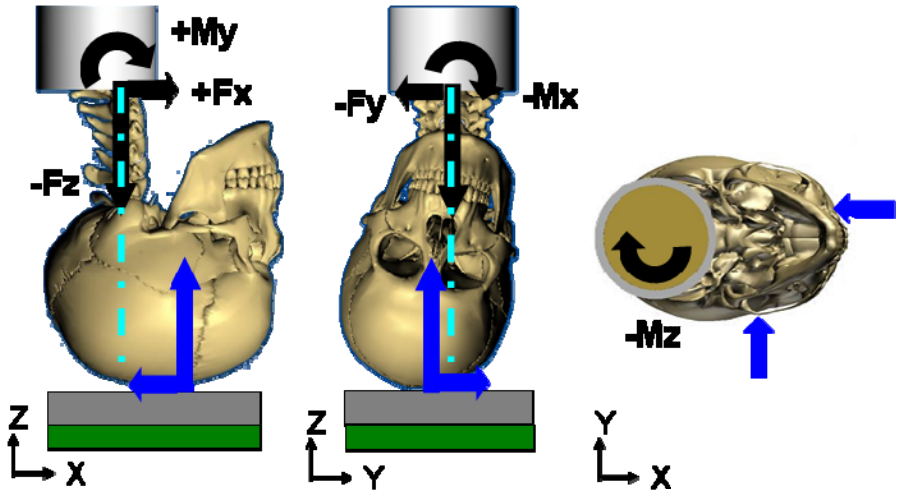

Figure 4.13: Primary forces and moments in cervical spine in test Configuration 2

Similar to Configuration 1, the torsional moment reaction was again negative or counter-clockwise when viewed from above. The torsional responses presented for both configurations in Figure 4.11 is oscillatory in nature but includes a more continuously applied and slightly greater magnitude response in Configuration 2, consistent with being driven by both anterior-posterior and lateral shear force components.

4.3.3 Cervical Spine Tolerance

Documented cervical damage is shown in Table 4.3. For Tests 1, 2 and 4, where impact speeds were below 3.1 m/s, the documented damage was less severe than for Tests 3 and 5 where the impact speed was 3.25 m/s or greater. This is consistent with the previous findings of Nightingale where the average impact speed for injurious rigid impacts was approximately 3.23 m/s (Nightingale et al. 1997a). The fractures observed were consistent with cervical spine injuries presenting clinically. In addition, in the more severe impacts of Test 3 and 5, the injuries showed a bias to the left side consistent with leftward asymmetric loading. The only unstable injury identified was at C4-C5 in Test 3. No fractures were identified in Test 1, however, increased laxity of the left facet capsule at C4-C5 was easily identifiable post-test compared to its pre-test range of motion. Note that the casting failure related fracture/dislocation of Test 2 occurred late in the event and was an artifact of the test method.

Table 4.3: Documented fractures during post-test dissection

Test ID	Left Side	Right Side
1	No fractures identified	
2	Casting Failure: T1-T2 dislocation, fracture through T1 body	
3	C1 lateral mass, C4 inf facet, C5 pedicle, C5 sup facet, C6 pedicle and lamina	C5 lamina, inf facet
4	C3-C4 ALL rupture, C4 – ant sup tear drop, C4 spinous process	
5	C5 inf facet, C6 pedicle and lamina	C6 lamina

Neck compressive fracture loads, timing and concurrent shear forces and bending moments are summarized in Table 4.4. The average fracture load was 2,795 +/- 1,107 N. The fracture loads for pre-laterally bent necks (Test 4 and 5) were similar to each other and larger than the single fracture in the neutrally oriented neck. The average time to fracture was 3.3 +/- 1.2 ms.

Table 4.4: Cervical spine forces and moments at the time of fracture

Test ID	Time (msec.)	Forces at Fracture (N)				Moments at Fracture (Nm)		
		X	Y	Z	R	X	Y	Z
3	4.5	305	-70	-1518	1549	-7.2	-21.8	-21.4
4	3.0	500	---	-3396	3433	---	-30.1	-44.5
5	2.2	454	-104	-3472	3503	-9.9	-17.2	-39.3

Axial force dominated the kinetic response at the time of fracture. In all 5 tests, the sagittal plane moment was primarily forward flexion at the base of the neck during the compressive phase, or first 30 to 40 milliseconds, of the response. However, the response in each test began with a 4 to 5 millisecond period of rearward extension. The initial point of failure from the axial load was identified during this period for test 3 through 5 and the injury pattern was consistent with compression-extension type injuries including posterior element fractures

and anterior longitudinal ligament rupture. Lateral shear force and lateral bending moments contributed the least to the mechanical response at the time of fracture.

In the current study, with a limited number of samples, overall torso and the first mode of head impulse served to accurately delineate the presence of fracture across test methods. A head impulse at or above 16.7 N·s. and a torso impulse at or above 42.6 N·s. correlated with the presence of cervical fracture. A head impulse at or below 14.0 N·s. and a torso impulse at or below 38.8 N·s. correlated with the lack of cervical fracture.

4.4 Discussion

This study provides a preliminary examination of the effects of asymmetric postures and asymmetric loading on cervical spine kinetics and kinematics. The results of these tests were compared to the sagittal plane dynamic responses of Nightingale et al. (1997a). The results indicate that moderate amounts of lateral bending resulting from asymmetric loading were similar to previous neutral posture sagittal plane compressive loading results. Impact speeds resulting in catastrophic injury in Tests 3 and 5 were approximately 3.25 m/s. A laterally pre-positioned posture increased the magnitude of the initial compressive force response and the axial force to failure. This is due to a pre-stiffening of the facet joints on the laterally compressed side of the cervical column. In Test 3 and Test 5 in which lateral shear force and bending moment at failure could be determined, the magnitude of these loads are small in comparison to sagittal plane shear and bending responses, however , the laterally eccentric loading caused increased loading through the facet joints which are lateral and posterior the vertebral body. This resulted in initial loading posterior to the center of the C7/T1 intervertebral disc and is consistent with the documented injury patterns.

4.4.1 Cervical Spine Response

Impact speeds in the current study that caused injury were consistent with previous findings, however, the overall head and neck kinetics varied, particularly between test configurations. In Configuration 1 (Tests 1 to 3), peak head impact forces and the resulting impulses were very similar to those reported in the past (Nightingale et al. 1997a). The average impulses due to the torso mass loading the cervical spine as well as the lag in the response at the base of the neck are consistent with previous research.

Corridors for head and neck load for the Nightingale data were reported by Camacho et al. (1999) and are presented in Figure 4.14 with the current data overlaid. Figures 4.14 (A) and (B) represent the current resultant head and neck test data from Configuration 1 (neutral neck with laterally inclined impact plate) and Figures 4.14 (C) and (D) contain the head and neck data from Configuration 2 (pre-positioned laterally flexed neck with horizontal impact plate). The data for the angled plate impacts are very similar to those found for neutral neck loading. Only one of the three tests is substantially above the upper limit of the corridor in Figure 4.14 (B). Figure 4.14 (A) and (B) also indicate that the overall head and neck loading duration is shorter than the respective corridors by approximately 5 ms.

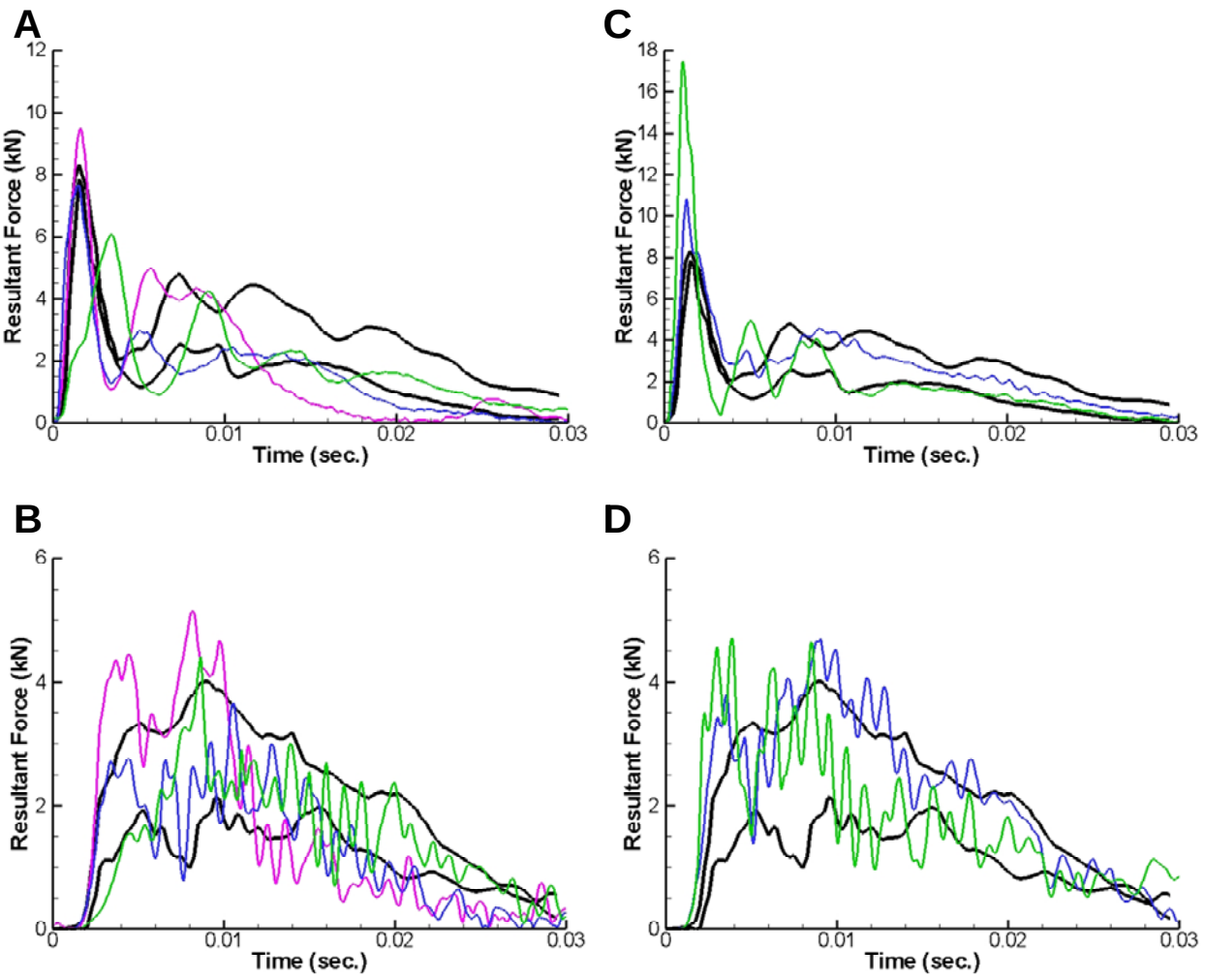

Figure 4.14: Resultant head force (A and C) and neck force (B and D) response comparison to previously published (Camacho et al. 1999) neutral neck / flat plate corridors for tests 1(magenta), 2 (blue) and 3 (green) (A and B) and 4 (blue) and 5 (green) (C and D)

Head contact loads for the lateral bending posture tests (Configuration 2) showed a trend for being substantially higher than head loads for tests with an angled impact plate. The head impulses measured for Configuration 2 were over 40% greater on average than those measured in Configuration 1 and presented in past studies. The contribution of inertial torso forces early in the event might be affecting the response of the neck. The impulses due to the torso mass were approximately 25 +/- 4% of the head impulse after the first mode of the head response which is substantially greater than the 2-10% reported previously (Nightingale et al. 1996b).

The increased head impulse in test Configuration 2 in comparison to the head momentum at impact indicates a more substantial rebound velocity and less of a an opportunity for the head to escape the following torso. In the lateral bending posture tests, the neck is preloaded resulting in stiffening the joints and more directly coupling the mass of the torso to the head. This would likely result in an increase in the effective mass of the head at initial contact. This may be one of the factors resulting in increased head loads in test Configuration 2. In addition, the lag between the head and neck loads is shorter for the pre-lateral bent tests consistent with a tighter couple between the head and the torso. Additionally, the torso impulse, or magnitude of torso momentum arrested, was greater for Configuration 2. Test 4 was the only case in which the torso impulse was greater than the torso momentum at contact. This is consistent with the observation from the test video that Test 4 was the only case in which the torso was fully arrested and rebounded slightly.

The sagittal plane bending moment was also compared to work previously conducted by Nightingale et al. (1997a). The moment responses for neutral neck / rigid flat plate tests were averaged and corridors defined by one standard deviation greater than and less than the mean response. Figure 4.15 displays the current experimental results overlaid on the calculated corridors. Similar to the axial neck load response, Figure 4.15 (A) shows that Configuration 1 tests follow the flat plate corridors well. Since the moment response is being driven by the axial load, it is not surprising that similar to Figure 4.14 (B), the overall duration is shorter than the respective corridors by approximately 5 ms. The response of the pre-laterally flexed necks are shown in Figure 4.15 (B). In general, the experimental moment response again fits reasonably well in the corridors. The peak magnitude response for Configuration 2 is slightly greater than the previous testing.

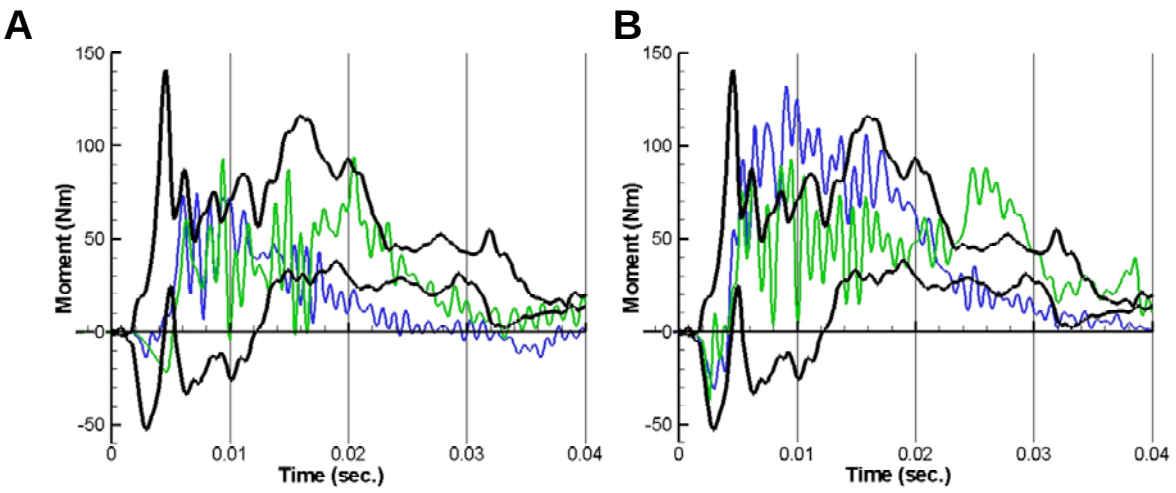

Figure 4.15: Sagittal plane bending moment response for tests 2 (blue) and 3 (green) (A) and 4 (blue) and 5 (green) (B) compared to previously neutral neck / flat plate tests (Nightingale et al. 1997a). A positive sagittal moment (My) indicates forward flexion at the base of the neck

4.4.2 Cervical Spine Tolerance

The failure load of 1,518 N in Test 3 with a neutrally oriented cervical spine is similar to reported tolerances by Nightingale et al. (1997a). The failure loads in Tests 4 and 5 using a pre-laterally flexed cervical spine were higher than one standard deviation above this same injury tolerance. The higher failure force is consistent with reported results from Pintar et al. (1995) who found mean failure loads of 3,326 N for the cervical spine in compression. The major difference in the test setup of Pintar compared to Nightingale and the current study was a pre-flexion of the head and neck that removed the resting lordosis of the cervical spine and aligned the vertebral column. Results indicate that pre-lateral flexion of the neck, while maintaining the resting lordosis of the spine, has a similar effect of increasing the compressive axial force tolerance. Figure 4.16 compares the failure loads in the current study to those reported by Nightingale et al. and Pintar et al. The increased axial force response in Tests 4 and 5 is due to a pre-stiffening of the facet joints on the laterally compressed side of the cervical column.

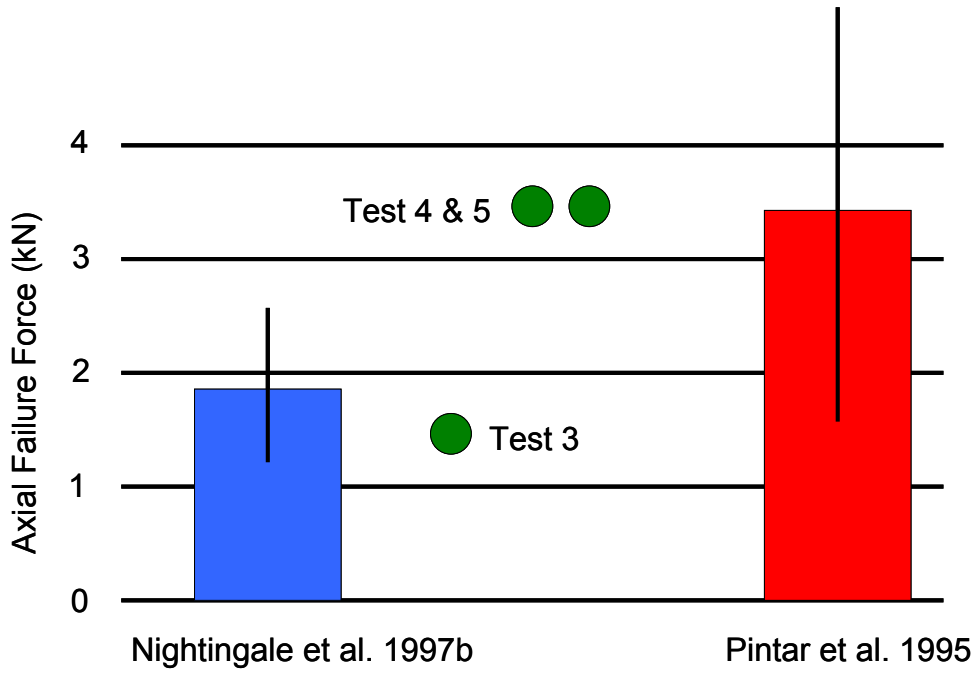

Figure 4.16: Average failure force reported by Nightingale et al. 1997a and Pintar et al. 1995 compared to the failure forces in Test 3, 4, and 5

Anterior – posterior shear force, lateral shear force and lateral bending moment do not contribute significantly to the kinetics at the time compressive failure of the cervical spine. The sagittal plane bending moment was primarily forward flexion at the base of the neck. However, this response began with a 4 to 5 millisecond period of rearward extension moment prior to buckling of the cervical spine. The initial point of failure was identified during this period of time. The negative sagittal plane moment, or posterior eccentricity, is consistent with the identified cervical damage and the geometry of a vertebra. Even though the lateral shear force and lateral bending moments contributed the least to the mechanical response at the time of initial failure, any degree of lateral eccentricity increases the loading through the facet joints, and consequently the posterior elements, which are lateral to the vertebral bodies. It is this loading through the facet joints that also explains the fairly significant torsional moments at failure as the facet joints are obliquely angled inferiorly as the joint extends posteriorly. The influence of these torsional moments on cervical tolerance is not currently well defined.

The numbers of specimens tested serve as limitation in drawing conclusions on a statistical basis. This preliminary investigation outlines general findings and trends that might help guide further research. Another limitation of the current study is lack of passive or active muscle contribution during the testing. Passive cervical spine muscle response has been shown to only slightly increase compressive cervical spine injury risk in finite element modeling (Hu et al. 2008). Active muscle response has been documented to occur 50 to 65 ms following head loading (Foust et al 1973, Schneider et al. 1975). Since the injuries in the current study have been identified to occur at 3.2 +/- 1.2 ms following head contact, the influence of cervical muscle reaction would be absent at the time of injury. Finally, four of the five test subjects utilized in the current study were 76 years of age or older. Test specimen number 5 was 55 years of age. Pintar et al. (1998b) has reported that the cervical spine failure force for loading rates between 2 m/s and 4 m/s decreases with age. The failure loads reported in the current study likely underestimate the failure loads for younger individuals.

4.5 Conclusions

Overall compressive neck injury dynamics and tolerances are similar to previous studies of purely sagittal plane dynamics based on these test results. Impact speeds for the five tests ranged from 2.9 to 3.25 m/s. Three of the five PMHS sustained compressive cervical vertebral fractures at loads ranging between 1,518 N and 3,472 N. The asymmetric postures and loading resulted in asymmetric fracture patterns. The pre-laterally flexed neck affected the neck axial force response and the average failure load in the current study. The initial axial response indicated a better coupling between the head and torso and the average failure load was approximately 50% greater than the average failure load reported for males in the past (Nightingale et al. 1997a). Although lateral pre-positioning of the head-neck complex influenced axial response, shear forces and the lateral bending moment magnitudes at failure were small in comparison to sagittal plane responses in both test configurations. These secondary kinetics primarily act to modify the location of the applied axial force relative to the cervical column and

in doing so, influence the magnitude of the axial response and specific injury outcomes. Based on the small sample of experiments conducted, Configuration 1 axial response and failure load appears consistent with the neutral posture sagittal plane studies of Nightingale et al. (1997a) while Configuration 2 failure loads appear consistent with the pre-flexed posture sagittal plane studies of Pintar et al. (1995).

CHAPTER 5

FURTHER INVESTIGATION INTO PMHS CERVICAL SPINE COMPERSSION TOLERANCE THROUGH COMBINATION OF MULTIPLE DATA SETS

5.1 – Introduction

Biomechanical investigations using PMHS have been an essential element in the current understanding of the complex dynamics of compressive cervical spine injury including cervical column buckling, injury timing with respect to head motion, and the effects of contact surface padding on neck injury risk (Nusholtz et al. 1983, Alem et al. 1984, Yoganandan et al. 1986, Pintar, Nightingale et al. 1996a, 1996b, Camacho et al. 2001). Compressive injury tolerance has historically been reported by identifying the peak axial force at injury measured at the base of the neck (Pintar et al. 1995 and Nightingale et al. 1997a). However, as an injury predictor, compressive force at failure exhibits wide variation and this has been attributed to the alignment of the cervical vertebra and the end conditions of test methodology used. Results from the previous chapter on the effects of lateral bending on compressive neck response and tolerance resulted in fracture loads consistent with the range of failure loads reported by Nightingale et al. (1997a) when the cervical spine's natural lordosis was maintained and Pintar et al. (1995) when the neck was pre-laterally flexed. Development and refinement of an injury criterion that incorporates the effects of compressive load eccentricity across the range of studies performed to date has the potential to lead to a more sensitive and robust injury predictor than axial force alone. Portions of the this chapter have been published in Traffic Injury Prevention.

5.1.1 Mechanistically Relevant Injury Criteria

Several composite neck injury tolerance criteria for compressive loading events have been proposed for both the upper and lower cervical spine that incorporate the effects of combined compressive loading modes including Nij. The linear combination of axial force and

bending moment has a basis in generalized mechanics. The upper neck Nij intercepts for combined tension and extension loading were derived by calculating the approximate maximum normal stress in the anterior longitudinal ligament (ALL) at the level of the occipital condyles (Mertz and Prasad 2000). In compressive loading, the maximum normal stress in a structural member (or strut), takes the form:

$$\text{(Equation 5.1)}\quad \sigma_{\max} = \frac{P}{A} + \frac{My_{\max}}{I} = \frac{P}{A} + \frac{Pey_{\max}}{I}$$

where P is the axial force, M is the moment, A is the cross sectional area of the strut, I is the second moment of the area, e is the distance from the central axis that the load is applied (eccentricity) and y is the distance from central axis for the location the stress is being calculated (see Figure 5.1A).

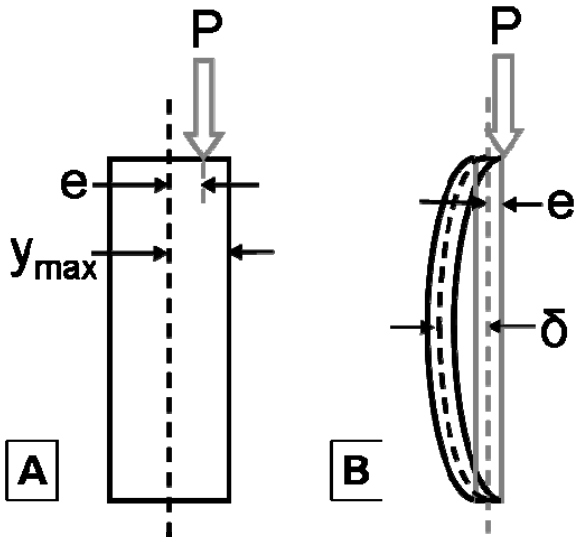

Figure 5.1: Generalized eccentric loading condition of a compressive strut (A) and a slender column (B)

As the cross sectional geometry of a compressive strut decreases while holding the length the same, the likelihood of buckling increases. In this case of a slender column as shown in Figure 5.1B, the maximum moment in Equation (5.1) is a function of not only the axial load

and its eccentricity but also the transverse deflection, δ, of the column (Equation 5.2). After solving for this deflection, the maximum normal stress is represented by Equation (5.3) known as the secant column formula (Shigley and Mischke, 1989). Regardless of whether the cervical spine is thought of as a compressive strut or slender column, the combination of axial force and the eccentricity at which it is applied has merit as a potential injury criteria based on fundamental mechanics.

(Equation 5.3) $$M_{\max} = -P(e+\delta)$$

(Equation 5.4) $$\sigma_n = \frac{P}{A}\left[1+\frac{ec}{k^2}\sec\left(\frac{l}{2k}\sqrt{\frac{P}{EA}}\right)\right]$$

5.1.2 PMHS Data Available for Consideration

In order to account for a range of applied loading vectors and cervical postures, a combined data set of relevant cervical spine tolerance data needs to include studies of whole cervical spine kinematics and inertial loading by the head. The minimum number of quantified parameters includes; known end conditions, spinal posture, injury outcomes and the kinetics at the base of the neck. Research conducted by three investigating groups meet the above criteria. They include Pintar et al. (1995 and 1998a), Nightingale et al. (1997a) and the experimentation conducted as part of this research. Amongst these three groups, two primary test methodologies have been used. Pintar et al. aligned the cervical column of a PMHS head-neck complex by pre-straitening the neck and impacted the apex of the head using an MTS machine and Nightingale et al. designed an inverted drop track with a simulated torso mass and mounted a head-neck complex with the cervical spine resting lordosis maintained. The current research adopted the general methodology of Nightingale at al. but investigated laterally oriented impact surfaces and pre-laterally positioned cervical spines.

The purpose of the following research is to attempt to identify a more sensitive and robust predictor of compressive injury in the PMHS cervical spine than the range of currently reported axial force tolerances. By including multiple data sets, a variety of conditions including head constraint, head-neck posture and test methodology can be evaluated while increasing to the overall number of test specimens considered for statistical analysis. A PMHS lower neck Nij, a combination of sagittal plane resultant force and its applied anterior-posterior eccentricity at the C7/T1 intervertebral disc, and axial impulse were evaluated for their ability to predict the presence of cervical damage in the PMHS.

5.2 Methodology

Combining the experiments of the studies outlined above results in a total of 57 experiments in which electronic data was available, 56 of which include the necessary information to transform the bending moments to the center of the C7/T1 disc. The data set of Nightingale et al. (1997a) includes 22 experiments of 21 PMHS, 16 of which resulted in cervical damage that was reported in detail. Pintar et al. (1995) conducted 20 PMHS experiments, all of which resulted in some form of documented injury. The 1998a study by Pintar et al. included an additional 10 PMHS experiments. Each experiment resulted in an injury outcome that was put into one of two groups of general injury descriptions, but injury specifics for each experiment were not available. Finally, the current research included 5 PMHS experiments, 3 of which resulted in cervical damage.

5.2.1 Data Processing

The data from each experiment was digitally filtered per SAE J211-1. Moment transformations were conducted as described in Chapter 4.2.4. The lower neck axial impulse was calculated by integrating the axial force at the center of the C7-T1 intervertebral disc. Integration was performed numerically using the trapezoidal rule. Integration began at the time of head contact and ended after the compression force returned to zero. In the case of impact

with a padded surface, the compressive load in the neck often did not return to zero and instead reached a steady state load approximately equal to the static force of the torso mass. In these cases, the integration was ended once the axial force reached a local minimum.

During impacts to the apex of the head, the location, magnitude and direction of the resultant load applied to the head directly influence the magnitude and direction of the lower neck reaction force and moment response. Figure 5.2 shows three equivalent depictions of a general loading scenario. The use of sagittal plane resultant force combined with eccentricity of the applied force relative to the center of the C7/T1 intervertebral disc allows for comparison of a range of initial neck orientations. The sagittal plane eccentricity (Exz) relative to the center of the C7-T1 intervertebral disc can be calculated using Equation (5.4) which only incorporates the neck reaction forces and moments. Eccentricity is fundamentally the perpendicular distance between the force line of action and center of the intervertebral disc.

(Equation 5.4) $$Exz = \frac{My}{Fxz} = \frac{My}{\sqrt{Fx^2 + Fz^2}}$$

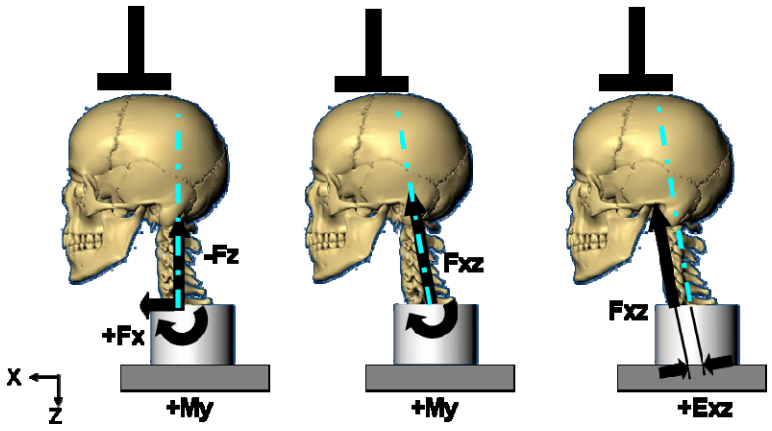

Figure 5.2: Equivalent representations of a generalized two-dimensional loading scenario depicting the relationship between sagittal plane kinetics and resultant sagittal plane force eccentricity

5.2.2 Injury Severity

The severity of cervical injuries in the AIS injury scaling system is highly dependent on neurological dysfunction and the magnitude of spinal cord involvement. Testing with PMHS limits the cervical damage documentation to clinically recognized orthopedic injuries. Each of the research groups whose studies are included in this combined data set utilized slightly different injury severity descriptions.

The experiments conducted as part of the current study and those conducted by Nightingale et al. used the clinical stability of the orthopedic damage sustained by the PMHS as an indication of cervical spine injury severity. Unstable injuries are more likely to involve the spinal cord and require surgical intervention (White and Panjabi, 1990). Pintar et al. used two similar injury severity scales in each of their studies. In the 1995 study, cervical damage was classified as either minor, moderate, or severe. Minor injuries were defined as trauma not requiring appreciable clinical intervention, moderate injuries were defined as trauma requiring moderate intervention with external and possibly internal (surgical) intervention and severe injuries were defined as trauma requiring appreciable internal (surgical) and external intervention. Finally, the 1998a Pintar et al. study defined injuries as either minor or major. Minor injuries included mainly disruption of lower cervical spine posterior ligaments at one level and major injuries included extensive liagamentous injury usually with vertebral fracture and/or complete dislocation. Spinal cord pressures were monitored and major injuries resulted in higher local cord pressure at the site of injury, increasing the risk for acute spinal cord trauma.

Based on the injury definitions from the various studies, stable and minor both describe injuries that do not likely require surgical intervention. Unstable, severe, and major describe injuries that likely require surgical intervention. The last category of injury severity is moderate from Pintar et al. (1995) which describes injuries that possibly require surgical intervention. Using the three column concept of spine stability, the classification of major and unstable groups can be interpreted to involve at least two columns and minor injuries one of the three

columns (Denis, 1984). The involvement of at least two of three columns often times leads to a more aggressive treatment regimen. The 10 experiments with documented injuries in the moderate category include complete posterior ligament rupture, anterior and posterior damage at the same cervical level, vertebral body fractures at multiple levels, and single vertebral body fractures including wedge and compression fractures. Two of the experiments with moderate injuries were subsequently included in the Pintar et al. 1998a study where they were classified in the major injury category. Based on the available injury descriptions, 7 of 10 experiments can reasonably be classified as more likely than not requiring surgical intervention due to involvement of two columns. Therefore, all 10 experiments were included with the unstable, severe and major group of injuries for purposes of statistical analysis.

5.2.3 Derivation of Injury Metrics

A two-dimensional plot of axial forces versus sagittal plane moment at failure was created using each experiment with an identified injury. A second two-dimensional plot was created using sagittal plane resultant force versus and its applied eccentricity at the time of identified failure. Linear regressions were conducted for both anterior and posterior moment and eccentricity to evaluate the presence or absence of a relationship between these variables.

In order to better define potential relationships between these variables, the data were categorized by gender, injury type and injury location and further analyzed using linear regression. The injury types included the presence of bony fracture or ligamentous only. Vertebral avulsion “fractures” were categorized as ligamentous damage. The injury locations included upper or lower cervical spine and anterior or posterior based on the mechanistic injury causing load eccentricity as defined by Winkelstein and Myers (1997) (see Figure 3.5). For example, wedge fractures and bilateral facet dislocations were identified as anterior injuries and pedicle or lamina fractures and anterior longitudinal ligament tears were categorized as posterior injuries.

Linear regressions were performed for anterior and posterior moment and eccentricity injuries. The linear regressions intercept values were constrained to be equal for both anterior and posterior regressions of a give two-dimensional plot. This was accomplished using Microsoft Excel solver to determine the three unknowns, the y-intercept (force), the anterior regression slope, and the posterior regression slope, while maximizing the coefficient of determination (R2) for the combined regressions.

5.2.4 Consideration of Donor Age

The peak force and failure force were scaled to account for PMHS donor age for each experiment. Riggs et al. (1981) reported unique linear relationships between bone mineral density and age for non-osteoporotic men and women (Figure 5.3). The reported linear regression equations for men and women are:

(Equation 5.5) $$BM_{MEN} = 1.33 - 0.0021 * age$$

(Equation 5.6 $$BM_{WOMEN} = 1.59 - 0.0092 * age$$

Nuckley and Ching (2005) have reported a linear relationship between vertebral bone mineral density and yield strength. Based on this relationship, the peak and failure loads for each PMHS were scaled to the age of 61, which is the average donor age of all PMHS included the combined cervical spine compressive data set. The linear regressions conducted as described in section 5.2.3 were repeated with the scaled loads to evaluate the influence of donor age on the regressions.

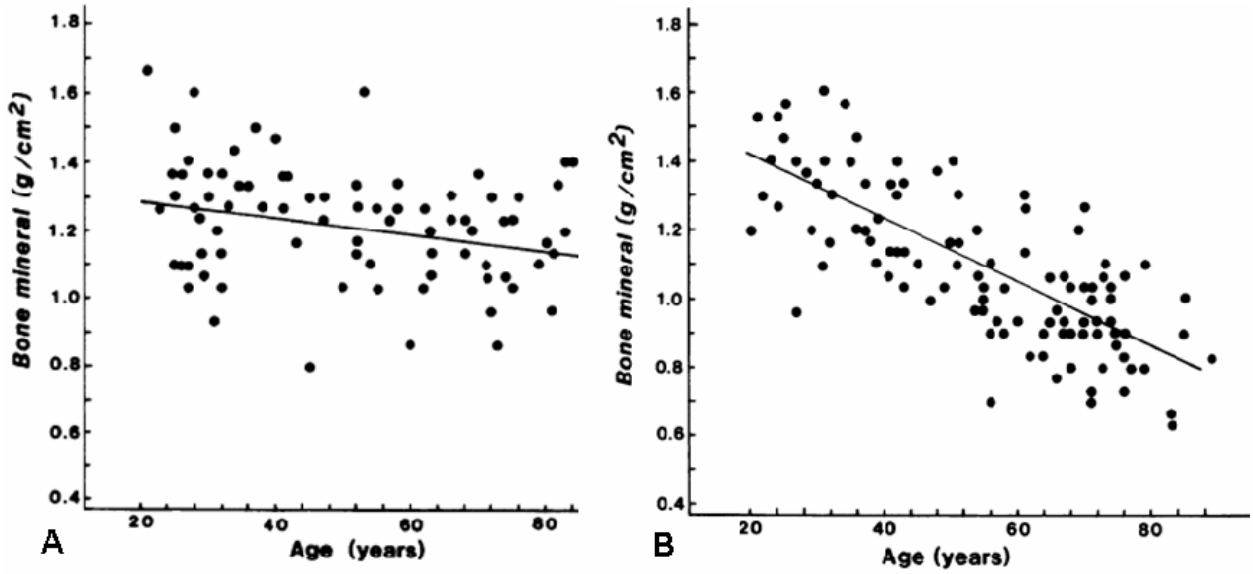

Figure 5.3: Linear regression of normal (no osteoporosis) men (A) and women (B) bone mineral density versus age taken directly from Riggs et al. (1981)

5.2.5 Statistical Methods and Distribution Analysis

Two statistical methods were used to evaluate the significance of differences between the means of two populations. The first method is the parametric t-test for unequal samples and unknown variances which assumes a t distribution. The second is the non-parametric Wilcoxon Rank-Sum test which is particularly useful when sample sizes are small and variances are unknown or unequal (Milton and Arnold, 1995). Significance levels were set at $p < 0.05$. When multiple qualitative independent variables exist in the two groups being compared, such as the test method utilized, the type of injury sustained, and the severity of the injury sustained, analysis of variance (ANOVA) was also conducted using XLSTAT Pro.

In physical experimentation, the mechanical stimulus at failure is traditionally used to define injury tolerance. Since PMHS without documented cervical damage has not yet failed, a direct comparison of mechanical responses between damaged and undamaged PMHS is problematic. These undamaged PMHS are right censored data as the mechanical stimulus necessary to cause a material failure is greater than what was applied during the experiment. Taking into account stronger or non-failed PMHS experiments that have been conducted is

necessary for a complete understanding of the probability of compressive cervical injury tolerance. Survival or reliability analysis allows for the analysis of a dichotomous dependant variable (injury or no injury) using censored data.

Survival analysis can be conducted with assumed parametric distributions or with a non-parametric distribution. Generally, non-parametric analyses more accurately represent the underlying data set so are better suited for comparison of two survival (failure) curves. A sensitive injury metric has the ability to predict the severity of an injury outcome based on the mechanical stimulus. The current study evaluates multiple injury predictors' ability to delineate the severity of injury using non-parametric distribution survival analysis techniques. The probability curve for sustaining a stable compressive cervical spine injury was constructed by using mechanical stimulus at the time of documented stable injury (uncensored) and the maximum stimulus for non-injured (right censored) PMHS experiments. Similarly, the probability curve for sustaining an unstable injury was developed using the mechanical stimulus at the time of documented unstable injury (uncensored) and the maximum stimulus in non-injured and stably injured (right censored) PMHS experiments. The primary assumption is that with more mechanical stimulus (regardless of which injury metric is used) the severity of orthopedic damage and thus risk of spinal cord involvement will increase. The Kaplan-Meier method was used to develop non-parametric survival curves (Kaplan and Meier, 1958). Log-Rank and Wilcoxon test methods were applied to stably and unstably injured PMHS failure curves to test for differences between them. The null hypothesis is that there is no difference between the two populations in the probability of a failure at any point in time. The Log-Rank test is more likely to detect a difference between groups when the risk of failure is consistently greater for one group versus the other and is most sensitive to differences at higher stimulus. The Wilcoxon test is more sensitive at detecting differences at low stimulus (Allison, 1995 and Maller and Zhou, 1996).

When ultimately creating an injury risk curve, parametric distributions are advantageous because the tails or extents of the injury curve are likely a better representation of the true injury risk at very low and very high stimuli where there is little experimental data. Multiple parametric distributions were evaluated using maximum likelihood methods and the goodness-of-fit of the data to assumed distributions was evaluated for each injury metric. The adjusted Anderson-Darling (A-D) statistic was used to assess the fit of the data. A smaller A-D statistic indicates the distribution fits the data better (Kent and Funk, 2004). In addition to assessing a given injury metrics ability to delineate the severity of injury using non-parametric methods, good fit of a parametric distribution increases the overall confidence that the derived injury risk, including at the extents of the risk curve, is accurate and appropriate. Minitab Version 16.2.2 was used for all parametric and non-parametric distribution analyses.

5.3 Results

A summary of the sagittal plane mechanical responses at the time of documented failure and at the time of peak axial force are summarized in Tables 5.1 for the inverted drop tests and in Table 5.2 for the superior to inferior impacts with an MTS machine. The results tables include PMHS gender, age and test conditions including impact velocity and either impact orientation or posture. Sagittal plane kinetics at the time of failure and peak load as well as the scaled kinetics at failure based on Riggs bone mineral density regressions are listed. The drop cart (torso) and impactor displacements at the point of failure and peak load are included. Finally, the calculated impulse from the base of the neck axial force and documented injury information is listed.

Table 5.1: Inverted drop test data from current study and Nightingale et al. 1997a

General Information					Failure Kinetics						Scaled Kinetics			Kinetics @ Peak Force							Injury Information	
Test ID	Age	Gender	Test Cond.	Vel. (m/s)	Time (msec.)	Fz (N)	Fxz (N)	My (Nm)	Ecc (mm)	Disp (mm)	Fz* (N)	Fxz* (N)	My* (Nm)	Time (msec.)	Fz (N)	Fxz (N)	My (Nm)	Ecc (mm)	Disp (mm)	Impulse (N·s)	Injury Stability	Injury Description
1	76	M	Config 1	2.91	-	-	-	-	-	-	-	-	-	8.2	-5122	5146	-	-	23.6	38.8	NI	
2	80	M	Config 1	3.07	10.6	-	-	-	-	-	-	-	-	10.6	-3643	3656	41.7	11.4	27.8	37.2	NI	
3	55	M	Config 1	3.25	4.5	-1518	1548	-21.8	-14.1	14.6	-1502	1532	-21.6	8.7	-4371	4407	37.5	8.5	26.2	42.6	unstable	C5 lamina/pedical/upper & lower facets
																					stable	C6 lamina and pedicle
																					stable	C1 left lateral mass
4	77	M	Config 2	2.91	3	-3396	3433	-30.1	-8.8	8.7	-3494	3531	-31.0	9.1	-4694	4695	131.9	28.1	21.8	64	stable	C4 spinous, C4 ant sup tear drop, C3-C4 ALL
5	88	M	Config 2	3.26	2.2	-3472	3502	-17.2	-4.9	7.3	-3644	3675	-18.1	3.8	-4669	4709	3.4	0.7	11.9	50.5	stable	C5 inf facet, C6 pedicle/lamina
N05	36	M	30	3.23	8.3	-1552	1593	-27	-17.0	25.8	-1487	1526	-25.9	16.3	-1858	1865	-4.7	-2.5	46.6	35.8	unstable	C3 burst
																					stable	C3-C4 disc / ALL
																					stable	C4-C5 ALL
N18	-	M	15	3.26	6.4	-1871	1895	13.2	7.0	19.8	-1871	1895	13.2	11.7	-2494	2531	12.9	5.1	32.9	62.7	unstable	C6-C7 BFD
																					unstable	C2 hangman, C2-C3 Disc/ALL
																					stable	C1 lateral mass
D41	69	M	15	3.11	-	-	-	-	-	-	-	-	-	5.7	-3839	3870	3.6	0.9	17.1	60.8	NI	
I32	78	M	15	3.18	3.9	-2416	2612	-0.8	-0.3	11.9	-2490	2691	-0.8	2.8	-2905	2921	58.3	20.0	8.9	40.6	stable	C5-C6 disc / ALL / L capsular lig
N26	65	M	0	2.43	-	-	-	-	-	-	-	-	-	8.9	-3877	4189	-19	-4.5	18.2	48.3	NI	
N24	62	M	0	3.2	2.2	-1845	1975	15.5	7.8	-	-1848	1978	15.5	8.5	-2308	2414	71.7	29.7	-	40.9	stable	C1 2 part posterior arch, C2 hangman
N22	71	M	0	3.26	6.5	-1966	2105	63.7	30.3	-	-2001	2142	64.8	14.1	-2814	2870	77.7	27.1	-	48.3	unstable	C1 3 part comminuted
N11	55	M	-15	3.14	-	-	-	-	-	-	-	-	-	6.6	-2539	2891	22.1	7.6	19.7	24.6	NI	
N13	35	F	-15	3.28	-	-	-	-	-	-	-	-	-	9.1	-1987	2087	47.5	22.8	27.7	22.6	NI	
UK3	62	F	-15	3.13	-	-	-	-	-	-	-	-	-	4.8	-3898	3977	-13.5	-3.4	14.6	37.3	NI	
N21	61	M	30	3.13	14.8	-1635	1662	19.7	11.9	45.6	-1635	1662	19.7	20.9	-1757	1760	9.6	5.5	61.2	44.3	stable	C5-C6 disc / ALL / L capsular lig
																					stable	C4 spinous fx
																					stable	C5 spinous fx
																					stable	C1 ant ring fx
N23A	46	M	30	3.03	-	-	-	-	-	-	-	-	-	22	-2052	2096	-23.8	-11.4	64.1	41.9	NI	
N23B	46	M	30	3.51	18.7	-2241	2350	-36.8	-15.7	62.2	-2183	2289	-35.9	18.7	-2241	2350	-36.8	-15.7	62.2	40.5	stable	C4-C5 disc / ALL
																					stable	C3-C4 disc / ALL
																					stable	C1 2 part right fx
I08	80	M	15	3.15	30.5	-2915	2918	42.2	14.5	74.5	-3015	3018	43.6	18.1	-4273	4309	50.8	11.8	55.2	78.6	unstable	C2 hangman and burst
I11	63	F	15	3.2	14	-967	972	19.5	20.1	-	-985	990	19.9	20.8	-2085	2096	26.3	12.5	-	71.8	unstable	C2 typeIII dens + comminution
																					stable	C4 body and R lamina
I04	63	M	15	3.19	18	-1675	1698	39.1	23.0	56.3	-1681	1704	39.2	22.1	-2218	2260	49.4	21.9	67.3	74.1	unstable	C2 hangman, C2-C3 dis ALL
																					stable	C1 2 part pos arch
																					stable	C7-T1 pos ligs
N03	75	M	0	3.08	18.2	-3473	3509	30.4	8.7	53.2	-3560	3596	31.2	21.3	-3937	4011	56.8	14.2	59.2	62.7	unstable	C6-C7 BFD
																					stable	C5-C6 disc
																					stable	C4-C5 capsular lig
N02	75	F	0	3.14	14.7	-787	800	12.3	15.4	45.9	-900	914	14.1	34.4	-2131	2149	20.1	9.4	93.2	76	unstable	C7 burst
																					stable	C6 R lamina/pedicle
																					unstable	C2 hangman + type III dens
																					stable	C1 ant ring
D40	53	F	0	3.16	16.7	-1438	1440	6.2	4.3	51.5	-1342	1344	5.8	38.7	-2486	2491	22.1	8.9	90.1	81.1	unstable	C5 burst, C5-C6 PLL
																					stable	C6 R lamina/pedicle
																					stable	C3-C4 disc / ALL / spinous
																					unstable	C1 3 part comminuted
N19	42	F	-15	3.07	18.8	-1013	1037	-1.3	-1.3	56.8	-866	887	-1.1	24.9	-1120	1221	-26.3	-21.5	73.7	24.5	stable	C3-C4 disc / ALL / C3 avulsion
																					stable	C2-C3 disc/ALL/C2 avulsion
NA2	61	M	-15	3.16	15.6	-1969	2091	45.2	21.6	48.5	-1969	2091	45.2	15.6	-1969	2091	45.2	21.6	48.5	35.1	stable	C3-4 disc/ALL/ L capsular lig
																					stable	C5-C6 disc / ALL
I25	59	M	-15	3.07	18.4	-2565	2585	30.9	12.0	54.9	-2556	2576	30.8	17.5	-3443	3448	33.8	9.8	52.5	39.7	unstable	C3-C4 disc/ ALL /PLL/ L capsular lig
																					stable	C1-C2 capsular lig

Table 5.2: MTS impactor test data from Pintar et al. (1995 and 1998a)

General Information					Failure Kinetics						Scaled Kinetics			Kinetics @ Peak Force							Injury Information	
Test ID	Age	Gender	Initial Ecc.	Vel. (m/s)	Time (msec.)	Fz (N)	Fxz (N)	My (Nm)	Ecc (mm)	Disp (mm)	Fz* (N)	Fxz* (N)	My* (Nm)	Time (msec.)	Fz (N)	Fxz (N)	My (Nm)	Ecc (mm)	Disp (mm)	Impulse (N·s)	Injury Stability	Injury Description
1	67	F	-0.5	3.13	7.0	-1186	1197	-0.3	-0.3	-	-1253	1265	-0.3	13.4	-1588	1597	13.2	8.3	-	21.1	minor	vertical frx C3 body
2	62	F	0	5.57	4.1	-3680	3682	4.5	1.2	20.5	-3713	3715	4.5	4.1	-3680	3682	4.5	1.2	20.5	25.6	severe	burst frx C5 body
3	77	F	0	6.36	3.9	-766	778	1.3	1.7	22.9	-893	908	1.5	7.7	-1179	1179	-9.8	-8.3	38.7	16	severe	wedge frx C4, comp frxs C2,C3
4	50	M	0	8.37	4.2	-5010	5011	-13.4	-2.7	24.6	-4915	4916	-13.1	4.2	-5010	5011	-13.4	-2.7	24.6	26.1	mod	wedge frx C6 body
5	38	F	0.5	7.99	3.5	-5857	6192	127.5	20.6	25.1	-4858	5135	105.7	3.5	-5857	6192	127.5	20.6	25.1	42.1	mod	C3-C4 ALL w. C3 avulsion
6	68	F	0.5	7.77	4.2	-3440	3442	22.9	6.7	27.1	-3669	3671	24.4	4.2	-3440	3442	22.9	6.7	27.1	26.5	severe	C2-C3 dislocation w. ligamentous rupture
7	67	M	0.5	-8.06	3.8	-4567	4970	77.6	15.6	25	-4615	5023	78.4	3.8	-4567	4970	77.6	15.6	25	29.4	mod	C4 frx ant body
8	48	M	0	-5.56	5.6	-3912	3925	14.4	3.7	26.6	-3825	3838	14.1	6.6	-4920	4937	0.4	0.1	29.6	41	mod	vertical frx C3 body w. lamina frx
9	50	M	0	-6	4.7	-5172	5221	-1.8	-0.3	24.6	-5074	5122	-1.8	6.2	-5638	5638	-20.2	-3.6	29.4	41	minor	ant-sup chip frx C3 body
10	59	M	0	-5.62	4.6	-3713	3778	15.8	4.2	25.4	-3700	3765	15.7	4.6	-3713	3778	15.8	4.2	25.4	34.1	mod	comp frxs C4 / C7 bodies
11	59	M	-0.5	-6.22	4.8	-4805	4824	-64.1	-13.3	26.7	-4788	4807	-63.9	4.8	-4805	4824	-64.1	-13.3	26.7	46.7	mod	C3-C4 ALL and C4, C5 spinous proc frx
13	82	M	2.5	-6.01	5.2	-2281	2372	12.6	5.3	23.5	-2368	2462	13.1	5.2	-2281	2372	12.6	5.3	23.5	17	minor	C6-C7 interspinous lig tear
14	60	F	0	-5.97	4.6	-3052	3073	107.5	35.0	26.7	-3025	3046	106.5	7.3	-3596	3603	132.8	36.9	36.3	27.1	severe	burst frx C5 body
15	95	F	-0.5	-3.08	11.8	-1336	1336	10.7	8.0	29.8	-1919	1920	15.4	14.9	-1645	1645	14.7	8.9	37.1	26.5	mod	C6-C7 ALL w. C6, C7 lamina frx
16	64	F	3	-6.07	5.4	-2554	3063	155	50.6	29.3	-2624	3147	159.3	5.4	-2554	3063	155	50.6	29.3	12.5	mod	C6-C7 posterior ligaments
17	66	M	0	-5.97	4.4	-2901	2902	88.7	30.6	22.8	-2927	2927	89.5	4.4	-2901	2902	88.7	30.6	22.8	22.9	mod	comp frx C5 body
18	54	M	0.5	-6.13	5.1	-2697	2732	97.5	35.7	27.1	-2664	2698	96.3	5.1	-2697	2732	97.5	35.7	27.1	31.7	minor	mild comp C7 body
19	76	M	2	-3.1	9.3	-2718	2846	-8.7	-3.1	23.2	-2792	2922	-8.9	15.1	-2927	3088	17.3	5.6	36.4	38.8	mod	C7-T1 posterior ligaments
20	29	F	1	-3.2	10.5	-2387	2422	-12.8	-5.3	26.1	-1856	1883	-10.0	11	-2462	2510	-13.6	-5.4	27.3	28.6	severe	burst frx C5 body w. C5-C6 posterior ligaments
21	76	M	0.5	-3.08	11.2	-3666	3690	-4.5	-1.2	27.7	-3764	3789	-4.6	11.2	-3666	3690	-4.5	-1.2	27.7	37.2	severe	burst frx C4 w. C3-C4 posterior ligaments
1	50	M	-	-5.14	2.0	-3521	3611	155	42.9	9.7	-3616	3708	159.2	2	-3521	3611	155	42.9	9.7	38.1	major	extensive lig w. fx and/or dislocation
2	46	M	-	-5.3	3.9	-4345	4600	8.7	1.9	20.5	-4462	4724	8.9	6.3	-4702	5120	42.2	8.2	30	39.9	major	extensive lig w. fx and/or dislocation
3	56	M	-	-3.6	5.4	-1915	2136	32.6	15.3	17.9	-1967	2193	33.5	9.1	-2177	2526	65.9	26.1	27.1	27.5	minor	lower cervical spine posterior ligament disruption
4	39	F	-	-3.6	10.9	-2386	2715	-21.6	-8.0	30.1	-2450	2788	-22.2	10.9	-2386	2715	-21.6	-8.0	30.1	38.2	major	extensive lig w. fx and/or dislocation
5	61	M	-	-3.26	7.1	-999	1109	12.6	11.4	18.4	-1026	1138	12.9	7.1	-999	1109	12.6	11.4	18.4	20	minor	lower cervical spine posterior ligament disruption
6*	76	F	-	-3.7	56.1	-591	591	37.9	64.1	-8.7	-607	607	38.9	-	-	-	-	-	-	-	minor	lower cervical spine posterior ligament disruption
7	58	F	-	-3.6	7.6	-1467	1521	53.4	35.1	23	-1506	1562	54.8	7.6	-1467	1521	53.4	35.1	23	16.1	minor	lower cervical spine posterior ligament disruption
9	49	M	-	-2.7	7.1	-640	754	43.6	57.8	17.9	-657	774	44.8	7.1	-640	754	43.6	57.8	17.9	7.6	minor	lower cervical spine posterior ligament disruption
10	43	M	-	-2.7	5.6	-2256	2377	11.5	4.8	15.1	-2317	2441	11.8	5.6	-2256	2377	11.5	4.8	15.1	35.6	major	extensive lig w. fx and/or dislocation
12	69	M	-	-5.7	3.6	-3258	3605	10.6	2.9	21.4	-3346	3702	10.9	3.6	-3258	3605	10.6	2.9	21.4	31.5	major	extensive lig w. fx and/or dislocation

* Short duration peak force present in the middle of the data trace that does not apear related to PMHS - reported failure kinetics are not reliable

5.3.1 Injury Metric Derivation

Experimental variables that describe the overall severity of impact, such as impact velocity, are often used to describe tolerance to injury. Impact velocity is not appropriate for combining the two different test methods based on their different initial conditions. For a given impact velocity, the inverted drop test methodology results in more severe impacts due to the greater mass and momentum subjected to the cervical spine. The torso cart and impactor displacement at the time of injury were also considered as potential injury indicators. However, these displacements are greatly influenced by the impact surface padding and are not true representations of the magnitude of the actual cervical spine compression.

Results for male PMHS with documented injuries in Tables 5.1 and 5.2 are plotted in Figure 5.4. The compressive axial force at failure was plotted against the sagittal plane moment at failure in Figure 5.4(A) and the sagittal plane resultant force at failure is plotted against the eccentricity at which it is applied at the time of failure in Figure 5.4(B). The experiments resulting in injury are separated into two groups by the direction of sagittal plane moment (flexion or extension) or the location of the load relative to the center of the C7-T1 disc (anterior or posterior). Linear regressions were performed and are drawn in Figure 5.4. There is no apparent relationship between compressive force and sagittal plane moment in Figure 5.4(A) and a weak relationship between sagittal plane resultant force and eccentricity in Figure 5.4(B).

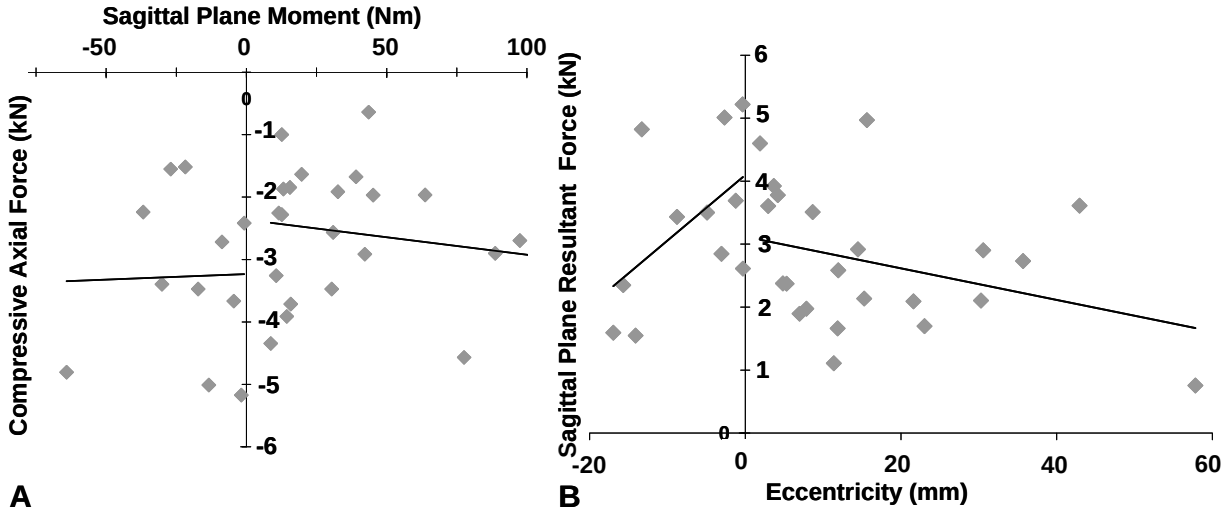

Figure 5.4: Male PMHS compressive force and sagittal plane moment (A) and sagittal plane resultant force and eccentricity (B) at the time of failure

To better define potential relationships between force and either moment or eccentricity, the data in Figure 5.4 was further analyzed and organized by both type of injury and mechanism of injury. The type of injury was defined as either including a bony fracture or being ligamentous only. Avulsion fractures were categorized as ligamentous only injuries. The mechanism of injury was defined as either being the result of anterior or posterior compressive load relative to the center of the nearest intervertebral disc to the site of injury (Winkelstein and Myers, 1997). Only experiments that could be confirmed to include documented lower cervical spine injuries are included in Table 5.3.

Table 5.3: Male PMHS experiments with documented lower cervical spine injuries

Test		Kinetics				Injury		
Study	ID	Fz (N)	Fxz (N)	My (Nm)	Ecc (mm)	Type	Mech Ecc	Description
Nightingale	N05	-1552	1593	-27	-17.0	B	P	C3 burst fx, C3-C4 disc/ALL, C4-C5 ALL
Nightingale	N23B	-2241	2350	-36.8	-15.7	L	P	C3-C4 disc/ALL, C4-C5 disc ALL
Current	3	-1518	1548	-21.8	-14.1	B	P	C5 lamina/ped/up&low facets, C6 lamina/ped
Pintar	11	-4805	4824	-64.1	-13.3	B	P	C4, C5 spinous proc frx, C3-C4 ALL
Current	4	-3396	3433	-30.1	-8.8	B	P	C4 spinous, C4 ant sup tear drop, C3-C4 ALL
Current	5	-3472	3502	-17.2	-4.9	B	P	C5 inf facet, C6 pedicle/lamina
Pintar	19	-2718	2846	-8.7	-3.1	L	A	C7-T1 posterior ligaments
Pintar	4	-5010	5011	-13.4	-2.7	B	A	wedge frx C6 body
Pintar	21	-3666	3690	-4.5	-1.2	B	A	burst frx C4, C3-C4 pos ligs
Pintar	9	-5172	5221	-1.8	-0.3	B	A	ant-sup chip frx C3 body
Nightingale	I32	-2416	2612	-0.8	-0.3	L	P	C5-C6 disc / ALL / L capsular ligament
Pintar	8	-3912	3925	14.4	3.7	B	A-P	vertical frx C3 body, C3 lamina frx
Pintar	10	-3713	3778	15.8	4.2	B	A	comp frxs C4 body & C7 body
Pintar	13	-2281	2372	12.6	5.3	L	A	C6-C7 interspinous lig tear
Nightingale	N18	-1871	1895	13.2	7.0	L	A	C6-C7 BFD
Nightingale	N03	-3473	3509	30.4	8.7	L	A	C6-C7 BFD
Pintar 98	5	-999	1109	12.6	11.4	L	A	pos ligs
Nightingale	I25	-2565	2585	30.9	12.0	L	A-P	C3-4 disc/ ALL /PLL/ L capsular lig
Pintar 98	3	-1915	2136	32.6	15.3	L	A	pos ligs
Pintar	7	-4567	4970	77.6	15.6	B	A	C4 frx ant body
Nightingale	NA2	-1969	2091	45.2	21.6	L	P	C3-4 disc/ALL/ L capsular lig
Nightingale	I04	-1675	1698	39.1	23.0	L	A	C7-T1 pos ligs
Pintar	17	-2901	2902	88.7	30.6	B	A	comp frx C5 body
Pintar	18	-2697	2732	97.5	35.7	B	A	mild comp C7 body
Pintar 98	9	-640	754	43.6	57.8	L	A	pos ligs

The experiments in Table 5.3 are listed in increasing order of the eccentricity of the force at failure. The failure kinetics are plotted in Figure 5.5(A) and 5.6(A). Bony fractures are represented by blue points if the injury is consistent with a posterior oriented load and green points for anterior oriented loads. Ligamentous only injuries with mechanisms of injury consistent with anterior oriented loads are represented by magenta data points. Only three experiments did not include a bony fracture and were consistent with a posterior eccentric load. These experiments are not plotted in Figures 5.5 and 5.6. Generally, the measured loads are consistent with the mechanism of the injury identified. In four cases, a measured posterior oriented load resulted in an injury whose mechanism is consistent with an anterior oriented load and in one case an anterior oriented load resulted in an injury whose mechanism is consistent with a posterior oriented load. In each of the cases in which the measured eccentricity at the C7-T1 intervertebral disc was inconsistent with the local injury mechanism, the magnitude of the

measured eccentricity was less than 5 mm. It is reasonable that there is not a clearly defined point at which the measured load's orientation will always correlate with the identified injuries' mechanism. Instead, there is a small area near the center of the vertebral body in which an injury can occur whose mechanism is consistent with either a posterior or anterior oriented load. This overlapping area is depicted by the gray box in Figures 5.5(A) and 5.6(A). The linear regressions conducted for the three injury type and mechanism combinations are depicted Figures 5.5(B) and 5.6(B). The data points in the overlapping area were used in both the anterior and posterior bony fracture injury regressions.

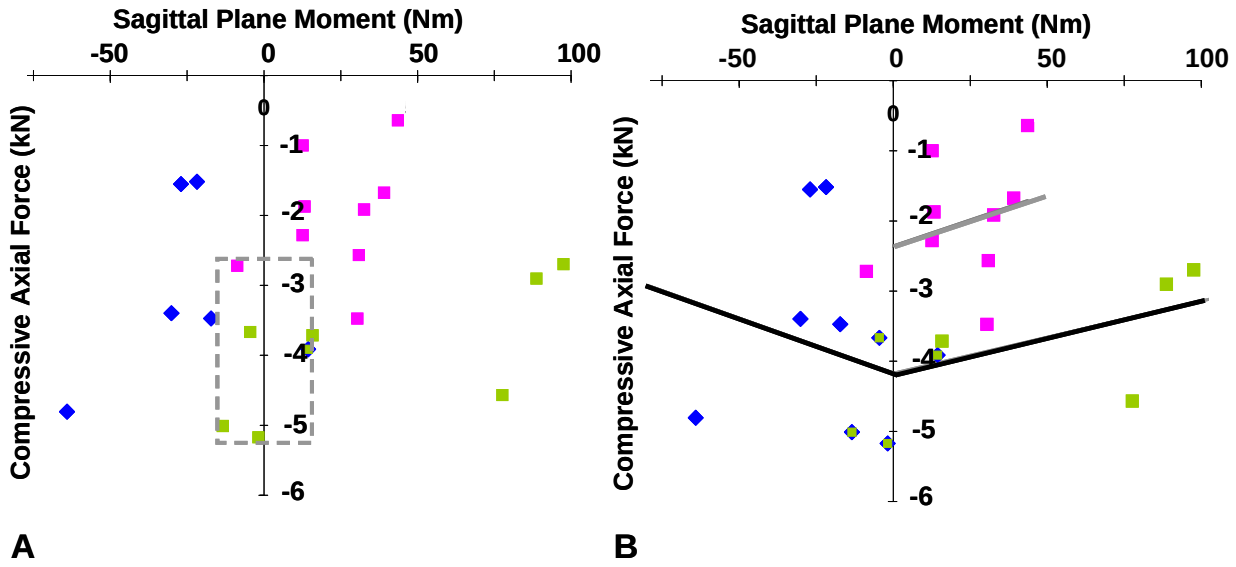

Figure 5.5: Male PMHS axial force and sagittal plane moment at failure for anterior-bony (green) posterior-bony (blue) and anterior-ligamentous only (magenta) injuries (A) and the linear regressions for the three injury mechanism-types (B)

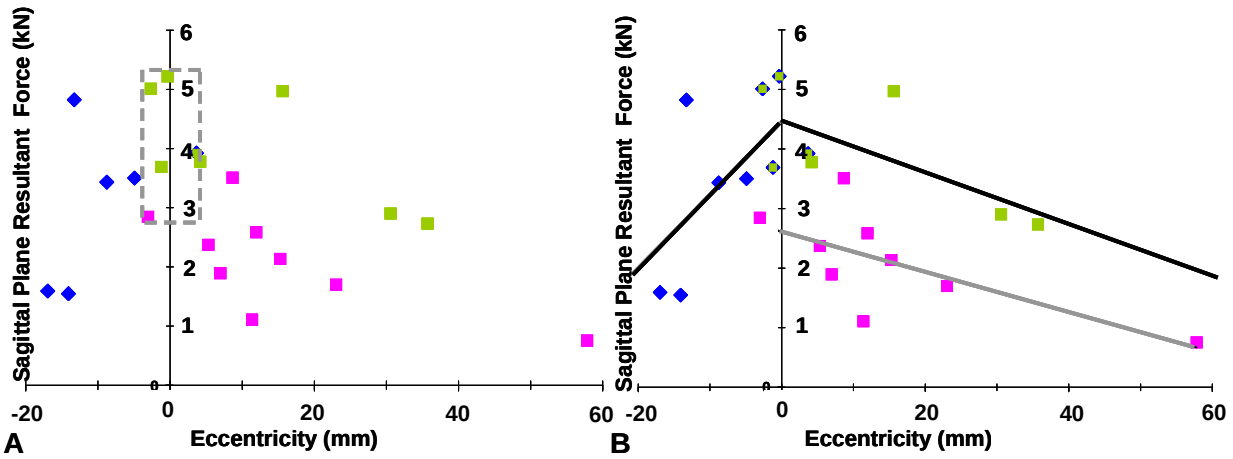

Figure 5.6: Male PMHS sagittal plane resultant force and eccentricity at failure for anterior-bony (green) posterior-bony (blue) and anterior-ligamentous only (magenta) injuries (A) and the linear regressions for the three injury mechanism-types (B)

The coefficient of determination (R2) for the bony fracture injury regression using axial force and sagittal plane moment in Figure 5.5(B) is only 0.14 compared to 0.43 in Figure 5.6(B) when sagittal plane resultant force and eccentricity at failure is used. The y-axis intercept for axial force is -4,171 N and sagittal plane moment intercepts are 405.6 Nm and -265.5 Nm for flexion and extension respectively. The y-axis intercept for sagittal plane resultant force is 4,472 N and eccentricity intercepts are 122.8 mm and -43.3 mm in the anterior and posterior direction respectively. The difference in kinetics at failure between injuries that include bony fracture and those that do not is apparent in Figures 5.5 and 5.6. The slope of the regressions for non-bony injuries is very similar to that of bony injuries suggesting the relative contribution of force and either moment or eccentricity is comparable for both injury types but the magnitudes are less. Similar to the regressions of bony fracture type injuries, the R2 for ligamentous only injury was 0.08 and 0.47 in Figures 5.5(B) and 5.6(B) respectively.

The addition of eccentricity to sagittal plane resultant force at failure resulted in a coefficient of determination greater than zero for bony fracture injuries, signifying that the addition of the eccentricity variable to resultant force better defined the failure data. The addition of sagittal plane moment to axial force at failure resulted in R2 nominally greater than zero

(0.14) indicating that the addition of moment to axial force at failure had a very small effect on the ability to characterize the failure data. This can be seen graphically in Figures 5.7(A) and 5.7(B). Figure 5.7 is a plot of the failure data with bony fracture linear regressions depicted all the way to their x-intercepts. Figure 5.7(A) depicts why addition of sagittal plane moment does little to improve the injury definition as all failure data is clustered near the y-axis at low magnitude moment values when compared to the moment intercepts. In Figure 5.7(B) the data is better distributed around the linear regression lines. However, all of the failure data lies at resultant forces greater than 750 N and eccentricities between 60 mm and -20 mm.

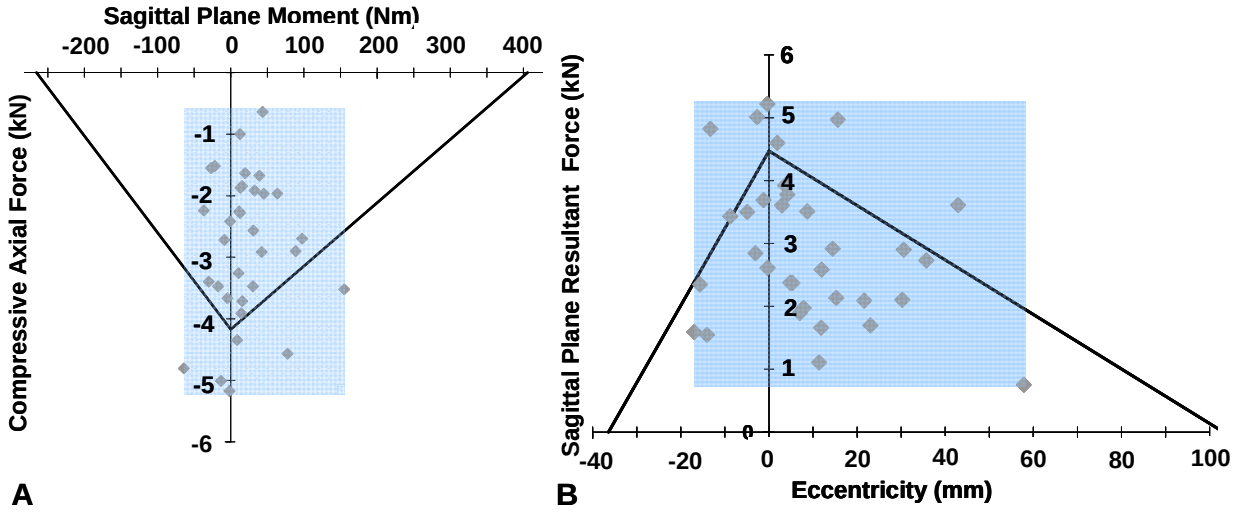

Figure 5.7: Male PMHS axial force and sagittal plane moment bony fracture linear regressions (A) and sagittal plane resultant force and eccentricity bony fracture linear regressions (B) at the time of failure

Since sagittal plane moment does not significantly improve the definition of injury for PMHS compared to axial force alone, the remainder of the analysis of PMHS compressive cervical spine tolerance will focus on the ability of axial force and the linear combination of resultant force and eccentricity to be predictive of cervical injury. The new metric, N_{ECC}, is defined as:

(Equation 5.7) $$N_{ECC} = \frac{Fxz}{F\,\mathrm{int}} + \frac{Exz}{E\,\mathrm{int}}$$

Where Fint equal 4,472 N and Eint equals 122.8 mm and -43.3 mm for anterior and posterior oriented loads respectively. When calculating a peak N_{ECC}, only forces greater than 500 N and eccentricities between 75 mm and -25mm where considered. When the maximum N_{ECC} was calculated over the time interval between the start of the experiment and the identified point of failure, the maximum value generally occurred at the point of failure. In two cases, the maximum axial force and N_{ECC} over this time interval occurred prior to the time of documented failure. In both of these cases, the PMHS avoided bony fracture at the peak mechanical stimuli and instead sustained ligamentous only injury as local bending moments and eccentricities increased due to local geometry changes.

5.3.2 Consideration Gender, Donor Age and Three-Dimensional Kinetic Responses

The same analysis conducted for male PMHS was also conducted for female PMHS. Of the 57 total experiments in the combined data set, only 18 were conducted with female PMHS. No meaningful trends were able to be identified when evaluating the combined kinetics at failure for the female PMHS. Therefore, no female specific injury criteria have been developed and the remainder of the analysis was conducted using only the 39 male PMHS experiments.

The derivation of injury criteria conducted for male PMHS was repeated with the scaled failure kinetics listed in Table 5.1 and 5.2 based on the finding of Riggs et al. (1981). The resulting R2 for the linear regressions are 0.43 for the combination of resultant force and eccentricity and 0.13 for the combination of axial force and sagittal plane moment. The resultant force and eccentricity intercepts are 4,449 N, 104.7 mm and -36.8 mm. The axial force and sagittal plane moment intercepts are -4,142 N, 423.4 Nm and -288.5 Nm. Since the donor age scaled findings are not appreciably different than the original findings, the remainder of the analysis has been conducted without consideration for donor age.

The majority of PMHS test results available for analysis are limited to sagittal plane forces and moments, thereby limiting the ability to evaluate potential injury metrics that include

three-dimensional kinetics such as the Neck Injury Index (NII). For the three experiments conducted as part of this study in which three dimensional failure kinetic data is available, the inclusion of the three-dimensional kinetics was considered. The resultant bending moment and eccentricity of the applied force was calculated by including the lateral bending moment. The nominally larger responses for these three experiments did not improve the linear regressions in Figures 5.5 and 5.6. There are multiple ways in which axial twist moment can be added to a mechanistically relevant injury criteria for a cylindrical structure (Bruhn, 1973). Without additional data beyond the three failure data points available, the best approach to include axial twist moment cannot be evaluated. The remainder of the analysis has been conducted using only sagittal plane kinetics.

5.3.3 Comparison of Injured Groups

The axial impulse at the base of the neck, axial force at failure and Necc at failure were considered as potential predictors of injury and compared across experiments that resulted in injury. Each of the three predictors was evaluated independently for its ability to delineate injury severity, injury type and whether the test methodology employed affected the predictor variable. Using both parametric and non-parametric test methods, it was found that impulse is significantly influenced by the test methodology employed ($p < 0.001$ parametric test, $p < 0.05$ non-parametric test). As cervical spine failure occurs before the end of the loading event, failure occurs before the peak impulse is reached. In the MTS method of experimentation employed by Pintar et al. (1995, 1998a), the stroke of the impactor is arrested by a hard stop, thus preventing the PMHS from resisting all of the initial inertia of the impactor. For this reason, impulse at the base of the neck was determined to not be an appropriate injury predictor variable across test methods.

The axial force at failure was able to distinguish between bony fracture injuries and ligamentous only injuries ($p = 0.023$ parametric test, $p < 0.05$ non-parametric test) but not

between stable and unstable injuries when only considering failure data. Similarly, N_{ECC} failure date was able to distinguish between bony fracture injuries and ligamentous only injuries ($p = 0.006$ parametric test, $p < 0.05$ non-parametric test) but not between stable and unstable injuries.

5.3.4 Survival Analysis

In order to evaluate to the ability of axial force and N_{ECC} to distinguish between less severe stable cervical orthopedic injuries and more severe unstable cervical orthopedic injuries, analysis of censored data, including non-injured PMHS experiments, was conducted. Table 5.4 includes the experiments used for this evaluation. All available male PMHS experiments that resulted in either lower cervical spine injury or no injury were included. The peak and failure axial force and N_{ECC} values are listed.

Table 5.4: PMHS data used in survival analysis

General Info		Documented Failure			Peak Injury Metrics				Injury	
Study	Test ID	Time (msec.)	Fz (N)	NECC	Time (msec.)	Fz (N)	Time (msec.)	NECC	Stability	Type
Current	1	-	-	-	8.2	-5122.4	-	-	NI	-
Current	2	-	-	-	10.6	-3643.3	10.6	0.93	NI	-
Current	3	4.5	-1517.5	0.73	8.7	-4371.4	8.6	1.07	unstable	B
Current	4	3	-3396	1.01	9.1	-4693.6	9.1	1.32	stable	B
Current	5	2.2	-3472	0.92	3.8	-4669	8.6	1.20	stable	B
Nightingale	N05	8.3	-1551.7	0.82	16.3	-1857.7	8.1	1.04	unstable	B
Nightingale	N18	6.4	-1871.3	0.49	11.7	-2493.9	2.0	0.74	unstable	L
Nightingale	D41	-	-	-	5.7	-3838.8	5.2	0.95	NI	-
Nightingale	I32	3.9	-2416.2	0.59	2.8	-2904.7	21.2	0.87	stable	L
Nightingale	N26	-	-	-	8.9	-3877	2.0	1.23	NI	-
Nightingale	N11	-	-	-	6.6	-2539.3	17.9	0.84	NI	-
Nightingale	N21	14.8	-1635.3	0.49	20.9	-1757.1	33.5	0.92	stable	B
Nightingale	N23A	-	-	-	22.0	-2051.6	29.9	0.91	NI	-
Nightingale	N23B	18.7	-2240.5	0.96	18.7	-2240.5	30.2	1.14	stable	L
Nightingale	N03	18.2	-3473	0.87	21.3	-3937.4	21.3	1.03	unstable	L
Nightingale	NA2	15.6	-1968.7	0.68	15.6	-1968.7	16.3	0.76	stable	L
Nightingale	I25	18.4	-2565.2	0.69	17.5	-3443.4	17.5	0.87	unstable	L
Pintar	4	4.2	-5009.9	1.19	4.2	-5009.9	4.5	1.28	unstable	B
Pintar	7	3.8	-4567.1	1.26	3.8	-4567.1	4.5	1.32	unstable	B
Pintar	8	5.6	-3912.2	0.91	6.6	-4919.5	6.0	1.17	unstable	B
Pintar	9	4.7	-5171.6	1.18	6.2	-5637.6	6.2	1.36	stable	B
Pintar	10	4.6	-3713.1	0.89	4.6	-3713.1	5.3	0.91	unstable	B
Pintar	11	4.8	-4805	1.44	4.8	-4805	4.6	1.50	unstable	B
Pintar	13	5.2	-2281.1	0.58	5.2	-2281.1	7.0	0.59	stable	L
Pintar	17	4.4	-2901.3	0.95	4.4	-2901.3	4.4	0.95	unstable	B
Pintar	18	5.1	-2696.5	0.96	5.1	-2696.5	8.3	0.97	stable	B
Pintar	19	9.3	-2718.4	0.72	15.1	-2926.9	15.3	0.76	unstable	L
Pintar	21	11.2	-3665.8	0.86	11.2	-3665.8	15.8	0.97	unstable	B
Pintar 98	1	2.0	-3521.1	1.22	2.0	-3521.1	2.0	1.22	unstable	-
Pintar 98	2	3.9	-4345.1	1.05	6.3	-4701.7	6.3	1.24	unstable	-
Pintar 98	3	5.4	-1915.1	0.63	9.1	-2176.7	39.1	0.85	stable	L
Pintar 98	5	7.1	-999	0.36	7.1	-999	26.6	0.87	stable	L
Pintar 98	9	7.1	-639.8	0.73	7.1	-639.8	9.5	0.85	stable	L
Pintar 98	10	5.6	-2256.4	0.58	5.6	-2256.4	53.5	0.60	unstable	-
Pintar 98	12	3.6	-3258.1	0.83	3.6	-3258.1	20.4	1.06	unstable	-

The non-parametric probability curves for sustaining cervical injury using axial force and N_{ECC} as the mechanical stimuli are presented in Figure 5.8. Right censored data for stable injury curves included the peak responses in experiments in which no injury was documented. The right censored data for the unstable injury curves was comprised of the peak responses in experiments with both stable injury and no injury outcomes.

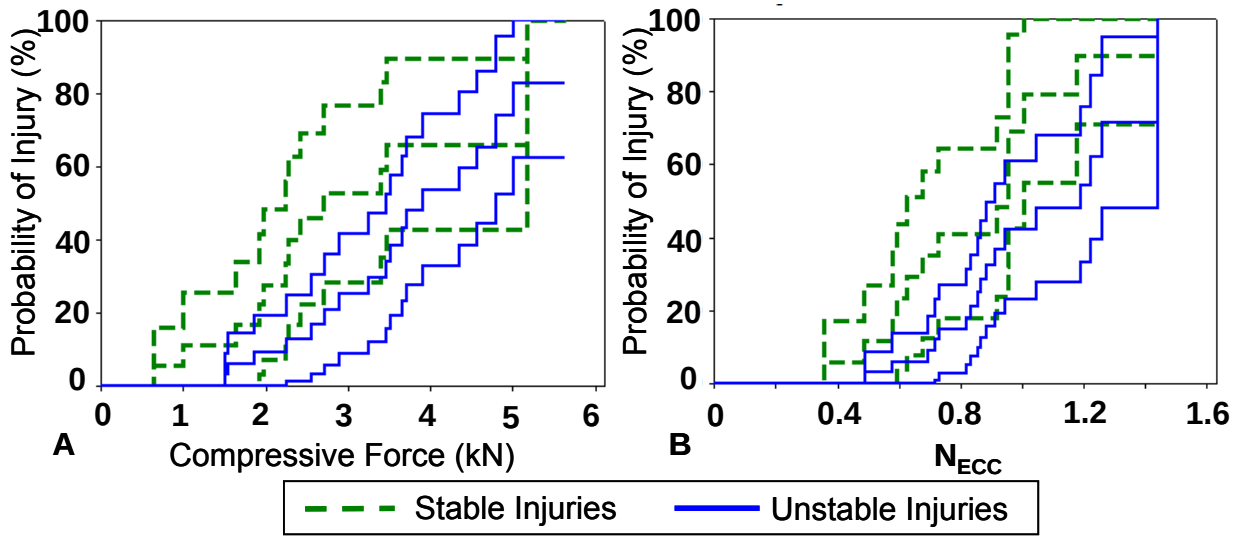

Figure 5.8: Probability of male PMHS stable and unstable cervical orthopedic injuries due to lower neck axial compressive force (A) and N_{ECC} (B) with 95th percentile confidence intervals

The stable and unstable injury curves in Figure 5.8 were tested for statistical difference between each other and the results are presented in Table 5.5. The Log-Rank p-value of 0.172 indicates that at higher stimulus, axial force does not differentiate the severity of injury well. In addition, the axial force stable and unstable curves cross prior to reaching 5 kN of force. Across the continuum of injury probabilities, N_{ECC} better delineates the severity of cervical spine compressive injuries.

Table 5.5: Results of tests comparing stable and unstable injury curves

Comparison of Survival Curves	Test	Chi-Square	P-Value
Fz - Stable vs. Unstable	Log-Rank	1.86748	0.172
	Wilcoxon	4.5312	0.033
N_{ECC} - Stable vs. Unstable	Log-Rank	3.96625	0.046
	Wilcoxon	3.46543	0.063

Injury probability curves based on the injury type were not created. Regardless of the type of injury, the most important factor in injury outcome is the level of spinal cord involvement which can occur with or without bony fracture. Additionally, data censoring assumptions are problematic when considering the type of injury. Unlike the assumption that an increase in mechanical stimulus will increase the risk of greater orthopedic damage, thus the risk of spinal cord involvement, the influence of increased mechanical stimulus on injury type is not clear.

5.3.5 Parametric Distribution

Axial force and N_{ECC} both showed promise in delineating the severity of orthopedic cervical damage depending on the statistical test method used, so both injury predictor data sets were evaluated using parametric distribution techniques. A total of eleven different distributions were evaluated for each the stable, unstable, and both stable and unstable injury outcomes. The adjusted Anderson-Darling statistic was used to assess the fit of the data to each assumed distribution. A smaller statistic indicates the distribution fits the data better. The results are presented in Table 5.6.

Table 5.6: Adjusted Anderson-Darling statistic for the parametric distributions evaluated

Distribution	Any Injury		Stable Injury		Unstable Injury	
	Fz	NECC	Fz	NECC	Fz	NECC
Weibull	2.183	1.506	9.761	8.659	20.921	10.949
Lognormal	2.297	1.403	9.61	8.663	20.99	10.69
Exponential	5.35	6.389	10.054	9.844	22.17	12.34
Loglogistic	2.167	1.347	9.614	8.654	20.944	10.74
3-Parameter Weibull	2.177	1.414	9.662	8.656	20.967	10.735
3-Parameter Lognormal	2.193	1.409	9.633	8.66	20.949	10.72
2-Parameter Exponential	4.221	3.711	9.814	9.088	21.369	11.176
3-Parameter Loglogistic	2.174	1.373	9.595	8.652	20.944	10.666
Smallest Extreme Value	2.569	1.977	10.308	8.715	20.961	11.344
Normal	2.277	1.51	10.071	8.678	20.935	10.982
Logistic	2.314	1.511	10.119	8.695	20.965	11.031

In almost all cases, N_{ECC} showed better fit to the underlying distribution than axial force alone. For both axial force and N_{ECC} across the various injury severities, the 3-Parameter Lognormal distribution fit the data well and was used to construct parametric injury probability curves. Figure 5.9 displays the probability of a male PMHS sustaining any injury due to axial force and N_{ECC} as mechanical stimuli. The black data points indicate uncensored PMHS failure data while the gray data points indicate right censored data in which no PMHS cervical damage was identified. Figures 5.10 and 5.11 display the probability of a male PMHS sustaining stable (5.10) and unstable (5.11) orthopedic damage due to axial force and N_{ECC} as mechanical stimuli. Dark green and blue data points indicate uncensored PMHS failure data while light

green and blue data points indicate right censored data. Figure 5.12 is a comparison of the stable and unstable injury probability curves.

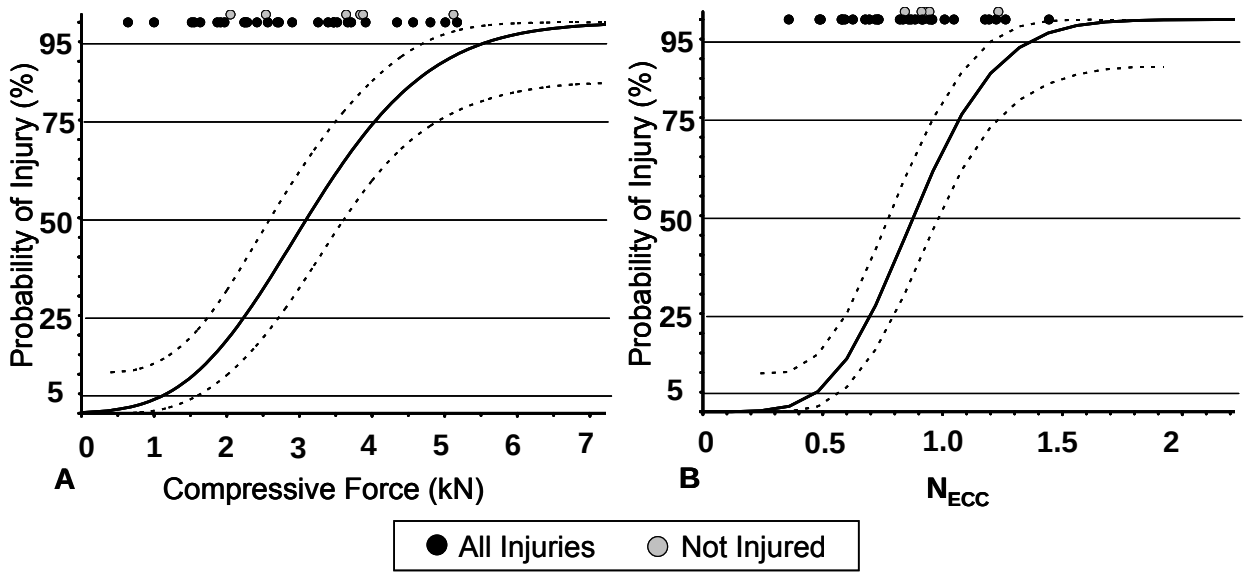

Figure 5.9: Probability of male PMHS sustaining cervical orthopedic injuries due to lower neck axial compressive force (A) and N_{ECC} (B) with 95th percentile confidence intervals

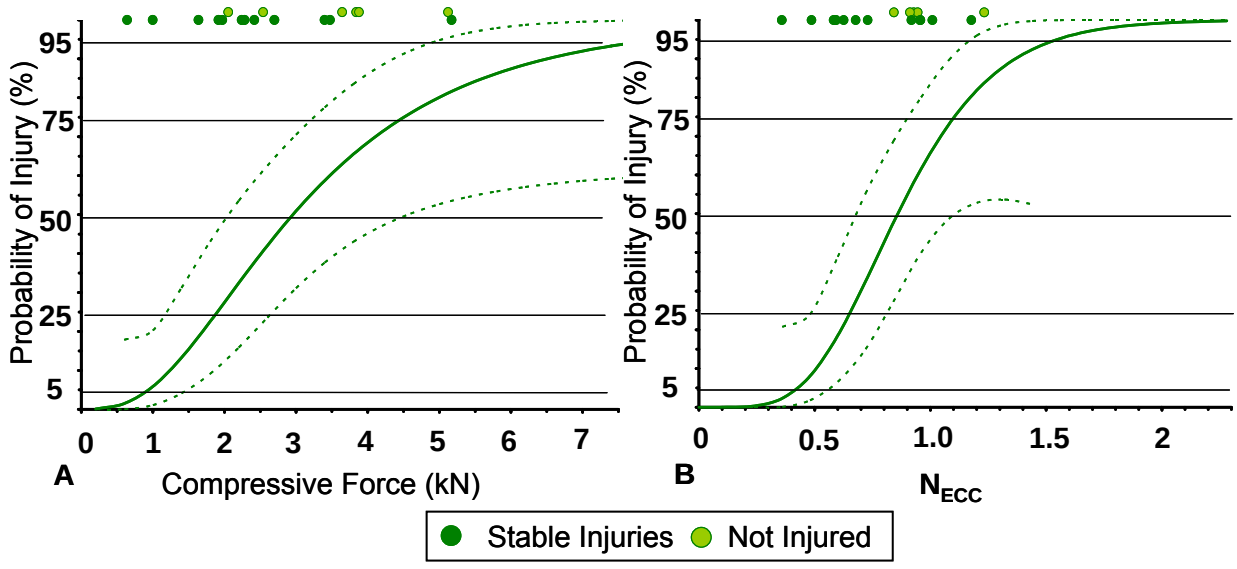

Figure 5.10: Probability of male PMHS sustaining stable cervical orthopedic injuries due to lower neck axial compressive force (A) and N_{ECC} (B) with 95th percentile confidence intervals

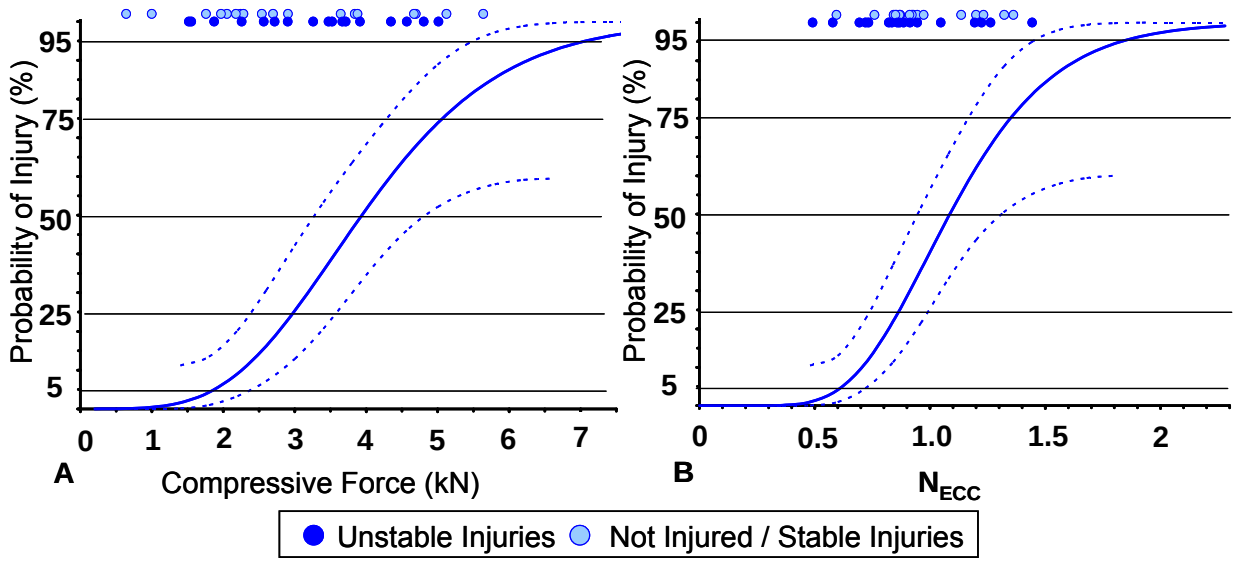

Figure 5.11: Probability of male PMHS sustaining unstable cervical orthopedic injuries due to lower neck axial compressive force (A) and N_{ECC} (B) with 95th percentile confidence intervals

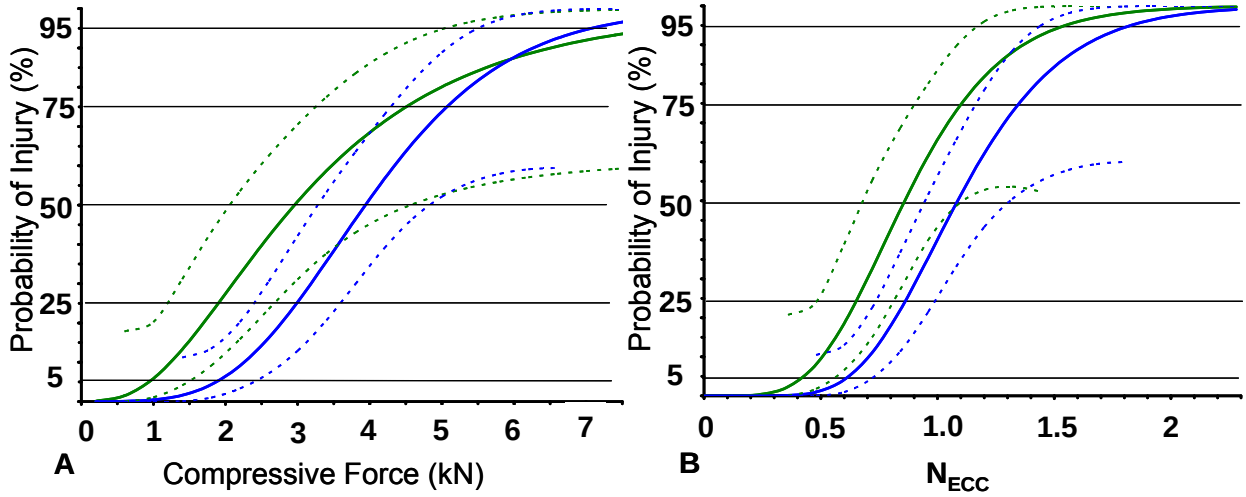

Figure 5.12: Comparison of the probability of male PMHS sustaining stable and unstable cervical orthopedic injuries due to lower neck axial compressive force (A) and N_{ECC} (B) with 95th percentile confidence intervals

Similar to the non-parametric probability of injury curves, the axial force stable and unstable injury curves cross at high stimulus in Figure 5.12(A). In general, the amount and distribution of the experimental data available limits the confidence level at both high and very low mechanical stimulus when stable and unstable injuries are evaluated separately. The probability curves for stable and unstable injury using N_{ECC} as the stimulus are similar in shape

and slope in Figure 5.12(B). The 5, 50, and 95 percent probability of injury for stable, unstable and any orthopedic injury of the cervical spine in compressive loading events are presented in Table 5.7.

Table 5.7: The 5, 50 and 95 percent probability of injury for axial force and N_{ECC}

	Any Injury		Stable Injury		Unstable Injury	
Probability	**Fz (N)**	**N_{ECC}**	**Fz (N)**	**N_{ECC}**	**Fz (N)**	**N_{ECC}**
5	1,167	0.48	940	0.43	1,873	0.62
50	3,109	0.88	2,956	0.86	3,938	1.09
95	5,595	1.38	8,078	1.55	7,074	1.83

The axial force that corresponds to a 95 percent probability of stable injury is greater than the force that corresponds to a 95 percent probability of unstable injury. This is due to the axial force probability curves crossing at high stimulus. In order to more accurately define the probability of injury in this region, more experimental data at high stimulus is necessary.

All of the male PMHS failure data has been plotted in Figure 5.13 with the 5 percent probability of stable and unstable boundaries defined in Table 5.7. Red data points represent unstable injury and green data points represent stable injury. In addition to the lower neck failure data represented by solid circles, the upper neck failure data is also included and is depicted by the hollow circles. For both the axial force stable injury boundary (Figure 5.13(A)) and the N_{ECC} stable injury boundary (Figure 5.13(B)), one stable injury lies within the boundary. Each of these experiments was part of the Pintar et al. (1998a) study and resulted in minor posterior ligament damage. With respect to the unstable injury boundaries, two experiments, one resulting in a upper cervical spine unstable injury another in a bilateral facet dislocation, are within the unstable boundary for both axial force and $N_{ECC.}$ Additionally, the axial force boundary does not delineate two unstable injuries that occurred at approximately 1,500 N of posteriorly oriented compressive force.

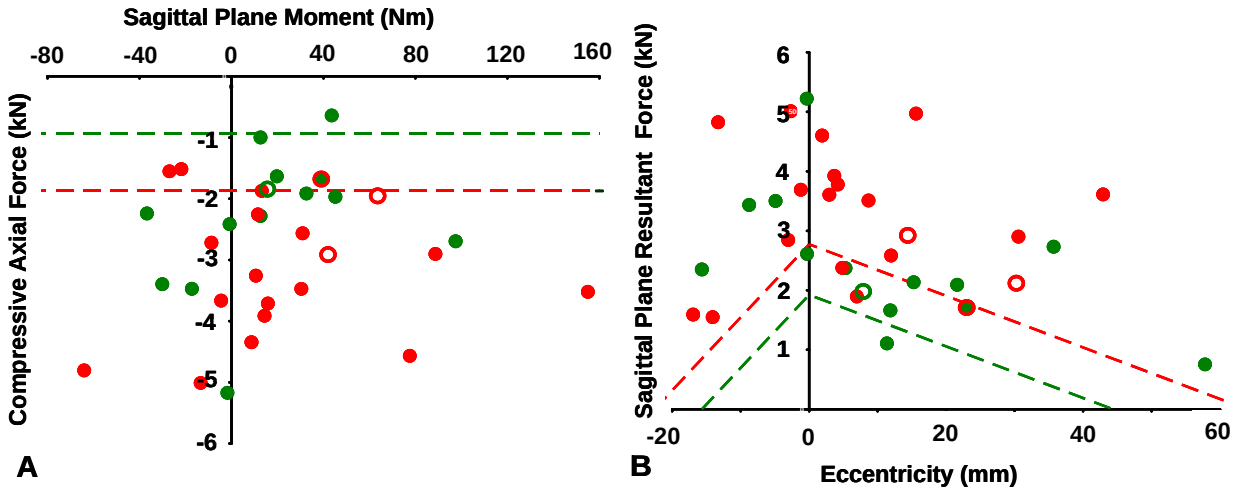

Figure 5.13: Male PMHS lower neck (solid circles) and upper neck (hollow circles), stable (green) and unstable (red) failure kinetics at the base of the neck. The 5 percent probability of stable and unstable injury is depicted for axial force (A) and N_{ECC} (B)

5.4 Discussion

Cervical spine compressive tolerance has traditionally been reported as an average axial force at failure. The current study combined all of the identifiable and available dynamic PMHS experimentation that included defined end conditions and kinetics at the base of the neck. Probability of injury curves were derived for all injuries, as well as by injury severity, further refining the PMHS cervical spine compressive force tolerance to injury. Based on fundamental compressive mechanics, a new injury metric, N_{ECC}, which takes into account the eccentricity at which the load is applied relative to the center of the C7/T1 intervertebral disc, was derived. N_{ECC} improves the ability to delineate between stable and unstable compressive cervical injuries. Additionally, by defining the location of the applied load, the type of injury likely to be sustained can also be estimated.

The current study did not address compressive cervical spine tolerance for female PMHS. A smaller number of experiments were available for analysis and the kinetics at failure exhibited significant scatter and did not follow an identifiable trend. A likely reason for this scatter is the wide range of bone mineral density in female PMHS of advanced age which is highly dependant on whether the donor experienced osteoporosis (Riggs et al. 1981). Since

bone mineral density for the PMHS used in experimentation were not available, variability due to this reason could not be accounted for. Similarly, donor age was also considered but did not have a large effect on male PMHS results. This is likely due to the fact that most of the donors were similarly advanced in age and male bone mineral density does not vary as significantly as female bone mineral density with age.

Nightingale et al. (1997a) averaged the cervical spine compressive failure loads in their study with those of Pintar et al. (1995) and determined the average failure load for a 61 year old PMHS male was 3,030 N. This is consistent with the distribution analysis in the current study which resulted in a 50 percent probability of a male PMHS sustaining any compressive orthopedic cervical spine injury at 3,109 N. Nightingale et al. (1997a) reported an average failure tolerance of 2,243 N when the resting lordosis of the spine was maintained while Pintar et al. (1998b) reported a tolerance of 3,900 N for a 50 year old PMHS male when the spine was pre-straightened. Pintar et al. (1998a) also reported a 50% probability of compressive cervical injury at 2,200 N when larger amounts of flexion were present due to the PMHS head being oriented anterior to the base of the neck at the onset of the experiment. By evaluating the primarily compressive load and its eccentricity, the range of failure loads and various injury outcomes in PMHS experimentation can be taken into consideration.

The eccentricity of the measured load at the base of the neck was generally consistent with lower neck injury mechanisms. As the eccentricity of the load increased, the magnitude of the sagittal plane resultant force generally decreased. This is consistent with the decreased compressive tolerances reported by Nightingale et al. (1997a) and Pintar et al. (1998a). The y-intercept derived for N_{ECC}, 4,472 N, is consistent with the initial Nij compression intercept advocated by NHTSA based on close to pure compression tests conducted by Pintar et al. (1990) which are not considered in this data set due to the lack of reported data other than force at failure. The 4,472 N intercept is also supported by results of Qingan et al. (1999) who impacted C2-C4 segments and found average peak compressive force for the non-damaged

segments was 4.11 +/- 0.11 kN and the average peak compressive force for the damaged specimens was 4.89 +/- 0.38 kN.

The coefficients of determination (R2) for the linear regressions of anterior oriented loads were consistently greater than for posterior oriented loads. This is likely due to the geometry of the vertebrae and the complexity of the interaction between facet joints during rearward extension or posterior oriented loading. The current study derived the relationship between sagittal plane resultant force and eccentricity using linear regression, however, based on fundamental mechanics of a slender column, it is likely that this relationship is non-linear. If more experimental data becomes available, various non-linear relationships can be evaluated.

Finally, the role of lateral bending moments and axial twist moments, which have been identified in the limited number of experiments not constrained to the sagittal plane, can also be further evaluated if more experiments including the three-dimensional dynamics become available for analysis. These five experiments were included in the combined data set because the lateral eccentricity magnitudes at failure did not add appreciably to the resultant eccentricity. Inclusion of lateral eccentricity at which the resultant force is applied increases the overall eccentricity relative to the center of the C7/T1 intervertebral disc by less than 2% in each of the failure cases.

5.5 Conclusions

A more refined PMHS cervical spine compressive injury tolerance was derived by combining the available dynamic PMHS experimentation including measured neck kinetics conducted by different laboratories using various test methodologies. The compressive force measured at the base of the neck associated with a 50% probability of stable and unstable orthopedic damage is 2,956 N and 3,938 N respectively. A new injury metric, N_{ECC}, was derived based on the kinetics of PMHS experimentation at the point of documented failure. N_{ECC} improves the ability to delineate between stable and unstable compressive cervical injuries and

by defining the location of the applied load, the type of injury likely to be sustained can be estimated. The N_{ECC} measured at the base of the neck associated with a 50% probability of stable and unstable orthopedic damage is 0.86 and 1.09 respectively.

CHAPTER 6

EVALUATION OF THE HYBRID III ATD NECK AND POTENTIAL LOWER NECK INJURY METRICS FOR DYNAMIC COMPRESSIVE LOADING SCENARIOS

6.1 Introduction

Physical biomechanical surrogates are critical for testing the efficacy of injury mitigating safety devices. Catastrophic cervical spinal cord injuries are most often associated with compression mechanisms of the cervical column (Roaf. 1972, Torg et al. 1990, Yogananadan et al. 1989, McElhaney et al. 2002). This can occur in any environment in which the apex of the head is loaded in a direction nearly parallel to the alignment of the cervical column including automobile crashes, swimming and diving, football, hockey, and motor sports. The Hybrid III family of ATDs has been used extensively in the automotive collision environment, including rollover applications (Orlowski et al. 1985, Bahling et al. 1990, Hare et al. 2002, Moffatt et al. 2003, McCoy and Chou 2007, Raddin et al. 2009, and Viano et al. 2009). In addition to the automobile crash environment, researchers evaluating devices intended to decrease the risk of cervical spine injury during athletic and motor sports often use the Hybrid III ATD to evaluate device performance (http://www.leatt-brace.com/company/leatt-lab/). The interpretation of measured neck loads and moments in these test scenarios would be aided by a better understanding of the correlation between the mechanical responses in the Hybrid III ATD and the probability of injury in the human cervical spine.

The current Hybrid III 50th male neck compressive IARV of 4,000 N was originally based on a reconstruction of a football injury sustained due to impact on the apex of the head with a talking block using the Hybrid III ATD (Mertz et al., 1978). The current compressive Nij intercepts were formulated by correlating Hybrid 3-years-old ATD responses to porcine tension – extension cervical injury through reconstruction of the porcine test conditions with the 3-years old ATD. The intercepts were subsequently scaled to the Hybrid III 50th male ATD. The compressive Nij

intercept was set equal to that of tension (Eppinger et al., 2000). The purpose of the following research is to evaluate the Hybrid III ATD neck response and potential neck injury metrics under dynamic compressive loading conditions comparable to those of PMHS tests with known injury outcomes to better define the correlation between measured neck responses in Hybrid III ATD and the risk of injury in the human cervical spine. This was accomplished by reconstructing the PMHS tests conducted as part of the current study and those conducted by Nightingale et al. (1997a) with the Hybrid III ATD head and neck assembly. Using this newly created matched data set, the injury predictability of ATD neck dynamics was evaluated and a refined injury risk relationship identified for evaluating neck compressive loading scenarios. In addition to current IARVs, neck injury metrics evaluated in the previous analysis of PMHS tests such as axial impulse and a combination of axial force and eccentricity (N_{ECC}) were also assessed.

6.2 Methodology

Male PMHS experiments from the current study and Nightingale et al. (1997a) were reconstructed with the Hybrid III 50th percentile head and neck. A total of 20 male PMHS experiments were evaluated, 5 impacts onto lubricated Teflon in lateral configurations from the current study and 15 experiments from Nightingale et al., 8 onto a lubricated Teflon impact surface and 7 onto 5 centimeters of open cell polyurethane foam.

6.2.1 Test Apparatus

A head and neck injury drop track apparatus, similar to that used for the PMHS tests, was designed to allow head-first impacts on an adjustable oblique surface (Figure 6.1). The Hybrid III 50th percentile male head and neck was mounted to a cart attached to a vertical track with linear sliders. The cart was weighted to 16 kg to simulate the effective mass of the torso, consistent with the PMHS tests.

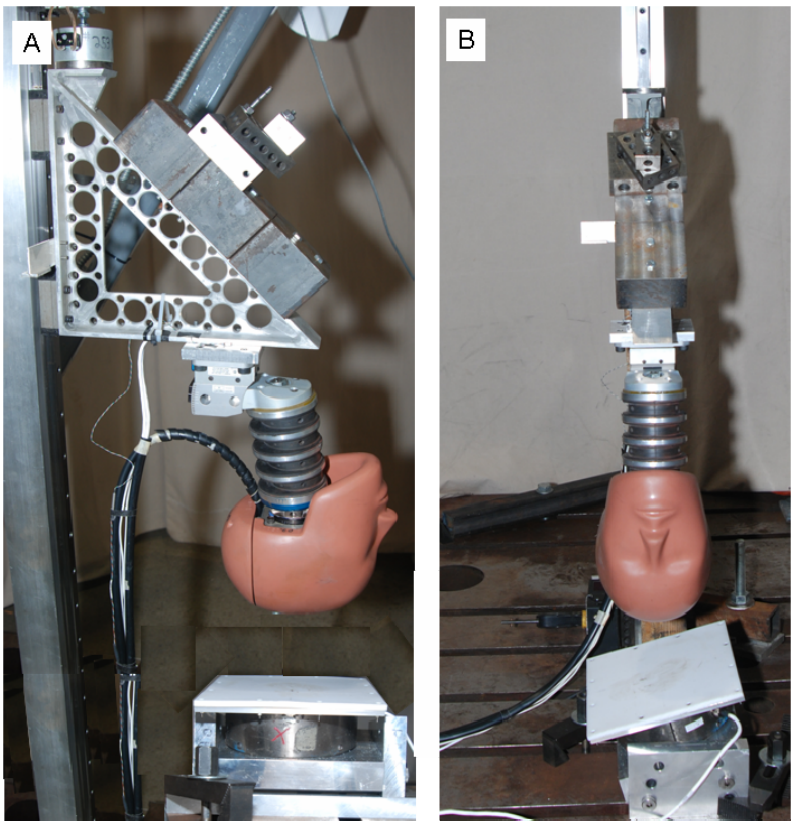

Figure 6.1: Lateral (A) and frontal (B) view of a Hybrid III 50th male head-neck mounted to the drop cart

6.2.2 Experimental Setup

The ATD head and neck assembly was inverted and mounted to the carriage on the drop track. Six different impact plate orientations were evaluated. The four anterior-posterior impact plate angles used by Nightingale et al. (1997a) (30, 15, 0 and -15 degrees) as well as the 15 degrees laterally inclined impact plate and pre-laterally flexed posture from the current study were evaluated. In addition to a lubricated Teflon impact surface, padded impact surface experiments in each of the Nightingale et al. impact plate orientations were also conducted. The closest match to the foam reportedly used by Nightingale et al. (1997b) was obtained. Open cell polyurethane foam with a density of 0.028 g/cm^3 was cut 5 cm thick and sized to cover the impact surface. Two sided carpet tape was used to keep the foam affixed and prevented

movement relative to the impact plate. The drop height for each experiment was defined by the drop heights used in the PMHS experiments.

Federal Motor Vehicle Safety Standard (FMVSS) 208 (CFR 49 part 572.208) dummy positioning procedures require the ATD head to be level (+/- 0.5 degrees) at the onset of frontal crash testing. When the ATD head is level, or perpendicular to the drop track motion, the neck angle is approximately 6 degrees from vertical (see Figure 6.2). The initial neck angles of the five PMHS conducted as part of the current study were identified in pre-test photographs. The initial neck angle, defined as the angle between a line drawn from the center of the C7/T1 intervertebral disc to the occipital condyles and vertical, ranged from 10 to 25 degrees. A 17.5 degree neck angle with respect to vertical was chosen to represent the mid point of the range of initial PMHS neck angles. The neck chord angle measured in human surrogates in an automotive driving position has previously been identified as 79 degrees or 11 degrees from vertical (Klinich et al. 2004). This is approximately halfway between the 6 and 17.5 degree neck angles chosen for the current study. Figure 6.2 compares the initial ATD neck angles to a sample PMHS pre-test photograph.

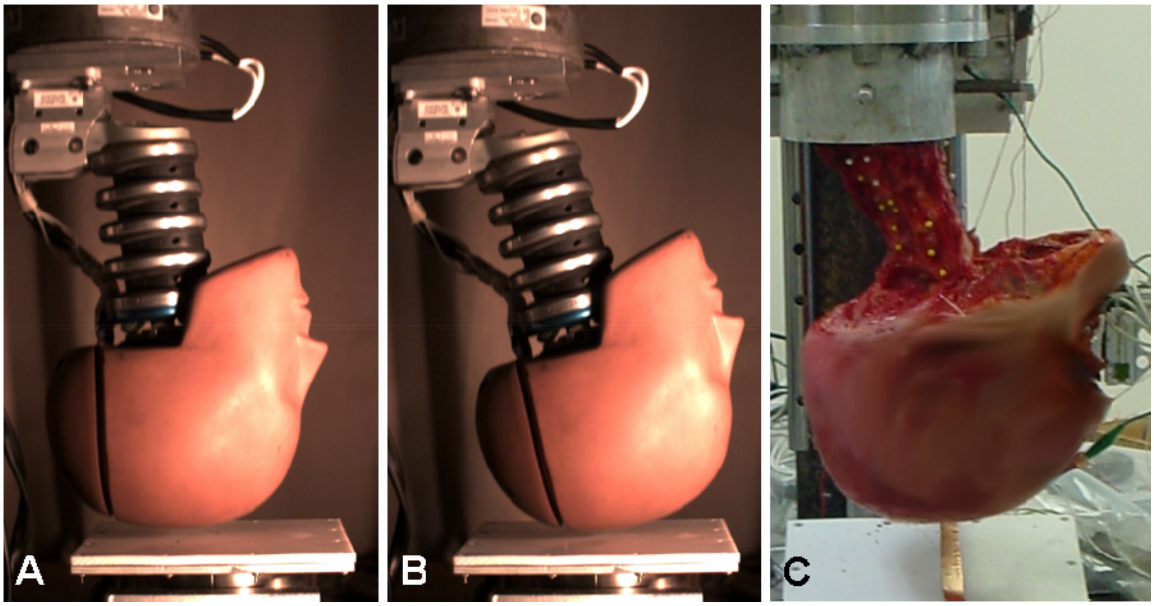

Figure 6.2: Lateral views of a Hybrid III 50th male head-neck mounted to the drop at neck angles of 6 degrees (A) and 17.5 degrees (B) compared to a sample PMHS pre-test orientation

The test matrix of the 26 ATD experiments conducted is listed in Table 6.1. The matrix consists of 13 tests conducted for each the 6 and 17.5 degrees neck angle. The current study evaluated PMHS response in two different lateral configurations, each from two different drop heights for a total of four test conditions. The Nightingale et al. (1997a) experiments included four different impact plate configurations with two different impact surface materials. One test condition, 0 degree impact onto lubricated Teflon, was conducted at two different drop heights for a total a nine different test conditions.

Table 6.1: PMHS test conditions reconstructed with the Hybrid III head and neck

.

Test #	Drop Height (cm.)	Impact Surface	Test Surface Angle (deg.)	Neck Angle (deg.)
1	53	Padded	30°	6
2	53	Padded	15°	6
3	53	Padded	0°	6
4	53	Padded	-15°	6
5	53	Teflon	30°	6
6	53	Teflon	15°	6
7	33	Teflon	0°	6
8	53	Teflon	0°	6
9	53	Teflon	-15°	6
10	45	Teflon	15° Lateral	6
11	53	Teflon	15° Lateral	6
12	45	Teflon	0° (15° Lateral Neck)	6
13	53	Teflon	0° (15° Lateral Neck)	6
14	53	Padded	30°	17.5
15	53	Padded	15°	17.5
16	53	Padded	0°	17.5
17	53	Padded	-15°	17.5
18	53	Teflon	30°	17.5
19	53	Teflon	15°	17.5
20	33	Teflon	0°	17.5
21	53	Teflon	0°	17.5
22	53	Teflon	-15°	17.5
23	45	Teflon	15° Lateral	17.5
24	53	Teflon	15° Lateral	17.5
25	45	Teflon	0° (15° Lateral Neck)	17.5
26	53	Teflon	0° (15° Lateral Neck)	17.5

6.2.3 Instrumentation and High Speed Digital Video

Upper and lower neck forces and moments were measured using the standard Denton 1716A six-axis upper neck load cell and the Denton 7992JTF adjustable six-axis lower neck

load cell. Drop cart vertical acceleration response was measured with a linear accelerometer. Drop cart displacement was measured using a laser CCD displacement sensor. All transducer data was acquired in accordance to the SAE J211 standard. Two Red Lake HG LE high-speed digital cameras were synchronized with the data acquisition and used to record each test at 1000 frames per second; one from the frontal perspective and one from the left lateral perspective.

The measurement range of the sagittal plane moment channel of the Denton 7992JTF adjustable lower neck load cell is +/- 340 Nm. It was determined at the onset of testing that the sagittal plane moment at the lower neck load cell sensitive axis would easily be exceeded during execution of the test matrix. Additionally, in rare circumstances, the axial load limit of 8,900 N could also be exceeded. Since a high capacity adjustable lower neck load cell (Humanetics model IF-219-HC) was not available for use, a six-axis Denton WSU-NMN-01 load cell was placed between the carriage and the lower neck load cell and positioned relative to the ATD head and neck so its operational range would not be exceed (Figure 6.3). The mass of the drop cart was decreased to accommodate the additional mass of this load cell. In the rare case that the lower neck load cell vertical force capacity was exceeded, the vertical force at the lower neck load cell sensitive axis was calculated by adding the product of the effective mass between the additional WSU-NMN-01 load cell and the lower neck load cell sensitive axes and the cart acceleration to the measured additional WSU-NMN-01 load cell vertical force (Equation 6.1). The sagittal plane moment at the lower neck load cell sensitive axis was determined by transforming the additional WSU-NMN-01 load cell sagittal plane moment using Equation 6.2. Validation of both transformation methods are shown in Figure 6.4.

(Equation 6.1) $$Fz_{NeckLC} = Fz_{AdditionalLC} + (M_{Effective} * A_{Cart})$$

(Equation 6.1) $$My_{NeckLC} = My_{AdditionalLC} + (Fx * Z) - (Fz * X)$$

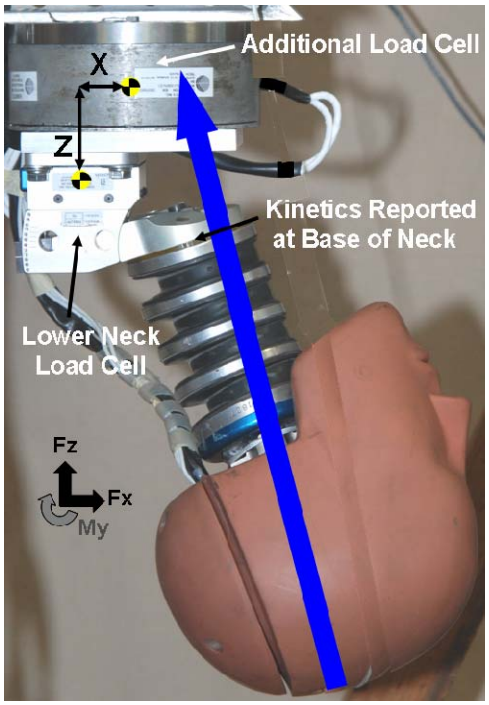

Figure 6.3: Load cell arrangement with approximate impact line-of-force drawn relative to the load cells sensitive axes and the base of the ATD neck

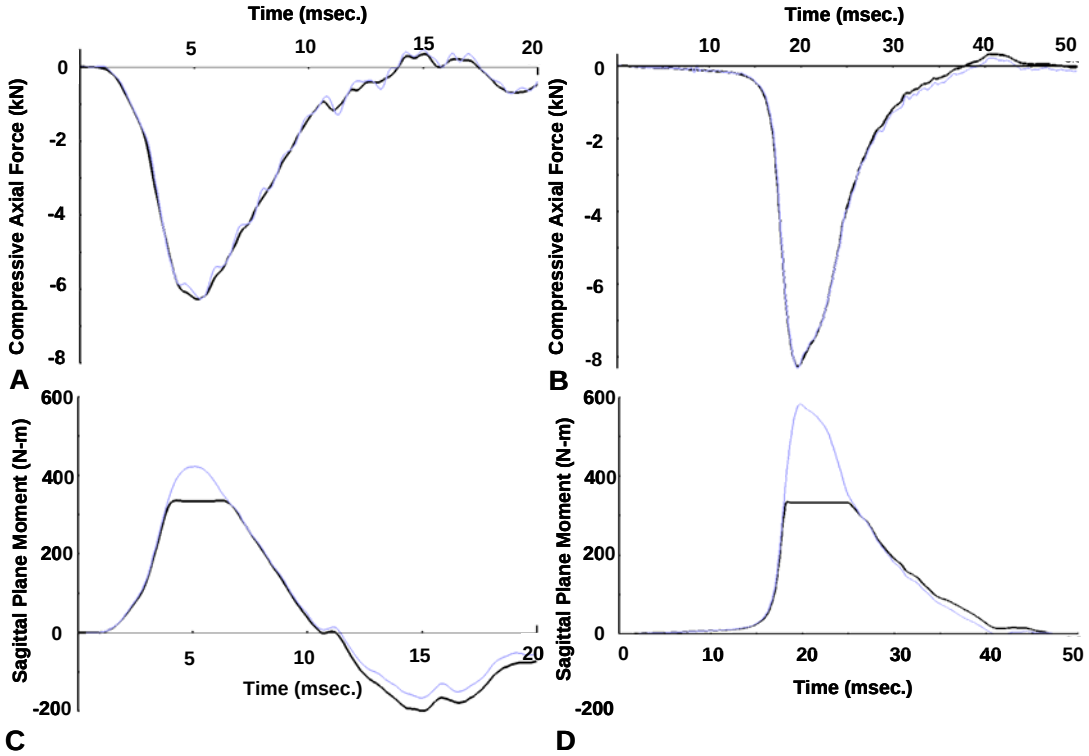

Figure 6.4: Comparison between measured lower neck load cell axial force and sagittal plane moment (black) channels with calculated lower neck force and moment (gray) from the additional Denton WSU-NMN-01 load cell for a 6 º neck impacting a 30 º Teflon surface (A and C) and a 17.5º neck impacting a 0 º padded surface (B and D)

Once the six axes loads were accurately defined at the adjustable lower neck load cell neutral axis, a final coordinate transformation was conducted so that the loads are reported aligned with the ATD neck orientation at the centerline of the base of the neck. Figure 6.5 depicts the transformation geometry of the adjustable lower neck load cell. The transformation equations are as follows:

(Equation 6.3) $$Fx_{Neck} = (Fx_{LC} * \cos\theta) + (Fz_{LC} * \sin\theta)$$

(Equation 6.4) $$Fy_{Neck} = Fy_{LC}$$

(Equation 6.5) $$Fz_{Neck} = (Fz_{LC} * \cos\theta) + (Fx_{LC} * \sin\theta)$$

(Equation 6.6) $$Mx_{Neck} = (Mx_{LC} - 1.72 * Fy)\cos\phi + (Mz_{LC} - 2.5 * Fy)\sin\theta$$

(Equation 6.7) $$My_{Neck} = My_{LC} + 1.72 * Fx + 2.5 * Fz$$

(Equation 6.8) $$Mz_{Neck} = (Mz_{LC} - 2.5 * Fy)\cos\phi + (Mx_{LC} - 1.72 * Fy)\sin\theta$$

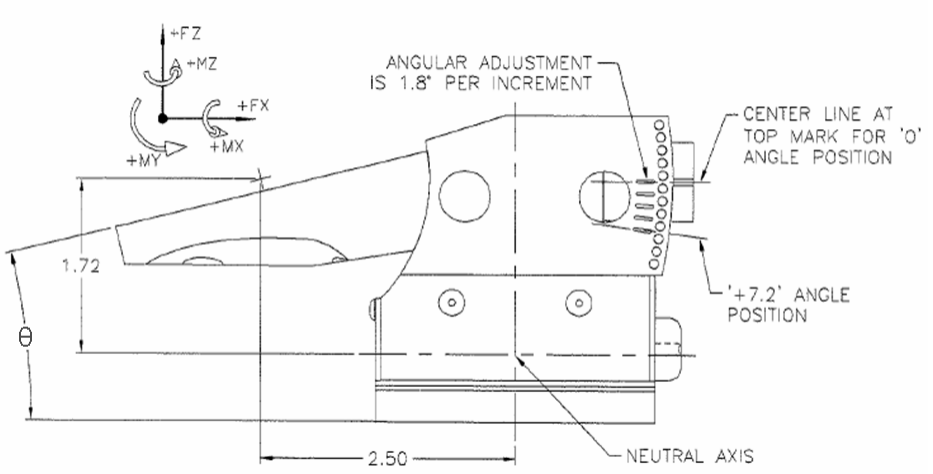

Figure 6.5: Drawing of the Denton 7992 adjustable lower neck six-axis load cell including dimension between the sensitive axis and the base of the ATD lower neck

Data processing was conducted in accordance was SAE J211-1. All head and neck forces were digitally filtered at SAE channel filter class 1000 Hz (CFC 1000 Hz) and neck moments at CFC 600. The SAE coordinate system outlined in J211 was utilized. The measured

neck forces were filtered at CFC 600 when Nij was calculated for the upper and lower neck load cells per the currently defined IARVs. Additionally, the axial force impulse was calculated for lower neck load cells by integrated the axial force channel.

6.2.4 Analysis of ATD Kinetic Responses and IARV Evaluation

The lower neck axial force versus time response of the Hybrid III 50th percentile ATD was compared to the responses of the male PMHS experiments whose injury outcomes the ATD responses are being matched. The 20 PMHS tests were divided into four groups: 3 experiments conducted with a laterally inclined plate, 2 experiments conducted with a pre-laterally flexed neck, 8 experiments constrained to sagittal plane motion on a Teflon impact surface and 7 experiments constrained to the sagittal plane conducted with a padded impact surface. For a given group of experiments' test conditions, the ATD axial response is presented as a corridor that represents the upper and lower extent of the response. Additionally, axial force versus the drop cart displacement response was evaluated. Head and neck axial deflection was not directly measured in the experiments. The cart displacement was measured in both the PMHS and ATD experiments and is a direct comparison of the combined response of the head and neck.

The current compressive neck injury assessment reference value of 4 kN was originally derived from reconstruction of an injurious football head impacts using the Hybrid III test device (Mertz et al., 1978). Due to their viscoelastic properties, the load carrying capability of biologic tissues often increase as the duration of loading decreases, Mertz et al. characterized a given axial loading event by the force maintained over prescribed durations (Figure 6.6). An upper and lower compressive limit was developed that is dependent on the duration of the force pulse and ranged from 4,000 N to 6,670 N for very short duration events. Loads above the upper limit (blue region) are defined as having the potential to cause serious neck injury. If the load falls in

the middle area (white region) the potential for injury is considered less likely and below the lower limit (green region) the probability of injury is considered remote.

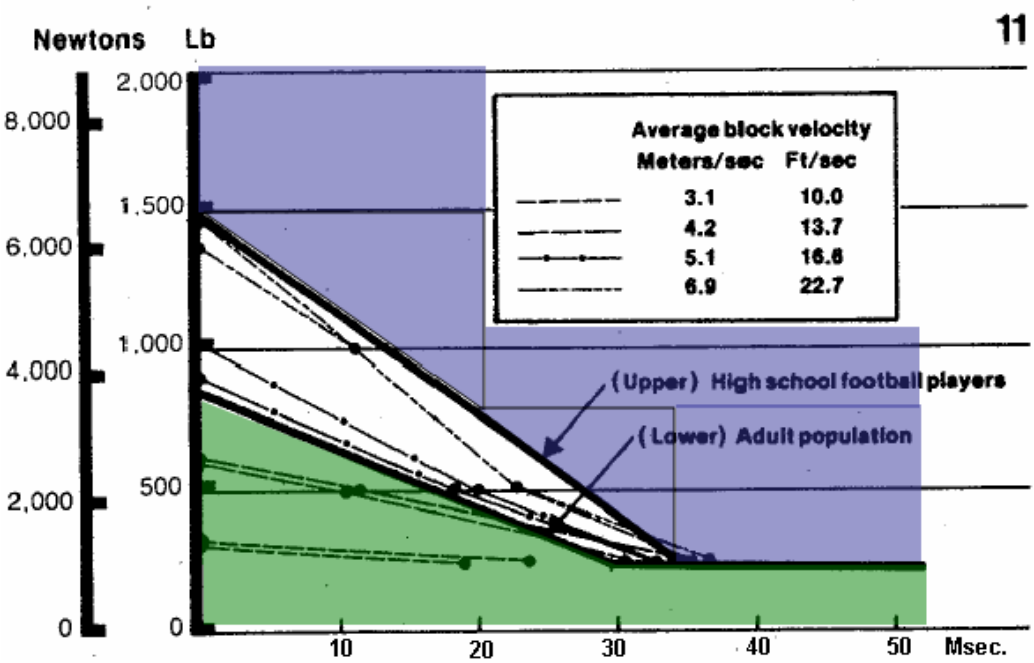

Figure 6.6: Axial compressive force IARV definition from Mertz et al. (1978)

The upper neck compression Nij intercepts adopted by NHTSA and incorporated into FMVSS 208 (CFR 49 part 571.208) for the Hybrid III 50th percentile male was set at 6,160 N, equal to the tension intercept derived from scaling the three-years-old ATD tension intercept based on the work of Mertz et al. (1997). The value of the compression intercept was deemed appropriate for the proper linear combination of sagittal moment and axial compressive load, however, a peak compressive load limit of 4,000 N was also maintained as an injury criteria limit consistent with the earlier work done by Mertz (1978). Lower neck IARVs have been reported by Mertz et al. (2003). The axial force limits and axial force Nij intercepts are identical to the upper neck. In addition to evaluating the peak axial forces in the current set of ATD experiments, the loading events were also characterized by the maximum compressive force maintained over durations of 1, 2.5, 5, 10, 15, and 20 milliseconds for direct comparison to the findings of Mertz et al. (1978).

Nij was evaluated to determine how effectively it could delineate ATD neck responses in test conditions of various PMHS injury outcomes. Nij is the linear combination of ATD neck axial force and sagittal plane moment and takes the form:

$$\text{(Equation 6.9)} \quad Nij = \frac{Fz(t)}{F_C} + \frac{My(t)}{M_C}$$

The upper and lower neck out-of-position Nij intercepts (Fc, Mc) were utilized. Impacts near the apex of the head were not one of the loading conditions used in the formulation of these intercepts. The historical derivation of these intercepts was presented in Chapter 3.5.

The sagittal plane eccentricity (Exz) relative to the center of the lower ATD neck and the occipital condyles of the upper ATD neck can be calculated using Equation (6.10), which only incorporates the neck reaction forces and moments. Eccentricity is fundamentally the perpendicular distance between the force line of action and a defined reference location.

$$\text{(Equation 6.10)} \qquad Exz = \frac{My}{Fxz} = \frac{My}{\sqrt{Fx^2 + Fz^2}}$$

The linear combination of lower neck sagittal plane resultant force and the eccentricity at which it is applied relative to the center of the C7/T1 intervertebral disc (N_{ECC}) has been shown to be a capable metric at delineating the severity of PMHS cervical spine orthopedic damage (Chapter 5). The mechanistically based criterion is evaluated using the Hybrid III 50th percentile head and neck response.

6.2.5 Statistical Methods

The mean peak ATD response or injury metric was compared across injury groups. Results were grouped to evaluate the responses that correlated with the presence of any PMHS injury outcome and unstable PMHS injury outcomes. Two statistical methods were used to evaluate the significance of the differences between the means of two populations. The first method is the parametric t-test for unequal samples and unknown variances which assumes a t distribution. The second is the non-parametric Wilcoxon Rank-Sum test which is particularly useful when sample sizes are small and variances are unknown or unequal (Milton and Arnold, 1995). Significance levels $p < 0.05$ and $p < 0.10$ were both evaluated using the non-parametric method.

In cases where a difference in the mean ATD response was identified between PMHS injury groups, binary logistic regressions were conducted in order to assess the relationship between biomechanical responses and the various injury outcomes. The logistic regression model takes the form of Equation 6.9.

$$\text{(Equation 6.9)}\quad P = \frac{1}{1 + e^{(\alpha + \beta x)}}$$

The constants α and β represent the coefficients associated with the independent variable. These coefficients were determined using the Maximum Likelihood method. The -2 log likelihood (-2LL) statistic was used to assess the fit of the model to the data using the Chi-squared distribution. The Wald statistic was used to assess the independent variables significance by testing the null hypothesis that there was no association between the independent variable and the injury outcome and compared to a chi-squared distribution. P values less than 0.05 were rarely achieved based on the matched data set of only 20 PMHS experiments, however, probability of injury curves for the upper and lower neck compressive force for injury definitions with the highest significance levels are presented for the purpose of comparison to the currently defined Hybrid III 50th percentile neck compressive IARVs. Finally,

the overall percent of accurately predicted outcomes for the various regressions are reported for the underlying data set along with the specificity and sensitivity of the regression model.

6.3 Results

6.3.1 General ATD Kinetics and Kinematics

A summary of the ATD sagittal plane upper and lower neck peak mechanical responses are summarized in Tables 6.1. The results tables include the impact surface material and orientation and the ATD neck angle. Upper and lower neck peak axial force and Nij, as well as the sagittal plane moment and eccentricity at the time of peak Nij are listed. The drop cart (torso) displacements at the point peak load and the calculated impulse from the lower neck axial force are included.

The response for the Hybrid III ATD head and neck was found to be extremely repeatable. Figure 6.7 depicts the lower neck axial force response in three experiments conducted from the same drop height onto a lubricated Teflon impact surface oriented laterally at 15 degrees. The traces are nearly indistinguishable from one another. The peak loads in this test condition are within approximately 1%.

Table 6.2: Kinetic results for 26 ATD experiments conducted

Test #	Impact Surface	Surface Angle (deg.)	Neck Angle (deg.)	ATD Lower Neck Kinetics @ Base Neck								ATD Upper Neck Kinetics @ Occipital Condyles					
				Fz Pk (N)	Cart Disp (mm)	Time (msec.)	Nij Pk	Time (msec.)	My^ (Nm)	Fz Ecc^ (mm)	Fz Imp (Nsec.)	Fz Pk (N)	Time (msec.)	Nij Pk	Time (msec.)	My^ (Nm)	Fz Ecc^ (mm)
1	Padded	30º	6	-7052	12.9	2.2	1.20	22	36.8	5.2	78.7	-7410	22.2	1.59	23.3	131.6	17.8
2	Padded	15º	6	-8502	13.3	20.2	1.48	20.1	69	8.1	74.7	-9396	21	1.78	22	86.9	9.2
3	Padded	0º	6	-9162	12.0	20.9	1.66	21.9	117.7	12.9	77.0	-10338	21.6	1.73	21.2	19.4	1.9
4	Padded	-15º	6	-7651	13.6	20.9	1.42	21.1	109.9	14.4	68.6	-7995	21	1.52	24.7	-80	-10.0
5	Teflon	30º	6	-6270	15.2	5.1	1.07	5	37.1	5.9	34.7	-6482	4.8	1.09	4.9	13.3	2.1
6	Teflon	15º	6	-8454	17.6	7	1.47	5	54.2	6.4	71.8	-9516	6	1.83	7.3	98.6	10.4
7	Teflon	0º *	6	-7553	13.6	6.2	1.35	5.7	90.4	12.1	61.7	-8564	6.6	1.42	6.1	13.8	2.0
8	Teflon	0º	6	-9665	16.3	6.5	1.86	6.1	174.2	18.1	75.4	-11145	6	1.86	5.9	17.9	1.6
9	Teflon	-15º	6	-7854	14.7	5	1.45	5.1	111.5	14.2	49.6	-8346	5.8	1.47	5.9	-19.6	-2.3
10	Teflon	15º Lat	6	-7743	68.4	4.7	1.39	4.8	87.5	11.3	49.3	-8438	5.5	1.39	5.6	13.7	1.6
11	Teflon	15º Lat	6	-8365	60.4	4.4	1.51	4.4	99.4	11.9	51.7	-9030	5.3	1.50	5.3	18	2.0
12	Teflon	0º **	6	-6744	61.0	4.4	1.23	4.4	86.7	12.9	44.6	-7066	5.9	1.16	4.9	7.3	1.0
13	Teflon	0º **	6	-7107	62.9	4.6	1.29	4.6	90.1	12.7	47.0	-8401	4.3	1.35	5.3	3.4	0.4
14	Padded	30º	17.5	-7745	12.6	21.9	1.39	21.9	84.6	10.9	83.7	-8503	22.9	1.70	23.6	112.9	13.3
15	Padded	15º	17.5	-9169	13.7	21.9	1.68	22.1	136.2	14.9	82.4	-10360	22	1.77	22.2	26.8	14.8
16	Padded	0º	17.5	-8558	13.3	19.6	1.63	19.7	153.3	17.9	69.7	-9214	20.7	1.66	20.8	-23.8	-2.6
17	Padded	-15º	17.5	-6503	13.4	20.2	1.27	20.3	132.9	20.4	71.6	-6613	20.1	1.43	23.1	-93	-14.1
18	Teflon	30º	17.5	-7698	14.8	5	1.38	5	81.8	10.6	60.4	-8449	5.7	1.58	6.8	88.7	10.5
19	Teflon	15º	17.5	-9676	16.8	6.5	1.82	6.5	155.6	16.1	80.6	-10943	6.8	1.93	6.8	43.5	4.0
20	Teflon	0º *	17.5	-6926	12.2	5.4	1.32	5.4	125.5	18.1	49.2	-7563	6.1	1.32	6.2	-15.2	-2.2
21	Teflon	0º	17.5	-8805	14.9	5	1.68	5.3	151.1	17.2	60.9	-9718	6.1	1.72	6.2	-21	-2.2
22	Teflon	-15º	17.5	-6659	15.3	5.1	1.29	5.1	134.7	20.2	35.7	-6731	4.7	1.36	6.1	-79.5	-11.8
23	Teflon	15º Lat	17.5	-7391	66.8	4.7	1.39	4.9	120.9	16.4	43.1	-7659	5	1.37	5.8	-20.9	-2.7
24	Teflon	15º Lat	17.5	-7888	63.1	4.6	1.49	4.7	134	17.0	45.4	-8272	5.6	1.42	5.6	-14.9	-1.8
25	Teflon	0º **	17.5	-6597	58.0	4.8	1.28	4.8	133.2	20.2	38.7	-6463	4.7	1.24	4.9	-26.2	-4.1
26	Teflon	0º **	17.5	-7215	63.1	4.4	1.40	4.4	144.3	20.0	40.3	-7151	4.9	1.35	4.8	-25.2	-3.5

*45 cm drop height

**ATD head-neck pre-flexed 15 degrees

^Reported at the time of peak Nij

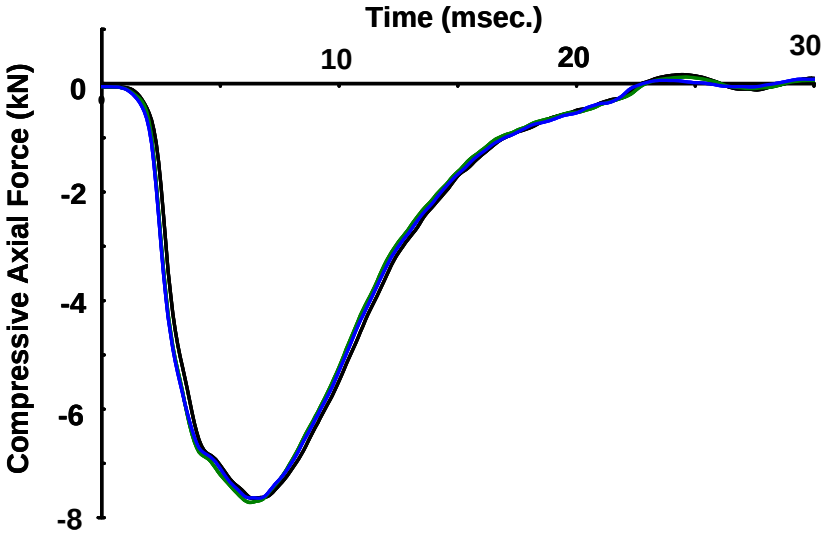

Figure 6.7: Lower neck axial force response for three experiments conducted using a 15º laterally inclined lubricated Teflon impact surface

The ATD neck angle with respect to vertical influenced the peak load measured at the upper and lower neck and polarity of the upper neck sagittal plane moment for a given impact plate orientation. In general, as the neck angle and impact plate become more perpendicular to one another, the neck loads increase. Thus, the highest loads with the 6 degree angle neck were measured with a 0 degree impact surface and highest loads for the 17.5 degree angle neck were measured in the 15 degree impact surface tests. This is generally consistent with PMHS testing in that the more perpendicular the axis of the spine is to the applied load, the higher the risk of injury. For flat surface impacts, the 6 degree neck angle results in flexion at the upper neck and the 17.5 degree neck results in extension, however in all cases, the upper neck moments were low in magnitude. Finally, peak loads were always anterior of the centerline of the base of the lower neck. This is consistent with peak loads in PMHS testing except for the 30 degree impact plate in which peak loads are generally posterior to the C7/T1 intervertebral disc in the PMHS. Figure 6.8 depicts the orientation of the ATD head and neck relative to the impact surface and the approximate line of action of the peak load for each sagittal plane impact plate orientation.

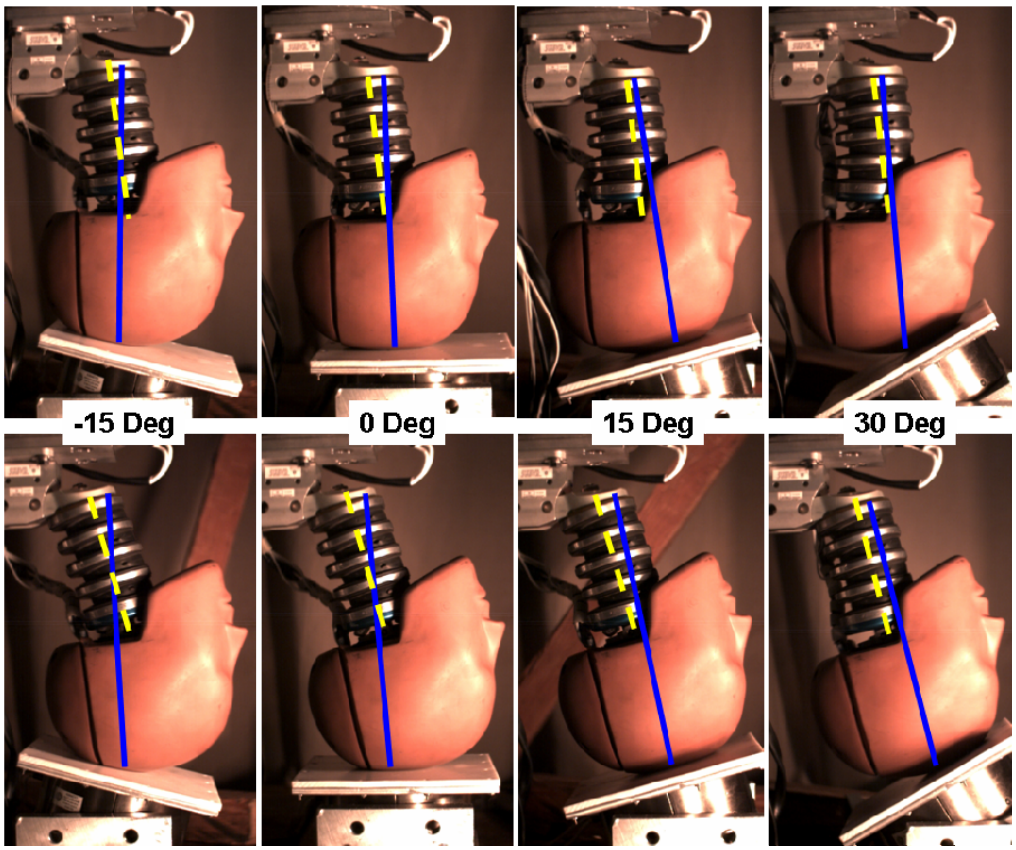

Figure 6.8: The line of force at peak load (blue) compared to the ATD neck centerline (yellow) for the 6 and 17.5 degree neck orientations for each the -15, 0, 15 and 30 impact plates

The ability of the ATD head to escape the following torso mass varied depending on impact plate orientation and surface material. The ATD head and neck kinematics at the approximate furthest extent of drop cart travel before either rebounding or coming to rest during the Nightingale et al. (1997a) impact conditions are depicted in Figures 6.9. In both the -15 degrees posterior oriented impact and the +30 degree anterior oriented impacted the ATD head escaped the following torso mass on lubricated Teflon, but not with the increased constraint caused by adding padding to the surface. During the 0 deg and +15 degree anterior oriented impacts, the ATD head was not able to escape with either a padded surface or a lubricated Teflon surface. In each of the lateral configurations, the head was able to escape whether it was a 15 degree laterally inclined surface or a 15 degree pre-laterally flexed ATD head-neck (Figure 6.10). Upper neck peak force ranged from 4 to 13 % greater than lower neck peak force across tests conditions due to the additional effective mass of the neck.

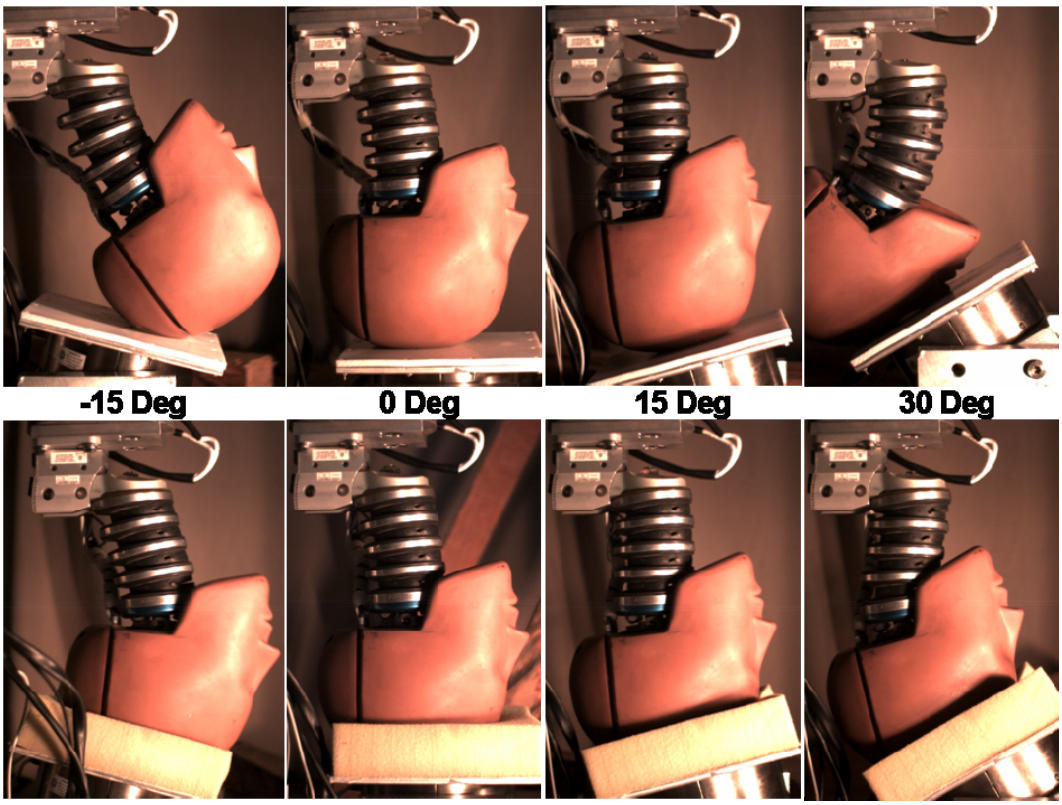

Figure 6.9: ATD kinematics for 6º neck angle in Nightingale et al. (1997a) impact surface and orientation conditions

I

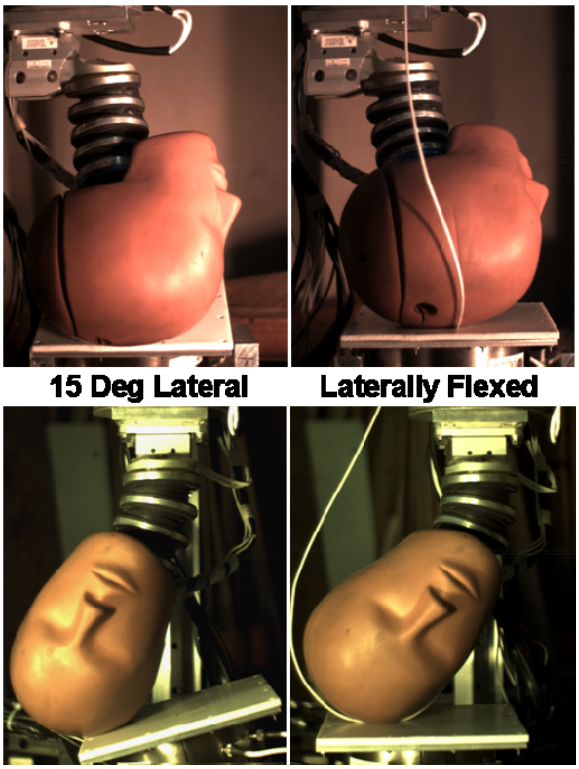

Figure 6.10: ATD kinematics for 6º neck angle in lateral Configurations 1 and 2 from the current study

In PMHS experimentation, increased head constraint increases the risk of cervical spine injury. If the head cannot escape the following torso, the torso is decelerated by forces transferred through the neck. Direct comparison between the ATD neck loads of lubricated Teflon and padded surface impacts shows that in the -15, 0, and 15 degree impact plate scenarios, the peak ATD upper and lower neck axial loads were reduced by approximately 2-7% by the introduction of padding. The exception is the 6 degree angle lower neck load on the 15 degree surfaces in which the loads were within 1%. In contrast, padding increased the ATD upper and lower neck loads in the 30 degree impact surface test condition. In the current set of experiments, once the angle between the axis of the ATD neck and the impact surface reached approximately 20 degrees, the increased constraint imposed on the ATD by padding resulted in higher neck loads.

The lower neck axial force impulse was also compared between lubricated Teflon and padded impacts. In every impact orientation, padding increased the impulse calculated from the lower neck axial force. The average increase was approximately 5% in 0 and 15 degree impacts and over 75% in 30 and -15 degree impacts. Unlike axial force, the axial impulse calculated at the lower neck increases with head constraint in all test condition and by a large margin in -15 degree posterior and 30 degree anterior impacts.

6.3.2 – Comparison to PMHS Response

The 20 PMHS tests reconstructed with the Hybrid III ATD were divided into four groups for comparison to ATD lower neck axial force response. The four groups include 3 experiments conducted with a laterally inclined plate, 2 experiments conducted with a pre-laterally flexed neck, 8 constrained to sagittal plane motion on a Teflon impact surface and 7 experiments constrained to the sagittal plane conducted with a padded impact surface. The range in the axial force responses for the ATD are depicted by the gray corridors and each PMHS experiment is plotted and depicted by the black lines in Figure 6.11.

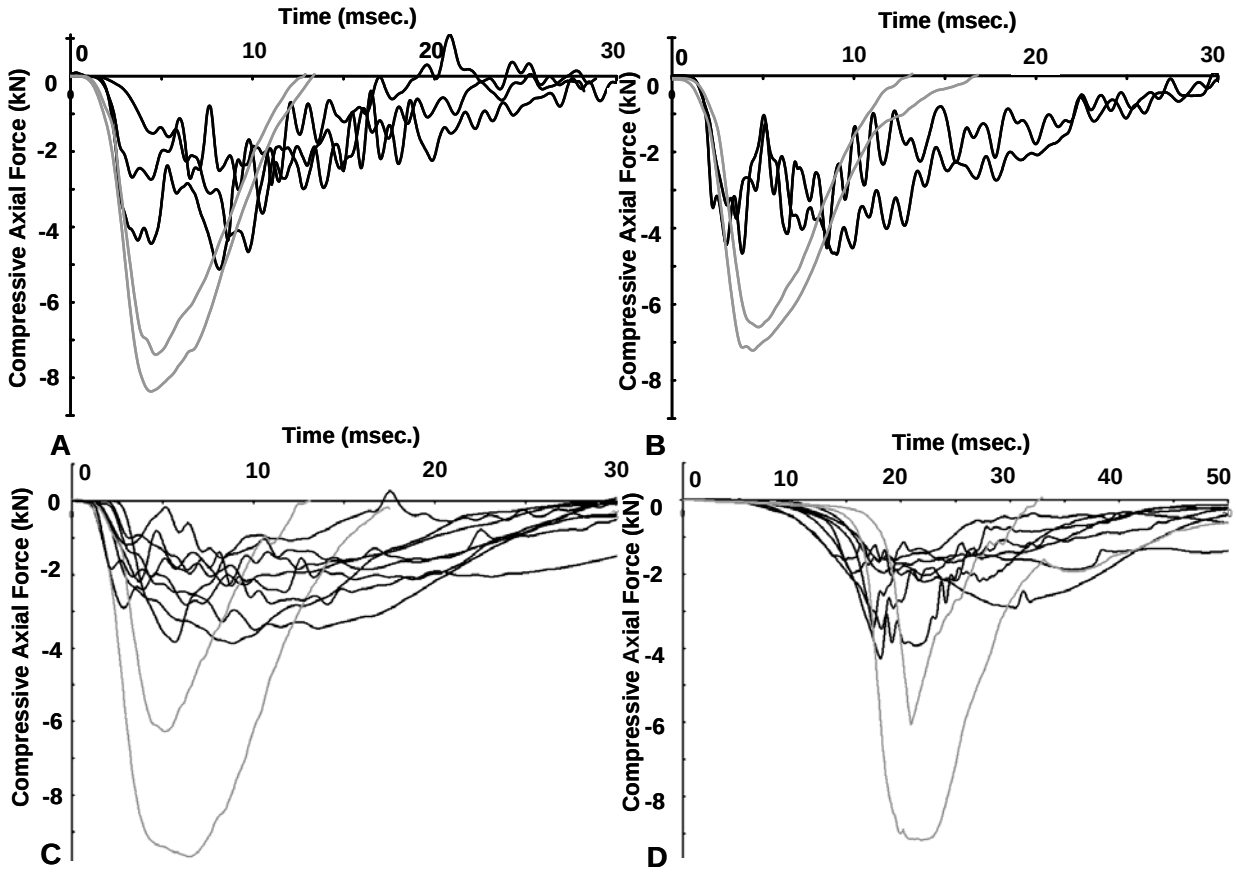

Figure 6.11: Comparison of PMHS and ATD lower neck axial force responses for 15 degree laterally inclined surface tests (A), 15 degree pre-laterally flexed head-neck tests (B) Nightingale et al. (1997a) lubricated Teflon tests (C) and Nightingale et al (1997a) padded tests (D)

The lower neck axial force response of the PMHS and ATD compares favorably for each of the groups of experiments during the initial loading. The rate of axial load onset is similar and does not begin to diverge until the PMHS fails or the cervical column buckles. Because the PMHS is force limited due to either material or structural failure, the peak forces cannot be directly compared. Across all 14 PMHS test conditions that resulted in a documented injury, the ATD peak load occurred, on average, within 2 milliseconds after the time of documented PMHS failure load. When evaluating rigid and padded impacts separately, the ATD peak load was measured, on average, approximately 1 and 2 milliseconds after the time of PMHS failure load respectively.

Similarly, the lower neck axial force versus cart displacement responses of the PMHS and ATD experiments compare favorably during the initial loading phase. The rate of axial load onset is similar and doesn't begin to diverge until the PMHS fails or the cervical column buckles.

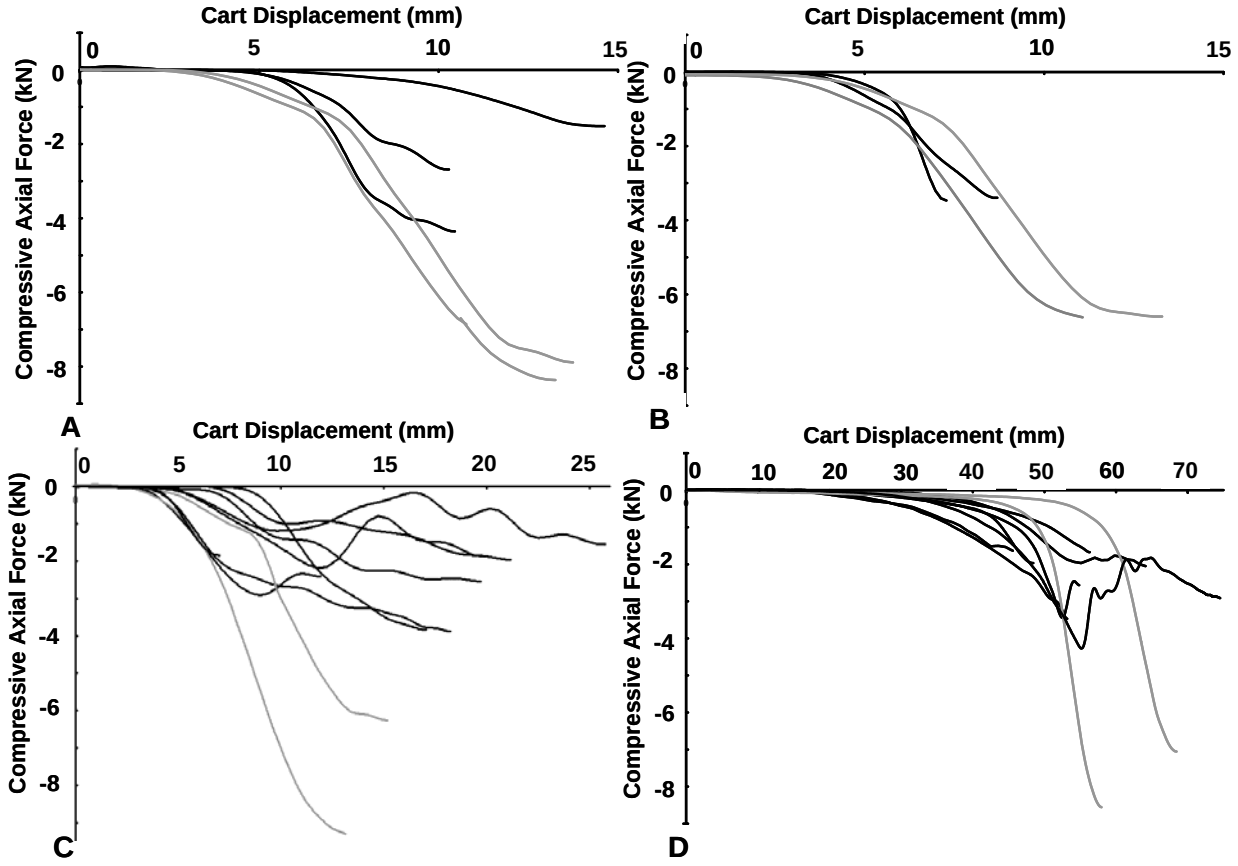

Figure 6.12: Comparison of PMHS and ATD lower neck axial force versus drop cart displacement for 15 degree laterally inclined surface tests (A), 15 degree pre-laterally flexed head-neck tests (B) Nightingale et al. (1997a) lubricated Teflon tests (C) and Nightingale et al (1997a) padded tests (D)

Across all 12 PMHS test conditions that resulted in a documented injury in which cart displacement data was available, the ATD peak load occurred with in approximately 4 millimeters of additional cart displacement, on average, compared to the documented PMHS failure cart displacement. When evaluating rigid and padded impacts separately, the ATD peak load occurred, on average, at less than 1 and 8 millimeters more displacement than the cart displacement at PMHS failure respectively. The greater variance in padded impacts can be explained by the onset of ATD load occurring later in padded impacts in Figure 6.12 (D). This

suggests the stiffness of the padding used in the PMHS and ATD tests was not exactly the same and highlights the influence of padding characteristics on the axial force response of the ATD neck.

6.3.3 ATD Neck Compressive Injury Metrics

Since PMHS are force limited by either structural (buckling) or material (fracture or ligament rupture) failure, direct comparison of PMHS loads to those measured in the ATD neck must be made carefully. In order for an injury criterion to be easily calculated and interpreted from the response of an ATD, peak loads are typically used. The peak kinetics measured in the ATD neck during test conditions that result in an increased risk of PMHS were generally greater in magnitude. The exception is the 0 and 15 degree anterior impacts on lubricated Teflon. The lower coefficient of friction in these impacts results in fewer and less severe injuries in the PMHS compared to impacts with a padded surface which have an increased probability of PMHS injury. In the 0 and 15 degree lubricated Teflon test conditions, the ATD head-neck is unable to escape the following torso mass and the loads measured exceed those in padded surface impacts. The head constraint present in the ATD reconstruction of these test conditions exceeds that of the PMHS and correlating to the respective injury outcomes may result in underestimation of the probability of injury. Analysis was conducted using two groups of matched ATD responses with PMHS outcomes. The first included all 20 experiments with known PMHS injury outcomes and second excluded the 0 and 15 degree Teflon impacts resulting in only 14 experiments with known PMHS injury outcomes.

The resulting p-values from comparison of upper and lower neck ATD peak axial forces across injury groups are presented in Table 6.3. The peak ATD lower neck axial force was found to delineate test conditions resulting in non-injury and stable injury from unstable injury when the 0 and 15 degree rigid impacts were excluded in both the 6 and 17.5 degree neck angle test conditions. The peak upper neck axial force delineates test conditions resulting in

non-injury from stable and unstable injury when all the test conditions were included for both the 6 and 17.5 degree neck angles. Equally important are the test conditions under which the lowest axial force was measured in a test condition that resulted in an unstable injury in the PMHS. These tests are the 30 degree lubricated Teflon impact surface for the 6 degree angle neck and the -15 degree padded impact surface for the 17.5 degree angle neck. The resulting upper neck axial compressive force for each test condition is -6,482 N and -6,613 N respectively. The resulting lower neck axial compressive force for each test condition is -6,290 N and -6,503 N respectively. These values are consistent with both the Nij compressive intercept and compressive IARV derived by Mertz et al. (1978).

Table 6.3: Comparison of peak ATD neck axial force across PMHS injury groups

	All Male PMHS Outcomes		Excluding 0° / 15° Teflon Outcomes	
	Any Injury p Value	Unstable Injury p Value	Any Injury p Value	Unstable Injury p Value
6° Upper Neck Fz	0.059*	0.497	0.140	0.540
17.5° Upper Neck Fz	0.056*	0.564	0.269	0.544
6° Lower Neck Fz	0.441	0.183*	0.836	0.097*
17.5° Lower Neck Fz	0.362	0.152	0.465	0.031*
6° Lower Neck Fz Impulse	0.450	0.555	0.577	0.538
17.5° Lower Neck Fz Impulse	0.232	0.227	0.255	0.194

*Wilcoxson Ranked Sum Test results is $p < 0.10$

The peak lower neck axial force in each test condition maintained for various length pulse durations are plotted in Figure 6.13. Each line on the plot represents a single test condition with multiple PMHS injury outcomes. Green lines represent test conditions in which no unstable injuries occurred, whereas red lines represent the presence of unstable injuries. Generally, the frequency of unstable injuries increases as the magnitude and duration of the axial neck load increases. The slope of the plotted lines is steeper than the results of Mertz et al. (1978) when the ATD impacted a football tackling block. The characteristics of the padding used in experimentation will have a significant influence on the overall pulse shape and duration measured by the ATD neck load cell. Based on Figure 6.13, in either the current test conditions

or those of Mertz et al., a peak ATD neck load of 6,000 N sustained for approximately 5 milliseconds results the “potential for serious neck injury” as defined by Mertz et al.

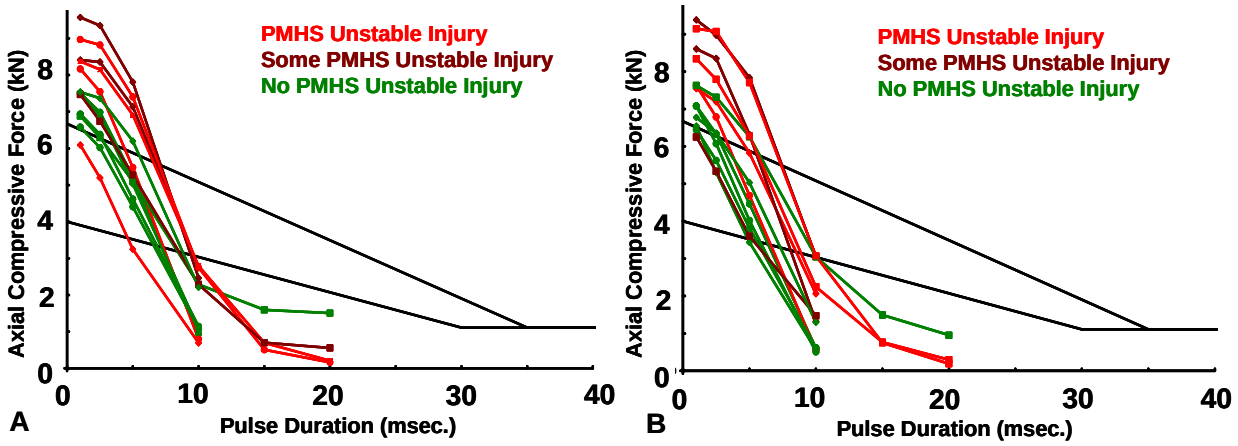

Figure 6.13: Comparison of the Hybrid III ATD reconstructions of Mertz et al. (1978) to the current study using a 6 degree (A) and 17.5 degree (B) neck

The lower neck axial impulse was sensitive to the additional head constraint from padding, however, the overall average magnitude of axial impulse between injury groups did not differ by a wide margin. The significance of the difference between injury groups was strongly influenced by the initial neck angle (Table 6.3). P values for differences in both the any injury and the unstable injury groups ranged between 0.2 and 0.25 for the 17.5 degree neck but ranged from 0.45 to 0.55 for the 6 degree neck.

The lower and upper neck Nij values were calculated. Similar to PMHS experimentation, the sagittal plane moment measured in the ATD neck did not add significantly to the ability to predict PMHS injury outcomes. The contribution of the sagittal plane moment to the Nij magnitude varied little between test conditions and was unable to delineate between test conditions that caused PMHS injury. The lower neck sagittal plane moment contributed 10.1 +/- 3.1% and 14.6 +/- 2.5% of the total lower neck Nij for the 6 degree and 17.5 degree neck orientations respectively. The upper neck sagittal plane moment contributed 4.1 +/- 4.1% and 4.9 +/- 3.7% of the total upper neck Nij for the 6 degree and 17.5 degree neck orientations respectively. The relatively small contributions are explained by how closely the force is applied

to the centerline of ATD neck in the loading scenarios investigated in the current study (Figure 6.8). Additionally, based on the geometry of the ATD head-neck complex, when the moments are calculated at the centerline of the base of the neck in these test conditions, they are almost exclusively of a positive polarity or forward flexion.

The eccentricity of the applied sagittal plane resultant force was calculated for each test condition in order to evaluate the possibility of defining an N_{ECC} injury metric for the ATD neck. The overall range of eccentricities was smaller than PMHS experiments. The magnitude of the lower neck eccentricities was 11.2 +/- 3.8 mm and 16.9 +/- 3.2 mm for the 6 and 17.5 degree neck orientations respectively for each of the test conditions evaluated. The magnitude of the upper neck eccentricities was 4.8 +/- 5.3 mm and 6.7 +/- 5.2 mm for the 6 and 17.5 degree neck orientations respectively. The ATD lower neck sagittal plane peak resultant force is plotted against the eccentricity from center of the base of the neck for each of the 17.5 degree neck angle test conditions evaluated in Figure 6.14.

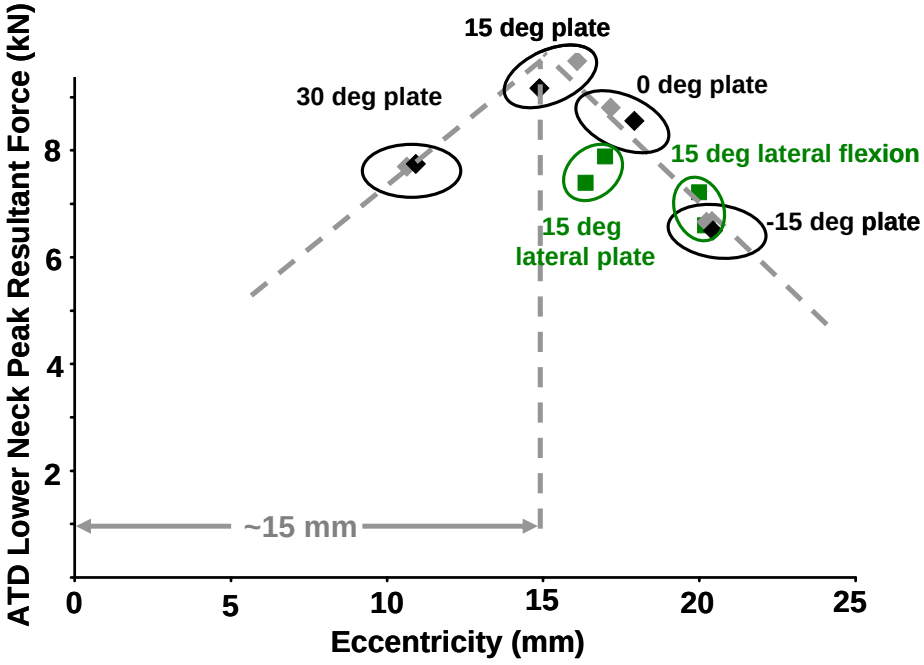

Figure 6.14: ATD peak lower neck sagittal plane resultant force versus eccentricity from the neck centerline for each of the test conditions evaluated

As the ATD neck and impact surface angle becomes more oblique, the peak force decreases and the eccentricity increases. During PMHS testing, the peak resultant load occurred at a positive (anterior) eccentricity for each test condition except for the 30 degree anterior oriented impacts which resulted in 5 to 10 millimeters of negative (posterior) eccentricity. For the 17.5 degree angled ATD neck, an eccentricity of approximately 15 millimeters appears to correlate with the center of the PMHS C7/T1 intervertebral disc. A similar analysis was conducted for the 6 degree neck angle and approximately 10 millimeters of eccentricity correlates with the center of the PMHS C7/T1 intervertebral disc. This is depicted in Figure 6.15 in which cervical vertebrae have been overlaid on the ATD neck. ATD lower neck kinetics are generally reported at the centerline of the base of the neck where the yellow lines intersect. Based on the measured responses in the current testing, this appears to be approximately 10 to 15 millimeter posterior of the point that would correlate to the kinetics of the center of the C7/T1 PMHS intervertebral disc.

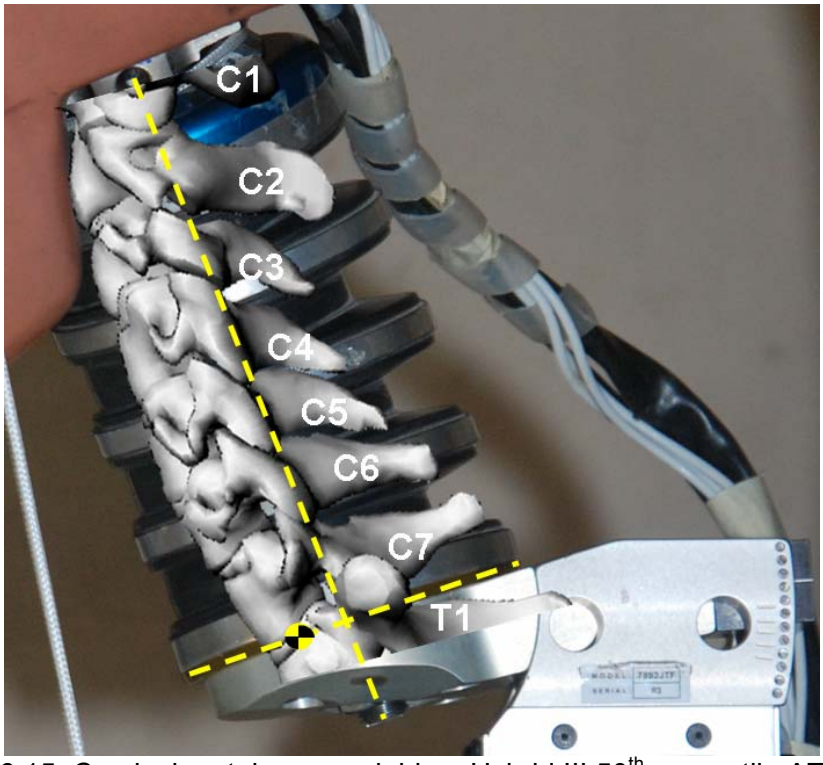

Figure 6.15: Cervical vertebrae overlaid on Hybrid III 50th percentile ATD neck

The point at which the lower neck forces and moments are reported is critical to deriving a N_{ECC} injury criteria based on the ATD neck response. This location varies depending on the neck angle used in the current study. Additionally, the derivation of a PMHS N_{ECC} was aided by a wider range of kinetic responses, some of which included eccentricities approaching 60 mm at failure. The Hybrid III ATD has a very narrow range of measured eccentricities in the test conditions evaluated in this study. Finally, the experiments reconstructed with the Hybrid III ATD head and neck are conducted very near the threshold for PMHS injury. A single test condition results in multiple PMHS injury outcomes with very little variation in the N_{ECC}. A wider range of test conditions with known PMHS injury outcomes is necessary to fully develop a N_{ECC} criterion for the Hybrid III ATD neck.

6.3.4 Logistic Regression

The limited number of male PMHS experiments able to be reconstructed limits the statistical significance of the findings. Analysis of the matched data set of Hybrid III ATD neck response and PMHS injury outcomes in the same test conditions resulted in only two correlations with significance levels better than $p < 0.1$. The peak ATD lower neck axial force was found to delineate test conditions resulting in non-injury and stable injury from unstable injury when the 0 and 15 degree rigid impacts were excluded. The peak upper neck axial force delineates the test conditions resulting in non-injury from stable and unstable injury when all the test conditions were included. Probability of injury curves for the injury definitions with the highest significance levels based on upper and lower neck compressive force are presented for the purpose of comparison to the currently defined Hybrid III 50^{th} percentile neck compressive IARVs. The 6 and 17.5 degree ATD neck angle are evaluated separately. Table 6.4 contains the matched data set of ATD upper and lower neck response and PMHS injury outcome.

Table 6.4: Matched ATD neck response and PMHS injury outcome data set

Test Information				PMHS Data							Hybrid III - 50th Percentile Neck Data					
				Documented Failure				Peak Force			Neck	Lower Neck		Upper Neck		
Study	Test ID	Age	Test Condition	Time (msec.)	Fz (N)	Cart Disp (mm)	Injury Stability	Time (msec.)	Fz (N)		Angle (deg.)	Time (msec.)	Fz (N)	Time (msec.)	Fz (N)	
Current	1	76	Config 1	-	-	-	NI	8.2	-5122		6	4.7	-7743	5.5	-8438	
Current	2	80	Config 1	-	-	-	NI	10.6	-3643		6	4.7	-7743	5.5	-8438	
Current	3	55	Config 1	4.5	-1518	14.6	unstable	8.7	-4371		6	4.4	-8365	5.3	-9030	
Current	4	77	Config 2	3	-3396	8.7	stable	9.1	-4694		6	4.4	-6744	5.9	-7066	
Current	5	88	Config 2	2.2	-3472	7.3	stable	3.8	-4669		6	4.6	-7107	4.3	-8401	
Nightingale	N05	36	30	8.3	-1552	25.8	unstable	16.3	-1858		6	5.1	-6270	4.8	-6482	
Nightingale	N18	-	15	6.4	-1871	19.8	unstable	11.7	-2494		6	7	-8454	6	-9516	
Nightingale	D41	69	15	-	-	-	NI	5.7	-3839		6	7	-8454	6	-9516	
Nightingale	I32	78	15	3.9	-2416	11.9	stable	2.8	-2905		6	7	-8454	6	-9516	
Nightingale	N26	65	0	-	-	-	NI	8.9	-3877		6	6.2	-7553	6.6	-8564	
Nightingale	N24	62	0	2.2	-1845	-	stable*	8.5	-2308		6	6.5	-9665	6	-11145	
Nightingale	N22	71	0	6.5	-1966	-	unstable*	14.1	-2814		6	6.5	-9665	6	-11145	
Nightingale	N11	55	-15	-	-	-	NI	6.6	-2539		6	5	-7854	5.8	-8346	
Nightingale	N21	61	30	14.8	-1635	45.6	stable	20.9	-1757		6	22	-7052	22.2	-7410	
Nightingale	N23A	46	30	-	-	-	NI	22	-2052		6	22	-7052	22.2	-7410	
Nightingale	I08	80	15	30.5	-2915	74.5	unstable*	18.1	-4273		6	20.2	-8502	21	-9396	
Nightingale	I04	63	15	18	-1675	56.3	unstable*	22.1	-2218		6	20.2	-8502	21	-9396	
Nightingale	N03	75	0	18.2	-3473	53.2	unstable	21.3	-3937		6	20.9	-9162	21.6	-10338	
Nightingale	NA2	61	-15	15.6	-1969	48.5	stable	15.6	-1969		6	20.9	-7651	21.2	-7995	
Nightingale	I25	59	-15	18.4	-2565	54.9	unstable	17.5	-3443		6	20.9	-7651	21.2	-7995	
Current	1	76	Config 1	-	-	-	NI	8.2	-5122		17.5	4.7	-7391	5	-7659	
Current	2	80	Config 1	-	-	-	NI	10.6	-3643		17.5	4.7	-7391	5	-7659	
Current	3	55	Config 1	4.5	-1518	14.6	unstable	8.7	-4371		17.5	4.6	-7888	5.6	-8272	
Current	4	77	Config 2	3	-3396	8.7	stable	9.1	-4694		17.5	4.8	-6597	4.7	-6463	
Current	5	88	Config 2	2.2	-3472	7.3	stable	3.8	-4669		17.5	4.4	-7215	4.9	-7151	
Nightingale	N05	36	30	8.3	-1552	25.8	unstable	16.3	-1858		17.5	5	-7698	5.7	-8449	
Nightingale	N18	-	15	6.4	-1871	19.8	unstable	11.7	-2494		17.5	6.5	-9676	6.8	-10943	
Nightingale	D41	69	15	-	-	-	NI	5.7	-3839		17.5	6.5	-9676	6.8	-10943	
Nightingale	I32	78	15	3.9	-2416	11.9	stable	2.8	-2905		17.5	6.5	-9676	6.8	-10943	
Nightingale	N26	65	0	-	-	-	NI	8.9	-3877		17.5	5.4	-6926	6.1	-7563	
Nightingale	N24	62	0	2.2	-1845	-	stable*	8.5	-2308		17.5	5	-8805	6.1	-9718	
Nightingale	N22	71	0	6.5	-1966	-	unstable*	14.1	-2814		17.5	5	-8805	6.1	-9718	
Nightingale	N11	55	-15	-	-	-	NI	6.6	-2539		17.5	5.1	-6659	4.7	-6731	
Nightingale	N21	61	30	14.8	-1635	45.6	stable	20.9	-1757		17.5	21.9	-7745	22.9	-8503	
Nightingale	N23A	46	30	-	-	-	NI	22	-2052		17.5	21.9	-7745	22.9	-8503	
Nightingale	I08	80	15	30.5	-2915	74.5	unstable*	18.1	-4273		17.5	21.9	-9169	22	-10360	
Nightingale	I04	63	15	18	-1675	56.3	unstable*	22.1	-2218		17.5	21.9	-9169	22	-10360	
Nightingale	N03	75	0	18.2	-3473	53.2	unstable	21.3	-3937		17.5	19.6	-8558	20	-9214	
Nightingale	NA2	61	-15	15.6	-1969	48.5	stable	15.6	-1969		17.5	20.2	-6503	20.7	-6613	
Nightingale	I25	59	-15	18.4	-2565	54.9	unstable	17.5	-3443		17.5	20.2	-6503	20.1	-6613	

Logistic regressions were conducted for both the upper and lower neck axial force responses in test conditions matched to PMHS human subject injury outcomes. Based on previous comparison between injury groups, the lower neck response data was used to generate the probability of unstable PMHS cervical damage whereas the upper neck data was used to evaluate the probability of any PMHS cervical damage. In both scenarios, the entire set of 20 experiments was evaluated as well as the set of experiments excluding 0 and 15 degree impacts on lubricated Teflon for the aforementioned reasons. The regression model and independent variable (axial force) statistics are presented in Table 6.5. Additionally, the percent of the time that the model accurately predicted the injury outcome based on the underlying data set is presented. The specificity (correctly predicted the lack of an injury outcome), sensitivity (correctly predicted the presence of injury outcome) and total percentages are listed.

Table 6.5: Logistic regression model and variable statistics

		Model Statistic		Variable Statistic		Model Predicted Correctly		
	Neck Angle	-2LL Chi^2	P value	Wald Chi^2	P value	Specificity	Sensitivity	Total
Lower Neck	6° Neck	1.998	0.158	1.768	0.184	91.7%	25.0%	65.0%
Compressive	17.5° Neck	2.264	0.132	2.060	0.151	0.0%	100.0%	71.4%
Force - Unstable	6° Neck*	3.280	0.070	2.437	0.118	100.0%	66.7%	85.7%
Injury	17.5° Neck*	5.293	0.021	3.124	0.077	100.0%	66.7%	85.7%
Upper Neck	6° Neck	4.210	0.040	3.025	0.082	33.3%	85.7%	70.0%
Compressive	17.5° Neck	4.180	0.041	3.094	0.079	33.3%	78.6%	65.0%
Force - Any	6° Neck*	2.817	0.093	1.945	0.163	25.0%	90.0%	71.4%
Injury	17.5° Neck*	1.529	0.216	1.261	0.261	0.0%	100.0%	71.4%

* Excluding 0° / 15° Rigid Impacts

Similar to the previous comparison of means between injury groupings, model and variable significance levels are highest when evaluating the entire data set for the upper neck loads and excluding the 0 and 15 degree lubricated Teflon impacts when evaluating the lower neck loads. Additionally, when attempting to delineate unstable injury with lower neck loads the specificity of the model is greater but upper neck loads are more sensitive at detecting the likelihood any cervical injury. Figure 6.16 depicts the probability of unstable injury based on lower neck loads and Figure 6.17 the probability of any injury based on upper neck loads.

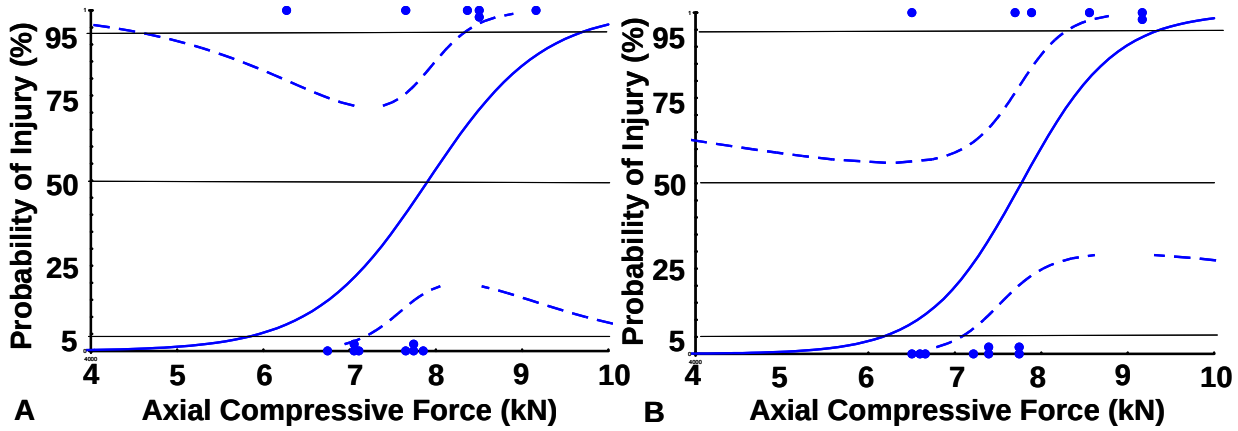

Figure 6.16: Probability of PMHS unstable orthopedic cervical damage based on the Hybrid III 50th percentile lower neck compressive force for a 6 degree (A) and 17.5 degree (B) neck angle

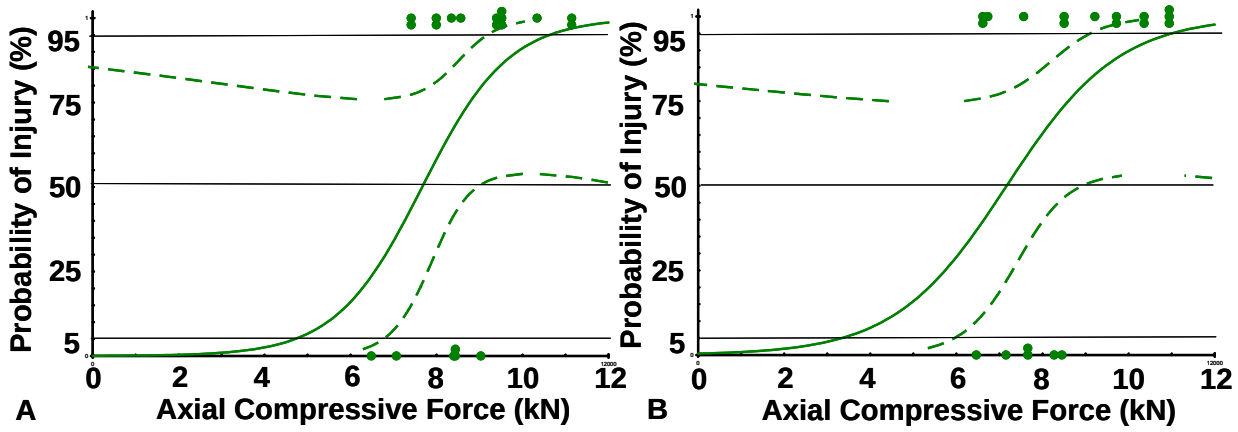

Figure 6.17: Probability of any PMHS orthopedic cervical damage based on the Hybrid III 50th percentile upper neck compressive force for a 6 degree (A) and 17.5 degree (B) neck angle

The 95% confidence intervals depicted in Figures 6.15 and 6.16 are very wide. The test conditions evaluated were all very near the threshold for PMHS injury. For a given test condition, in many cases multiple different PMHS injury outcomes were observed. Combined with the fact that the data set is relatively small, this likely is the major influence on the size of the confidence intervals. Although the confidence intervals are large, the underlying data are a good representation of outcomes in test conditions that are very near the PMHS injury threshold in the test methodology utilized.

The 5 and 50% probability of any injury ranged from approximately 3,340 to 4,710 N and 7,170 to 7,660 N of upper neck axial force depending on ATD neck angle. The wide range at low probability of injury is due to the limited underlying data near the tail of the probability curve. The 5 and 50% probability of unstable injury ranged from approximately 5,950 to 6,160 N and 7,770 to 7,910 N of lower neck axial force depending on ATD neck angle.

6.4 Discussion

The Hybrid III family of ATDs is often used to evaluate the potential for catastrophic compressive cervical spine injury. A limited number of direct correlations between the Hybrid III ATD response and human injury outcomes are available in the literature. The interpretation of measured neck loads and moments in various loading scenarios would be aided by a better understanding of the correlation between the mechanical responses in the Hybrid III ATD and the risk of injury in the human cervical spine. This was accomplished by creating a matched data set of ATD response and PMHS injury outcomes through experimental reconstruction of 20 PMHS experiments with the Hybrid III ATD head and neck.

The Hybrid III ATD head and neck assembly was found to be robust and extremely repeatable in severe impact scenarios. The initial axial force response of the ATD head-neck is very comparable to PMHS experiments up to the point of PMHS cervical column buckle or material failure. The time and displacement of the drop cart at the peak ATD response occurred very close to the time and displacement of the drop cart at documented PMHS failure. The Hybrid III ATD head and neck best matched the response of PMHS experiments with a pre-laterally flexed posture which better couples the head to the torso (Figures 6.10(B) and 6.11(B)). Based on the geometry and construction of the Hybrid III ATD neck, it is expected that its response would even closer match dynamic PMHS experiments with pre-forward flexed resulting in an aligned cervical column (Pintar et al. 1995).

In most of the impact scenarios evaluated, the overall head kinematics of the ATD were similar to the PMHS. The exception was the 0 and 15 degree lubricated Teflon impacts. Several factors may contribute to this difference including greater coupling of the ATD head to the drop cart torso mass, the straighter geometry of the ATD neck and increased scalp friction of the ATD resulting in greater head constraint of the ATD in these scenarios then a PMHS. The practical result of this increased effective constraint is to make the response of Hybrid III head and neck a conservative predictor of injury in these impact conditions. However, there is not a high likelihood of interacting with a surface with a similar coefficient of friction as lubricated Teflon in real-world impact scenarios. As the friction in a real-world impact scenario increase, the ATD response and correlation to PMHS injury outcomes in padded impacts will better predict the probability of sustaining a cervical injury.

Two ATD neck angles with respect to vertical were chosen to evaluate a reasonable range of potential ATD head-neck orientations with the impact surfaces. A 6 degree neck angle was chosen as a representation of ATD neck head-neck orientations at the onset of automotive crash testing and 17.5 degree neck angle was chosen to more closely represent the orientation of the PMHS experiments being reconstructed. The neck angle relative to vertical used in the experiments did not have a large influence on the 50% probability of sustaining a cervical injury. It did have more influence on the range of loads estimated for probabilities of injury near the tails of the regression curves. Since the different neck angles evaluated changes the overall geometry of the ATD head-neck complex relative to the impact surface, neck angle did influence which impact conditions were associated with the highest or lowest loads and subsequently highest or lowest probability of injury. The 6 degree neck is least likely to result in a predicted injury in a 30 degree anterior impact on lubricated Teflon and the 17.5 degree neck is least likely to result in a predicted injury in a – 15 degree posterior impact on a padded surface. One PMHS unstable injury was documented in both of these scenarios resulting in a minimum range of

peak ATD lower neck axial force associated with unstable injury of 6,270 to 6,502 N for the current data set.

The number of experiments in the matched data set limits the statistical significance of the injury probability curves generated. The presented probability of injury curves are not recommended as definitive risk assessment, however, the logistic regressions are valuable for comparison to the currently defined neck compressive load IARVs and strengthen the basis for the IARVs by adding to the number of PMHS injury outcomes that the Hybrid III ATD has been correlated to. As more data becomes available, the ATD response and probability of human cervical injury relationship can be improved and potentially expanded to include additional injury criteria.

The average of the 6 and 17.5 degree neck angle *peak* ATD upper neck load associated with a 5% probability of any injury in a PMHS was found to be 4,025 N which is nearly equal to the current upper neck compressive force IARV. The average of the 6 and 17.5 degree neck angle *peak* ATD lower neck load associated with a 5% probability of an unstable injury in a PMHS was found to be 6,055 N. The lowest lower neck compressive force associated with a PMHS unstable injury producing test condition ranged from 6,290 N to 6,503 N depending on the initial neck angle of the ATD used in the experiment. Each of these values is consistent with both the Nij compressive intercept (6,200 N) and the upper compressive force threshold (6,670 N) above which there is a potential to cause serious neck injury as defined by Mertz et al. (1978). In the loading environment evaluated as part of the current study, where ATD head, neck and torso mass impact speeds are at the threshold for causing catastrophic cervical injury in the PMHS, the difference between 4,000 N and 6,000 N in the ATD neck is a matter of approximately 2 to 3 millimeters of additional torso cart displacement.

6.5 Conclusions

The Hybrid III ATD head and neck assembly was found to be robust and extremely repeatable in severe impact scenarios. The initial axial force response of the ATD head-neck is very comparable to PMHS experiments up to the point of PMHS cervical column buckle or material failure. AIS injury scaling of the cervical spine is highly dependant on the magnitude of spinal cord involvement. Unstable cervical orthopedic injuries have a greater risk of spinal cord injury and the need for surgical intervention. The smallest lower neck peak compressive force measured using the current set of PMHS test conditions with known injury outcomes that was associated with a PMHS unstable injury ranged from 6,290 N to 6,503 N depending on the initial neck angle of the ATD used in the experiment. The 5% probability of unstable injury ranged from approximately 5,950 to 6,160 N of lower neck axial force depending on ATD neck angle. These values are consistent with the both the reported finding of Mertz et al. (1978) and the current Nij compressive force intercept. The 5% probability of any injury ranged from approximately 3,340 to 4,710 N of upper neck axial force depending on ATD neck angle. This is consistent with the current FMVSS 208 compressive axial force limit of 4,000 N.

CHAPTER 7

CONCLUSIONS AND RECOMMENDATIONS

Overall compressive neck injury dynamics and tolerances in laterally inclined impacts and postures are similar to previous studies of purely sagittal plane dynamics based on these test results. Impact speeds for the five tests ranged from 2.9 to 3.25 m/s. Three of the five PMHS sustained compressive cervical vertebral fractures at loads ranging between 1,518 N and 3,472 N. The asymmetric postures and loading resulted in asymmetric fracture patterns. The pre-laterally flexed neck affected the neck axial force response and the average failure load in the current study. The initial axial response indicated a better coupling between the head and torso and the average failure load was approximately 50% greater than the average failure load reported for males by Nightingale et al. (1997a). Although lateral pre-flexion of the head-neck complex influenced axial response, shear forces and the lateral bending moment magnitudes at failure were small in comparison to sagittal plane responses in both test configurations. These secondary kinetics primarily act to modify the location of the applied axial force relative to the cervical column and in doing so, influence the magnitude of the axial response and specific injury outcomes. The axial response and failure load of a neutrally oriented neck against a laterally inclined impact plate is consistent with the neutral posture sagittal plane studies of Nightingale et al. (1997a). The failure loads of the pre-laterally flexed necks impacted onto a flat surface are consistent sagittal plane studies of Pintar et al. (1995) in which the cervical column was aligned through anterior pre-flexion.

A more refined PMHS cervical spine compressive injury tolerance was derived by combining the available dynamic PMHS experimentation including measured neck kinetics conducted by different laboratories using various test methodologies. The compressive force measured at the base of the neck associated with a 50% probability of stable and unstable orthopedic damage is 2,956 N and 3,938 N respectively. A new injury metric, N_{ECC}, was derived

based on the kinetics of PMHS experimentation at the time of documented failure. N_{ECC} improves the ability to delineate between stable and unstable compressive cervical injuries and by defining the location of the applied load, the type of injury likely to be sustained can be anticipated. The N_{ECC} measured at the base of the neck associated with a 50% probability of stable and unstable orthopedic damage is 0.86 and 1.09 respectively.

The Hybrid III ATD head and neck assembly was found to be robust and extremely repeatable in severe impact scenarios. The initial axial force response of the ATD head-neck is very comparable to the PMHS experiments up to the point of PMHS cervical column buckle or material failure. AIS injury scaling of cervical injury above AIS level 1 and 2 is highly dependent on the magnitude of spinal cord involvement. Unstable cervical orthopedic injuries have a greater risk of spinal cord injury and the need for surgical intervention. The smallest lower neck peak compressive force measured using the current set of PMHS test conditions with known injury outcomes that was associated with a PMHS unstable injury ranged from 6,290 N to 6,503 N depending on the initial neck angle of the ATD used in the experiment. The 5% probability of unstable injury ranged from approximately 5,950 to 6,160 N of lower neck axial force depending on ATD neck angle. These values are consistent with the both the reported finding of Mertz et al. (1978) and the current Nij compressive force intercept. The 5% probability of any injury ranged from approximately 3,340 to 4,710 N of upper neck axial force depending on ATD neck angle. This is consistent with the current FMVSS 208 compressive axial force limit of 4,000 N.

The test methodologies used by Pintar et al. (1995) and Nightingale et al. (1997a) are limited in their ability to define local kinetics at the site of injury and their ability to delineate injuries sustained at multiple vertebral levels in a single test. Analysis of individual cervical motion segment kinematics is limited to high speed video which is heavily dependent on the visible anatomical landmarks and the light necessary for clear depiction of motion at high frame rates. Use of advanced instrumentation techniques such as high speed bi-planar x-ray and acoustic sensors would aid in the definition of the local kinematics and kinetics at the site of

injury. These dynamics are especially important to injuries that result during the cervical spine's post-buckled orientation. Once these dynamics are more accurately defined, further investigation of oblique or three-dimensional cervical spinal response can be conducted. Currently, it is difficult to assess the influence of the fairly large axial twist moments measured in lateral test configurations. The quantification of PMHS bone mineral density used in experimentation is important in order to better define female cervical spine compressive injury tolerance and to more accurately assess the influence of donor age.

Additional PMHS experiments conducted over a wider range of impact conditions, including more test conditions that do not result in PMHS material failure, are necessary for a more rigorous statistical analysis of injury outcomes and their relationship to physical biomechanical surrogates' responses. The potential to include the natural lordosis of the human cervical spine in future physical surrogates should be evaluated, but a repeatable mechanical response must be maintained for consistency of results between laboratories.

REFERENCES

Alem, N.M., Nusholtz, G.S., Melvin, J.W., 1984. Head and neck response to axial impacts. 28th Stapp Car Crash Conference Proceedings, 127-40.

Alker, G.J., Oh, Y.S., Leslie, E.V., Lehotay, J., Panaro, V.A., Eschner, E.G., 1975. Postmortem radiology of head and neck injuries in fatal traffic accidents. Radiology, 114, 611-7.

Allen, B.L., Ferguson, R.L., Lehmann, T.R., O'Brien, R.P., 1982. A mechanistic classification of closed, indirect fractures and dislocations of the lower cervical spine. Spine, 7 (1), 1-27.

Allison, P.D., 1995. Survival analysis using the SAS® system: a practical guide. SAS Institute Inc., Cary, NC.

Babcock, J.L., 1976. Cervical spine injuries. Arch Surg, 111, 646-51.

Bahling, G.S., Bundorf, R.T., Kaspzyk, G.S., Moffatt, E.A., Orlowski, K.F., Stocke, J.E., 1990. Rollover and drop tests – the influence of roof strength on injury mechanics using belted dummies. 34th Stapp Car Crash Conference Proceedings, 101-12.

Bass, C.R., Donnellan, L., Salzar, R., Lucas, S., Folk, B., Davis, M., Rafaels, K., Planchak, C., Meyerhoff, K., Ziemba, A., Alem, N., 2006. A new neck injury criterion in combined vertical/frontal crashes with head supported mass. In Proceeding of International Research Council on the Biomechanics of Impact, Madrid (Spain), September 2006, 75-91.

Bass, C.R., Salzar, R.S., Lucas, S.R., Rafaels, K.A., Damon, A.M., Crandall, J.R., 2010. Re-evaluating the neck injury index (NII) using experimental PMHS tests. Traffic Injury Prevention, 11, 194-201.

Bostrom, O., Svensson, M.Y., Aldman, B., Hansson H.A., Haland, Y., Lovsund, P., Seeman, T., Suneson, A., Saljo, A., Ortengren, T., 1996. A new neck injury criterion candidate based on injury findings in the cervical spinal ganglia after experimental neck extension trauma. In Proceeding of International Research Council on the Biomechanics of Impact, Dublin (Ireland), September 2006, 123-36.

Bruhn, E. F., 1973. Analysis and Design of Flight Vehicle Structures, Jacobs Publishing, Inc., Indianapolis.

Bucholz, R.W., Burkhead, W.Z., Graham, W., Petty, C., 1979. Occult cervical spine injuries in fatal traffic accidents. J Trauma, 19(10), 768-71.

Camacho, D., Nightingale, R.W., Myers, B.S., 1999. Surface friction in near-vertex head and neck impact increases risk of injury. J Biomech, 32, 293-301.

Carter, J.W., Ku, G.S., Nuckley, D.J., Ching, R.P., 2002. Tolerance of the cervical spine to eccentric axial compression. 46th Stapp Car Crash Conference Proceedings, 441-59.

CFR 49 part 572.208, Code of Federal Regulations (CFR) Title 49 (Transportation) Chapter V (NHTSA, DOT), Part 571-208, Occupant Crash Protection

Cheng, R., Yang, K.H., Levine, R.S., King, A.I., Morgan, R., 1982. Injuries to the cervical spine caused by a distributed frontal load to the chest. 26th Stapp Car Crash Conference Proceedings, 1-40.

Ching, R.P., Elias, P.Z., Harrington, R.M., Nuckley, D.J., 2004. Proceedings of the Thirty-Second International Workshop, 271-6.

Clemons, H.J., Burrow, K., 1972. Experimental investigation on injury mechanism of cervical spine at frontal and rear-front vehicle impacts. 16th Stapp Car Crash Conference Proceedings, 76-104.

Culver, R., Bender, M., Melvin, J., 1978. Mechanisms, tolerances and responses obtained under dynamic superior-inferior head impact. University of Michigan Highway Safety Research Institute, Report No. UM-HSRI-78-21.

Denis, F., 1984. Spinal instability as defined by the three-column spine concept in acute spinal trauma. Clin Orthop Relat Res, 189, 65-76.

Duma, S.M., Crandall, J.R., Rudd, R.W., Kent, R.W., 2003. Small female head and neck interaction with a deploying side airbag. Accident Analysis & Prevention, 35, 811-6.

Eggers, A., Zhu, F., Yang, K.H., King, A.I., 2005. Predictions of neck load due to combined compression and lateral bending. Int J Veh Safety, 1 (1/2/3), 118-28.

Eppinger, R., Sun, E., Bandak, F., Haffner, M., Khaewpong, N., Maltese, M., Kuppa, S., Nguyen, T., Takhounts, E., Tannous, R., Zhang, A., Saul, R., 1999. Development of improved injury criteria for the assessment of advanced automotive restraint systems – II. NHTSA Docket No. 1999-6407-5, November 1999.

Eppinger, R., Sun, E., Kuppa, S., Saul, R., 2000. Supplement: development of improved injury criteria for the assessment of advanced automotive restraint systems – II. NHTSA Docket No. 2000-7013-3, March 2000.

Eriksson, L., Kullgren, A., 2006. Influence of seat geometry and seating posture on NICmax long-term AIS 1 neck injury predictability. Traffic Injury Prevention, 7, 61-9.

Fife, D., Kraus, J., 1985. Anatomic location of spinal cord injury – relationship to the cause of injury. Spine, 11(1), 2-5.

Foster, J.K., Kortge, J.O., Wolanin, M.J., 1977. Hybrid III – a biomechanically-based crash test dummy. 21st Stapp Car Crash Conference Proceedings, 975-1014.

Foust, D.R., Chaffin, D.B., Snyder, R.G., Baum, J.K., 1973. Cervical range of motion and dynamic response and strength of cervical muscles. 17th Stapp Car Crash Conference Proceedings, 285-308.

Frechede, B., McIntosh, A., Grzebieta, R., Bambach, M., 2009. Hybrid III ATD in inverted impacts: influence of impact angle on neck injury risk assessment. Annals of Biomedical Engineering, 37 (7), 1403-14.

Hare, B.M., Lewis, L.K., Hughes, R.J., Ishikawa, Y., Iwasaki, K., Tsukaguchi, K., Doi, N., 2002. Analysis of rollover restraint performance with and without seat belt pretensioner at vehicle trip. Society of Automotive Engineers, Warrendale, PA. Paper No. 2002-01-0941.

Harris, J.H., Edeiken-Monroe, B., Kopaniky, D.R., 1986. A practical classification of acute cervical spine injuries. Orthopedic Clinics of North America, 17 (1), 15-30.

Heitplatz, F., Sferco, R., Fay, P., Riem, J., Kim, A., Prasad, P., 2003. An evaluation of existing and proposed injury criteria with various dummies to determine their ability to predict the levels of soft tissue neck injury seen in real world accidents. In Proceedings of the 18th International Technical Conference on the Enhanced Safety of Vehicles (ESV), Nagoya (Japan), Paper #504.

Hodgson, V.R., Thomas, L.M., 1980. Mechanisms of cervical spine injury during impact to the protected head. 24th Stapp Car Crash Conference Proceedings, 17-42.

Hosmer, D.W., Lemeshow, S., 1989. Applied logistic regression. John Wiley & Sons, New York.

Hu, J., Yang, K.H., Chou, C.C., Chen, R.J., King, A.I., 2007a. Field data analysis of occupant injury during rollover crashes. Int. J Vehicle Safety, 2(3), 261-77.

Hu, J., Chou, C.C., Yang, K.H., King, A.I., 2007b. A weighted logistic regression analysis for predicting the odds of head/face and neck injuries during rollover crashes. 51st Annual Proceedings Association for the Advancement of Automotive Medicine, Melbourne (Australia), October 15-17, 363-79.

Hu, J., Yang, K.H., Chou, C.C., King, A.I., 2008. A numerical investigation of factors affecting cervical spine injuries during rollover crashes. Spine, 33(23), 2529-35.

Huelke, D.F., Mendelsohn, R.A., States, J.D., Melvin, J.W., 1978. Cervical fractures and fracture-dislocations sustained without head impact. J Trauma, 18(7), 533-8.

Huelke, D.F., Mackay, G.M., Morris, A., Bradford, M., 1992. Non-head impact cervical spine injuries in frontal car crashes to lap-shoulder belted occupants. Society of Automotive Engineers, Warrendale, PA. Paper No. 920560.

ISO 1323-5:2005(E), 2005. Motorcycles – test and analysis procedures for research evaluation of rider crash protective devices fitted to motorcycles – Part 5: Injury indices and risk/benefit analysis. International Standards Organization, Geneva (Switzerland).

Kallieris, D., Schmidt, G., 1990. Neck response and injury assessment using cadavers and the US-SID for far-side lateral impacts of rear seat occupants with inboard-anchored shoulder belts. 34th Stapp Car Crash Conference Proceedings, 93-100.

Kaplan, E., Meier, P., 1958. Non parametric estimation from incomplete observations. Journal of the American Statistic Association, 53

Keaveny, T.M., Hayes, W.C., 1993. A 20-year perspective on the mechanical properties of trabecular bone. J Biomech Eng, 115 (4B), 534-42.

Kent, R.W., Funk, J.R., 2004. Data censoring and parametric distribution assignment in the development of injury risk functions from biomechanical data. Society of Automotive Engineers, Warrendale, PA. Paper No. 2004-01-0317.

King, A.I., 2002. Injury to the thoracolumbar spine and pelvis In: Nahum, A.M., Melvin, J.W., (Ed.) Accidental Injury: Biomechanics and Prevention. Springer-Verlag, New York, 454-90.

Klinich, K.D., Saul, R.A., Auguste, G., Backaitis, S., Kleinberger, M., 1996. Techniques for developing child dummy protection reference values. NHTSA child injury protection team. NHTSA Docket No. 74-14, Notice 97, Item 069, October 1996.

Klinich, K.D., Ebert, S.M., VanEe, C.A., Flannagan, C.A.C., Prasad, M., Reed, M.P., Schneider, L.W., 2004. Cervical spine geometry in the automotive seated posture: variations with age, stature and gender. 48th Stapp Car Crash Conference Proceedings.

Lund, A.K.. 2003. Recommended procedures for evaluating occupant injury risk from deploying side airbags. Technical Working Group Report, First Revision, Insurance Institute for Highway Safety.

Maiman, D.J., Sances, A., Myklebust, J.B., Larson, S.J., Houterman, C., Chilbert, M., El-Ghatit, A.Z., 1983. Compression injuries of the cervical spine: a biomechanical analysis. Neurosurgery, 13 (3), 254-60.

Maiman, D.J., Yoganandan, N., Pintar, F.A., 2002. Preinjury cervical alignment affecting spinal trauma. J Neurosurg (Spine 1), 97, 57-62.

Maller, R., Zhou, X., 1996. Survival analysis with long-term survivors. Wiley and Sons, New York.

Matsushita, T., Sato, T.B., Hirabayashi, K., Fujimara, S., Asazuma, T., Takatori, T., 1994. X-ray study of the human neck motion due to head inertia loading. 38th Stapp Car Crash Conference Proceedings, 55-64.

McCoy, R.W., Chou, C.C., 2007. A study of kinematics of occupants restrained with seat belt systems in component rollover tests. Society of Automotive Engineers, Warrendale, PA. Paper No. 2007-01-0709.

McElhaney, J.H., Roberts, V., 1971. Mechanical properties of cancellous bone. AIAA 9th Aerospace Science Meeting, New York, January 25-27.

McElhaney, J.H., Snyder, R.G., States, J.D., Gabrielsen, M.A., 1979. Biomechanical analysis of swimming pool injuries. Society of Automotive Engineers, Warrendale, PA. Paper No. 790137.

McElhaney, J.H., Paver, J.G., Mc Crackin, H.J., Maxwell, G.M.., 1983. Cervical spine compression responses. 27th Stapp Car Crash Conference Proceedings, 163-77.

McElhaney, J.H., Doherty, B.J., Paver, J.G., Myers, B.S., Gray, L., 1988. Combined bending and axial loading responses of the human cervical spine. 32nd Stapp Car Crash Conference Proceedings, 21-8.

McElhaney, J.H., Nightingale, R.W., Winkelstein, B.A., Chancey, V.C., Myers, B.S., 2002. Biomechanical aspects of cervical trauma In: Nahum, A.M., Melvin, J.W., (Ed.) Accidental Injury: Biomechanics and Prevention. Springer-Verlag, New York, 324-73.

McIntosh, A.S., Kallieris, D., Frechede, B., 2007. Neck injury tolerance under inertial loads in side impacts. Accident Analysis and Prevention, 39, 326-33.

Mertz, H.J., Patrick, L.M., 1971. Strength and response of the human neck. 15th Stapp Car Crash Conference Proceedings.

Mertz, H.J., Hodgson, V.R., Thomas, L.M., Nyquist, G.W., 1978. An assessment of compressive neck loads under injury-producing conditions. Physician and Sports Medicine, 6(11), 95-106.

Mertz, H.J., Driscoll, G.D., Lenox, J.B., Nyquist, G.W., Weber, D.A., 1982a. Response of animals exposed to deployment of various passenger inflatable restraint system concepts for a variety of collision severities and animal positions. In Proceedings of the 9th International Technical Conference on the Enhanced Safety of Vehicles (ESV), Kyoto (Japan), 352-68.

Mertz, H.J., Weber, D.A., 1982b. Interpretations of the impact responses of a 3-year-old child dummy relative to child injury potential. In Proceedings of the 9th International Technical Conference on the Enhanced Safety of Vehicles (ESV), Kyoto (Japan), 368-76.

Mertz, H.J., 1984. Injury assessment values used to evaluate hybrid III response measurements. NHTSA Docket 74-14, Notice 32. General Motors Submission USG 2284, Attachment 1, Enclosure 2, March 22, 1984.

Mertz HJ, Prasad P., Irwin, A.L., 1997. Injury Risk Curves for Children and Adults in Front and Rear Collisions. 41st Stapp Car Crash Conference Proceedings.

Mertz HJ, Prasad P, 2000. Improved Neck Injury Risk Curves for Tension and Extension Moment Measurements of Crash Dummies. 44th Stapp Car Crash Conference Proceedings.

Mertz, J.H., Irwin, A.L., Prasad, P., 2003. Biomechanical and scaling bases for frontal and side impact injury assessment reference values. 47th Stapp Car Crash Conference Proceedings, 155-188.

Miller, T., Romano, E., Zaloshnja, E., Spicer, R., 2001. Harm 2000: crash cost and consequence data for the new millennium. 45th Annual Proceedings Association for the Advancement of Automotive Medicine, San Antonio, September 24-26, 159-84.

Milton, J.S., Arnold, J.C., 1995. (Ed.) Introduction to probability and statistics – principles and applications for engineering and the computing sciences. Irwin/McGraw-Hill, Boston.

Moffatt, E.A., Cooper, E.R., Croteau, J.J., Orlowski, K.F., Marth, D.R., Carter, J.W., 2003. Matched-pair rollover impacts of rollcaged and production roof cars using the controlled rollover impact system (CRIS). Society of Automotive Engineers, Warrendale, PA. Paper No. 2003-01-0172.

Moore, K.L., Dalley, A.F., 1999. (Ed.) Clinical oriented anatomy. Lippencott Williams & Wilkins, Philadelphia.

Moore, K.L., Agur, A.M.R., 2002. (Ed.) Essential clinical anatomy. Lippencott Williams & Wilkins, Philadelphia.

Mow, V.C., Hayes, W.C., 1997. (Ed.) Basic orthopaedic biomechanics. Lippencott-Raven, Philadelphia.

Munoz, D., Mansilla, A., Lopez-Valdes, F., Martin, R., 2005. A study of current neck injury criteria used for whiplash analysis, proposal of a new criterion involving upper and lower neck load cells. In Proceedings of the 19th International Technical Conference on the Enhanced Safety of Vehicles (ESV), Washington D.C., June 6-9.

Myers, B.S., McElhaney, J.H., Doherty, B.J., Paver, J.G., Nightingale, R.W., Ladd, T.P., Gray, L., 1989. Responses of the human cervical spine to torsion. 33rd Stapp Car Crash Conference Proceedings, 215-22.

Myers, B.S., Richardson, W.J., Doherty, B.J., Nightingale, R.W., McElhaney, J.H., 1991a. The role of head constraint in the development of lower cervical compression flexion injury. 35th Stapp Car Crash Conference Proceedings, 391-9.

Myers, B.S., McElhaney, J.H., Doherty, B.J., Paver, J.G., and Gray, L., 1991b. The role of torsion in cervical spine trauma. Spine, 16 (8), 870-4.

Myers, B.S., Winkelstein, B.A., 1995. Epidemiology, classification, mechanism, and tolerance of human cervical spine injuries. Critical Reviews in Biomedical Engineering, 23 (5&6), 307-409.

Nightingale, R.W., McElhaney, J.H., Richardson, W.J., Best, T.M., Myers, B.S., 1996a. Experimental impact injury to the cervical spine: relating motion of the head and the mechanism of injury. J Bone Joint Surg Am, 78, 412-21.

Nightingale, R.W., McElhaney, J.H., Richardson, W.J., Myers, B.S., 1996b. Dynamic responses of the head and cervical spine to axial impact loading. J Biomech., 29, 307-18.

Nightingale, R.W., McElhaney, J.H., Camacho, D.L.A., Kleinberger, M., Winkelstein, B.A., Myers, B.S., 1997a. The dynamic responses of the cervical spine: buckling, end conditions, and tolerance in compressive impacts. 41st Stapp Car Crash Conference Proceedings, 451-71.

Nightingale, R.W., Richardson, W.J., Myers, B.S., 1997a. The effects of padded surfaces on the risk for cervical spine injury. Spine, 22(20), 2380-7.

Nightingale, R.W., Winkelstein, B.A., Knaub, K.E., Richardson, W.J., Luck, J.F., Myers, B.S., 2002. Comparative strengths and structural properties of the upper and lower cervical spine in flexion and extension. J Biomechanics, 35, 725-32.

Nightingale, R.W., Chancey, V.C., Ottaviano, D., Luck, J.F., Tran, L., Prange, M., Myers, B.S., 2007. Flexion and extension structural properties and strengths for male cervical spine segments. J Biomechanics, 40, 535-42.

NSCISC, 2009. Spinal cord injury facts and figures at a glance. National Spinal Cord Injury Statistical Center, Birmingham, AL. April 2009.

Nuckley D.J., Ching, R.P., 2005. Relationship between vertebral bone mineral density and strength. In Proceedings Society of Experimental Mechanics Annual Conference and Exposition on Experimental and Applied Mechanics.

Nucholtz, G.S., Melvin, J.W., Huelke, D.F., Alem, N.M., Blank, J.G., 1981. Response of the cervical spine to superior-inferior head impact. 25th Stapp Car Crash Conference Proceedings, 197-237.

Nusholtz, G.S., Huelke, D.E., Lux, P., Alem, N.M., Montalvo, F., 1983. Cervical spine injury mechanisms. 27th Stapp Car Crash Conference Proceedings, 179-207.

Orlowski, K., Bundorf, R., Moffatt, E., 1985. Rollover crash tests – the influence of roof strength on injury mechanics. 29th Stapp Car Crash Conference Proceedings, 181-203.

Panjabi, M.M., Oda, T., Crisco, J.J., Oxland, T.R., Katz, L., Nolte, L., 1991. Experimental study of atlas injures I – biomechanical analysis of their mechanisms and fracture patterns. Spine, 16 (10), S460-5.

Pintar, F.A., Sances, A., Yoganandan, N., Reinartz, J., Maiman, D.J., Suh, J.K., Unger, G., Cusick, J.F., Larson, S.J., 1990. Biodynamics of the total human cadaveric cervical spine. 34th Stapp Car Crash Conference Proceedings, 55-72.

Pintar, F.A., Yoganaandan, N., Voo, L., Cusick, J.F., Maiman, D.J., Sances, A., 1995. Dynamic characteristics of the human cervical spine. 39th Stapp Car Crash Conference Proceedings, 195-202.

Pintar F.A., Voo L.M., Yoganadan N., Cho T.H., Maiman D.J., 1998a. Mechanisms of hyperflexion cervical spine injury. Proceeding of International Research Council on the Biomechanics of Impact, Goteborg (Sweden), September 1998, 249-260.

Pintar, F.A., Yoganandan, N., Voo, L., 1998b. Effect of age and loading rate on human cervical spine injury threshold. Spine, 23(18), 1957-62.

Portnoy, H.D., McElhaney, J.H., Melvin, J.W., Croissant, P.D., 1972. Mechanisms of cervical spine injury in auto accidents. Proceedings of the 15th Conference of the American Association for Automotive Medicine, New York NY, 58-83.

Prasad, P., Daniel, R.P., 1984. Biomechanical analysis of head, neck, and torso injuries to child surrogates due to sudden acceleration. 28th Stapp Car Crash Conference Proceedings, 25-40.

Prasad, P., Kim, A., Weerappuli, D., 1997, Biofidelity of anthropomorphic test devices for rear impact. 41st Stapp Car Crash Conference Proceedings, 387-415.

Qingan, Z., Jun, O., William, L., Haijun, L., Zhonghua, L., Xinhui, G., Shizhen, Z., 1999. Traumatic instabilities of the cervical spine caused by high-speed axial compression in a human model: an in virtro biomechanical study. Spine, 24 (5), 440-4.

Raasch, C.C., Carhart, M.R., Ivarsson, B.J., Lucas, S.R., 2010. Development of lower neck injury assessment reference values based on comparison of ATD and PMHS tests. Society of Automotive Engineers, Warrendale, PA. Paper No. 2010-01-0140.

Raddin, J., Cormier, J., Smyth, B., Croteau, J., Cooper, E., 2009. Compressive neck injury and its relationship to head contact and torso motion during vehicle rollovers. Society of Automotive Engineers, Warrendale, PA. Paper No. 2009-01-0829.

Riggs B.L., Wahner, H.W., Dunn, W.L., Mazess, R.B., Offord, K.P., Melton III, L.J., 1981. Differential changes in bone mineral density of the appendicular and axial skeleton with aging: relationship to spinal osteoporosis. J. Clin. Invest. 67, 328-335.

Roaf, R., 1963. Lateral flexion injuries of the cervical spine. J Bone Joint Surg, 45B (1), 36-8.

Roaf, R., 1972. International classification of spinal injuries. Paraplegia, 10, 78-84.

SAEJ211-1, 2007. Instrumentation for impact test – part 1 – electronic instrumentation. Society of Automotive Engineers Surface Vehicle Recommended Practice, Warrendale, PA. July 2007.

Sances, A., Myklebust, J., Cusick, J.F., Weber, R., Houterman, C., Larson, S.J., Walsh, P., Chilbert, M., Prieto, T., Zyvoloski, M., Ewing, C., Thomas, D., Saltzberg, B., 1981. Experimental studies of brain and neck injury. 25th Stapp Car Crash Conference Proceedings, 149-94.

Schmitt, K., Muser, M.H., Walz, F.H., Niederer, P.F. 2002. Nkm – a proposal for a neck protection criterion for low-speed rear-end collisions. Traffic Injury Prevention, 3, 117-26.

Schneider, L.W., Foust, D.R., Bowman, B.M., Snyder, R.G., Chaffin, D.B., Abdelnour, T.A., Baum, J.K., 1975. Biomechanical properties of the human neck in lateral flexion. 19th Stapp Car Crash Conference Proceedings, 455-85.

Shigley JE, Mischke CR, 1989. Mechanical Engineering Design Fifth Edition. McGraw-Hill Inc., New York.

Tilley, A.R., 1993. The measure of man and woman: human factors in design. The Whitney Library of Design, New York.

UNECE Regulation No.94. Uniform provisions concerning the approval of vehicles with regard to the protection of occupants in the event of a frontal collision. United Nations Economic Commission for Europe –Transport Division, May 8, 2007.

Viano, D.C., Parenteau, C.S., 2008. Analysis of head impacts causing neck compression injury. Traffic Injury Prevention, 9, 144-52.

Viano, D.C., Parenteau, C.S., Gopal, M.M., James, M.B., 2009. Vehicle and occupant responses in a friction trip rollover test. Society of Automotive Engineers, Warrendale, PA. Paper No. 2009-01-0830.

White, A.A., Panjabi, M.M., 1978. (Ed.) Clinical biomechanics of the spine. Lippencott-Raven, Philadelphia.

White, A.A., Panjabi, M.M., 1990. (Ed.) Clinical biomechanics of the spine. Lippencott-Raven, Philadelphia.

Wilber, V.H., 1998. American Automobile Manufactures Association Comments to Docket No. NHTSA Docket No. 98-4405; Notice 1 Advanced Technology Airbags: Attachment C. American Automobile Manufactures Association, December 17, 1998 (NHTSA Docket 98-4405-79).

Winkelstein, B.A., Myers, B.S., 1997. The biomechanics of cervical spine injury and implications for injury prevention. Medicine & Science in Sports & Exercise, 29 (7), 246-55.

Wismans, J., Spenny, C.H., 1983. Performance requirements for mechanical necks in lateral flexion. 27th Stapp Car Crash Conference Proceedings, 137-48.

Yamaguchi, G.T., Carhart, M.R., Larson, R., Richards, D., Pierce, J., Raasch, C.C., Scher, I., Corrigan, C.F., 2005. Electromyographic activity and posturing of the human neck during rollover tests. Society of Automotive Engineers, Warrendale, PA. Paper No. 2005-01-0302.

Yoganandan, N., Sances, A., Maimam, D.J., Myklebust, J.B., Pech, P., Larson, S.J., 1986. Experimental spinal injuries with vertical impact. Spine, 11 (9), 855-60.

Yoganandan, N., Pintar, F.A., Haffner, M., Jentzen, J., Maiman, D.J., Weinshel, S.S., Larson, S.L., Nichols, H., Sances, A., 1989a. Epidemiology and injury biomechanics of motor vehicle related trauma to the human spine. 33rd Stapp Car Crash Conference Proceedings, 223-42.

Yoganandan N., Sances, A., Pintar, F., 1989b. Biomechanical evaluation of the axial compressive responses of the human cadaveric and manikin necks. J Biomechanical Eng, 111, 250-5.

Yoganandan, N., Pintar, F.A., Sances, A., Reinartz, J., Larson, S.J., 1991. Strength and kinematic response of dynamic cervical spine injuries. Spine, 16 (10), S511-7.

Yoganandan, N., Pintar, F.A., Maiman, D.J., Philippens, M., Wismans, J., 2009. Neck forces and moments and head acceleration in side impact. Traffic Injury Prevention, 10, 51-7.

ABSTRACT

CERVICAL SPINE TOLERANCE AND RESPONSE IN COMPRESSIVE LOADING MODES INCLUDING COMBINED COMPRESSION AND LATERAL BENDING

by

DANIEL E. TOOMEY

May 2013

Advisor: King H. Yang, Ph.D.

Co-Advisor: Chris A. Van Ee, Ph.D.

Major: Biomedical Engineering

Degree: Doctor of Philosophy

Injuries in motor vehicle accidents continue to be a serious and costly societal problem. Automotive safety researchers have observed noticeable lateral bending of the anthropomorphic test device (ATD) neck prior to or in conjunction with head impact with the vehicle roof in rollover crash tests. Since there is scant data available about the effects of lateral bending on overall compressive tolerance of the human cervical spine, it is unknown if the presence of lateral bending is important to consider during impacts with the apex of the head. Compressive injury tolerance has historically been reported by identifying the axial force at the time of injury measured at the base of the neck, however, axial force at failure exhibits variation and this has been attributed to the alignment of the cervical vertebra and the end conditions of test methodology used. Robust and sensitive injury metrics for human compressive cervical spine tolerance that can be applied to a wide range of loading conditions and head-neck postures would be useful in evaluating and developing mechanically meaningful and robust anthropomorphic test devices (ATDs) and their associated injury assessment reference values (IARVs). As the Hybrid III ATD continues to be used in automotive rollover applications, interpretation of measured neck loads in this

testing mode would be aided by a better understanding of human cervical spine response and tolerance in compression dominated combined loading scenarios and their correlation to Hybrid III ATD neck responses.

The effects of lateral bending on the compressive cervical spine dynamic response and tolerance was investigated through post mortem human subject (PMHS) head-neck complex experimentation. Similar to findings of previous researchers, the initial cervical posture influenced the mechanical response of the spine and the loads at failure. The results were combined with available historical compressive cervical spine tolerance studies that include head and neck dynamics, cervical kinetics and known end conditions. A re-evaluation of the axial force tolerance of the PMHS cervical spine as well as derivation of a mechanistically relevant eccentricity based injury tolerance metric that can be applied to a wider range of loading vectors and initial cervical spine postures were conducted. Finally, the Hybrid III ATD neck compressive injury assessment reference values (IARVs) were evaluated through reconstruction of PMHS experiments with known injury outcomes using the Hybrid III head and neck assembly. Results are consistent with the currently defined IARVs and provide additional experimental support of the IARVs in loading modes that are known to result in PMHS compressive cervical injuries.

AUTOBIOGRAPHICAL STATEMENT

DANIEL E. TOOMEY

EDUCATION:

2013	Ph.D.	Biomedical Engineering Wayne State University – Detroit, MI
2003	MSE	Mechanical Engineering University of Michigan – Dearborn, MI
2001	BSE	Mechanical Engineering University of Michigan – Ann Arbor, MI

PROFESSIONAL EXPERIENCE:

2001 to Date	Design Research Engineering, LLC. – Novi, MI *Project Engineer / Senior Project Engineer*
2000	TRW Automotive - Livonia, MI *Co-op Engineer*

LICENSURE: Professional Mechanical Engineer, Michigan #6201056035

PUBLICATIONS:

Toomey D.E., Yang K.H., Yoganandan N., Pintar F.A., VanEe C.A. (2013) "Towards a More Robust Lower Neck Compressive Injury Tolerance - An Approach Combining Multiple Test Methodologies," *Traffic Injury Prevention*, Accepted.

Toomey D.E., Mason M.J., Hardy W.N., Yang K.H., Van Ee C.A. (2009) "Exploring the Role of Lateral Bending Postures and Asymmetric Loading on Cervical Spine Compression Responses," 2009 ASME International Mechanical Engineering Congress & Exposition, IMECE2009-12911, Lake Buena Vista, Florida, November 13-19.

Toomey D.E., Paddock E.M., Winkel E.S., Burnett, R. (2009) "Vehicle Chassis, Body, and Seat Belt Buckle Acceleration Responses in the Vehicle Crash Environment," *SAE Int. J. Passeng. Cars – Mech.Syst.* 2(1): 1151-1170.

Toomey D.E., Klima M.E., Cooper E.R. (2009) "Evaluation of Seat Belt Assembly Physical Evidence in Properly Functioning and Intentionally Disabled Retractor Demonstrations," SAE Paper No. 2009-01-1245, Warrendale, PA.

Shim T., **Toomey, D.E.**, Ghike, C. Sardar, H.M. (2008) "Vehicle Rollover Recovery Using Active Steering/Wheel Torque Control," *International Journal of Vehicle Design* 46(1) : 51-71.

Toomey D.E., VanEe C.A., Klima M.E. (2006) "Safety Restraint System Physical Evidence and Biomechanical Injury Potential Due to Belt Entanglement," SAE Paper No. 2006-01-1670, Warrendale, PA.

Klima M.E., **Toomey D.E.**, Weber M.J. (2005) "Seat Belt Retractor Performance Evaluation in Rollover Crashes," *J. Passeng. Cars – Mech.Syst.* Section 6 – Vol 114: 2016-2023.

Klima M.E., **Toomey D.E.**, Weber M.J. (2005) "Seat Belt Buckle Performance in High Energy Wheel-to-Ground Impacts," *J. Passeng. Cars – Mech.Syst.* Section 6 – Vol 114: 2034-2041.

Toomey D.E., Shim T. (2004) "Investigation of Active Steering/Wheel Torque Control at the Rollover Limit Maneuver," *J. Passeng. Cars – Mech.Syst. .* Section 6 – Vol 113: 1133-1140